Lab on a Chip

CRITICAL REVIEW

View Article Online
View Journal

Cite this: DOI: 10.1039/d5lc00957j

Integrated microfluidic biosensors: shaping the future of quantitative life sciences and on-chip molecular diagnostics

Ty Naquin,[a] Chloe Naquin,[a] Qian Wu,[a] Ying Chen,[a] Aidan Canning,[a] Kaichun Yang,[a] Yuna Li,[a] Shuaiguo Zhao,[a] Yun Ling,[a] Zhiteng Ma,[a] Ke Jin,[a] Ye He,[a] Shujie Yang,*[ab] Luke P. Lee*[cde] and Tony Jun Huang*[a]

Integrated microfluidic biosensors have rapidly evolved into powerful platforms to meet the increasing demand for ultrasensitive and high-throughput quantitative analysis. By seamlessly combining sample handling through microfluidics with real-time detection *via* biosensors, these systems provide unmatched benefits in sensitivity, speed, portability, and immediate monitoring, thereby transforming diagnostics in human and animal health, environmental sensing, and point-of-care testing. In this review, we provide a comprehensive overview of integrated microfluidics with biosensors, highlighting the synergistic interplay between these two complementary fields and their various biomedical applications. We begin by examining different microfluidic technologies, including 3D dynamic cell culture systems, inertial microfluidic separation, acoustofluidics, dielectrophoresis, optofluidics, and immunoassays. Next, we discuss integrated microfluidic systems that incorporate various biosensor technologies, including electrochemical, electrophysiological, plasmonic, Raman, and quantum sensors. These are designed to detect and analyze DNA, RNA, proteins, exosomes, cells, and small organisms, covering a size range from nanometers to millimeters. Additionally, we discuss the wide range of applications for integrated microfluidic biosensors and examine significant challenges and future opportunities that will influence their ongoing development and practical use. Finally, we highlight successful commercial products developed with integrated microfluidic technologies.

Received 11th October 2025,
Accepted 9th April 2026

DOI: 10.1039/d5lc00957j

rsc.li/loc

1. Introduction

There is a growing demand for biological analysis tools that are sensitive, accessible, and capable of handling complex samples with minimal processing. Such platforms are crucial for next-generation diagnostics, enabling the detection of disease at earlier stages and delivering results directly at the point of care.[1,2] Beyond the clinic, they also support broader research needs, enabling high-throughput screening and real-time monitoring that accelerate discovery and therapeutic development.[3–5]

Traditionally, however, sample isolation, enrichment, and detection have been treated as separate processes, requiring multiple preparation steps that introduce inefficiencies, sample loss, and potential contamination.[6,7] Conventional methods, such as centrifugation, filtration, and chromatography, often require large sample volumes, specialized equipment, and extensive processing time, making them impractical for integration with biosensors in rapid or point-of-care applications.[8–10] Furthermore, matrix effects often affect biosensing techniques that rely on unprocessed biological samples, where interfering substances obscure target signals, reducing sensitivity and specificity.[11] These challenges highlight the need for approaches that streamline preparation and detection into a unified process.[12]

Microfluidic technologies have emerged as a powerful response to this need. By integrating sample processing with biosensing, microfluidic platforms enable seamless transitions from isolation and enrichment to detection. Early biosensors relied on coarse methods, such as filtration and

[a] *Thomas Lord Department of Mechanical Engineering and Materials Science, Duke University, Durham, NC 27708, USA. E-mail: shujie.yang@seas.upenn.edu, tony.huang@duke.edu*
[b] *Department of Mechanical Engineering and Applied Mechanics, University of Pennsylvania, Philadelphia, PA, 19104, USA*
[c] *Division of Engineering in Medicine, Renal Division, Department of Medicine, Brigham and Women's Hospital, Harvard Medical School, Boston, MA 02115, USA. E-mail: lplee@bwh.harvard.edu*
[d] *Department of Bioengineering, University of California, Berkeley, Berkeley, CA 94720, USA*
[e] *Department of Electrical Engineering and Computer Science, University of California, Berkeley, Berkeley, CA 94720, USA*

sedimentation, which limited their efficiency and throughput. As microfluidic technologies matured, approaches such as dielectrophoresis (DEP),[13,14] acoustofluidics,[15–17] and inertial microfluidics[18,19] enabled more selective enrichment, reduced background noise, and enhanced biosensor response. These capabilities are especially valuable in clinical diagnostics, liquid biopsy, environmental monitoring, and personalized medicine, where the accurate detection of rare biomarkers, such as circulating tumor cells or extracellular vesicles, is critical.[20–26] By unifying processing and sensing in one unit, integrated systems minimize reagent use, reduce assay time, and expand opportunities for single-cell analysis, biomarker discovery, and early disease detection.

This review examines the fundamental principles underlying microfluidic and sensing technologies, highlighting significant advancements in sample isolation techniques, including electrophoresis, acoustofluidics, inertial microfluidics, immunoaffinity capture, and microfluidic filtration. We will also examine a variety of biosensing modalities, including electrochemical, optical plasmonic, Raman, and quantum biosensors, that are being integrated into microfluidic platforms to enhance analytical performance. Finally, we will discuss the challenges and prospects of these technologies in both research and clinical settings.

2. Microfluidics for sample handling and manipulation

Microfluidic technologies have become essential tools for sample processing and manipulation in biological and biomedical research, enabling the efficient and high-resolution handling of complex samples across various applications.[27,28] Their ability to integrate critical operations, such as isolation, enrichment, and purification, into compact, automated platforms has streamlined workflows across diverse applications, from basic cell biology to

Table 1 Comparison of microfluidic technologies commonly used for sample preparation, manipulation, and integration with biosensing platforms, highlighting their primary functions, advantages, limitations, and application contexts

Microfluidic technology	Subtype	What it measures	Key advantages	Primary constraints	When to choose this modality
Passive microfluidics (hydrodynamic/physical property-based)	Inertial microfluidics	Size-based focusing, separation, and enrichment	High throughput and label-free processing, simple hardware	Limited post-fabrication tunability, geometry dependent resolution	When high-throughput preprocessing or enrichment is needed upstream of sensing
	Deterministic lateral displacement	Size and trajectory-based separation	Precise size cutoffs, continuous and label-free operation	Clogging susceptibility, strict fabrication requirements, reduced nanoscale throughput	When precise size fractionation is required
	Filtration/sieving	Size-based isolation	Simple operation, compatible with unprocessed samples	Membrane fouling, clogging, limited device lifetime	When simplicity and whole-sample compatibility are prioritized
Active field-driven microfluidics	Acoustofluidics	Contactless manipulation *via* acoustic radiation forces and streaming	Contactless and biocompatible manipulation, tunable field strength	External actuation hardware, power requirements	When tunable, label-free manipulation is required
	Dielectrophoresis	Electrical phenotype-based trapping, separation, and concentration	High selectivity, nanoscale sensitivity, strong sensor integration	Conductivity sensitivity, electrode fouling, joule heating	When electrical contrast provides discrimination beyond size or affinity
	Optofluidics	Optical actuation, trapping, or photothermal flow control	Wireless actuation, high spatial precision	Optical alignment, photothermal effects	When electrical contact is undesirable and optical access is available
	Digital microfluidics	Programmable droplet transport, merging, and splitting	Highly reconfigurable, automated workflows	Surface fouling, dielectric breakdown, voltage requirements	When assay flexibility and automation outweigh raw throughput
Affinity-based microfluidics	Immunoaffinity capture	Target-specific capture *via* antibodies or ligands	High molecular specificity, strong sensing integration	Reagent dependence, nonspecific binding	When molecular specificity is essential
Microenvironment engineering	Dynamic 3D culture/organ-on-chip	Controlled tissue culture and physiological modeling	Human-relevant models, long-term functional readouts	System complexity, limited scalability	When modeling tissue function or drug response

therapeutic development.[29,30] These systems minimize sample loss, accelerate processing, and enable high specificity for rare or delicate targets that are challenging to obtain using conventional methods. In this section, we introduce several foundational microfluidic strategies—including dynamic 3D cell culture, inertial microfluidics, acoustofluidics, electrophoretic manipulation, and immunoaffinity capture—that have advanced the frontiers of sample handling for biosensing and clinical diagnostics (Table 1).

2.1 Passive microfluidics

Passive hydrodynamic and physical property-based microfluidic operations leverage channel geometry, flow fields, and intrinsic particle or cell properties to achieve manipulation without external actuation.[31] These approaches are particularly attractive for applications requiring high-throughput, label-free processing with minimal system complexity, as they rely on fixed device architectures rather than active fields or control hardware. By exploiting size, deformability, density, or inertia-dependent effects, passive methods are well suited for preprocessing large sample volumes, including enrichment, filtration, and buffer exchange prior to downstream analysis.[32,33] However, their performance is tightly coupled to device geometry and flow conditions, introducing trade-offs between throughput and selectivity, limited post-fabrication tunability, and constraints on integration with downstream sensing or analytical modules. As such, passive strategies represent a foundational design choice when simplicity, scalability, and robustness are prioritized in microfluidic system design.

2.1.1 Inertial and secondary-flow-driven microfluidics. Separating, manipulating, and enriching cells or nanoparticles at high throughput is challenging because conventional methods often rely on external labels, introduce sample loss, and are challenging to scale for clinical or industrial use. These limitations become particularly problematic when working with rare or delicate targets that require quick and gentle isolation. Inertial and secondary flow-driven microfluidics address these challenges by exploiting hydrodynamic forces that arise at finite Reynolds numbers within microchannels.[34,35] Rather than relying on externally applied electric, magnetic, or optical fields, these approaches leverage inertial lift forces and secondary flow structures—such as Dean vortices—generated by channel geometry and curvature to manipulate particles and cells. At sufficiently high flow rates, particles experience inertial lift forces that cause them to migrate and concentrate in specific channel regions. By harnessing these flow-induced phenomena through rational channel design, inertial and secondary-flow-driven microfluidics enable high-throughput, label-free separation and sorting of diverse biological entities, including cells, exosomes, and other micro- or nanoscale particles.[36–38] Because these systems operate without external actuation, they offer low hardware complexity and strong scalability, making them well suited for industrial and clinical workflows.

In a straight channel, particles experience focusing due to the balance between inertial lift forces and the drag force from the fluid. This results in the formation of particle bands at specific positions, typically near the center of the channel. Using this concept, Bhagat *et al.* showcased the separation of 590 nm polystyrene particles from a mixture containing both 1.9 μm and 590 nm particles using a straight microfluidic channel with a rectangular cross-section.[39] Jeon *et al.* demonstrated that by adding polymers, viscoelastic forces can be harnessed in conjunction with inertial lift forces to achieve submicron resolution in particle separation at high throughput (Fig. 1A).[40] In a clinically significant example, vortex microfluidic technology has been applied for label-free isolation of prostate circulating tumor cells (CTCs), showcasing the translational potential of inertial-based platforms for rare cell enrichment without relying on external labels (Fig. 1B).[41] These principles also extend to droplet microfluidic systems; Li *et al.* demonstrated size-based sorting of hydrogel droplets, separating smaller cell-laden droplets from larger empty ones with high purity while preserving cell viability (Fig. 1C).[42] Here, inertial effects provide a passive quality-control mechanism that integrates naturally into droplet workflows.

When fluid flows through a curved channel, the higher-momentum fluid near the centerline moves outward due to centrifugal forces, while the slower-moving fluid near the walls is displaced inward. This displacement creates two counter-rotating vortices, known as Dean vortices, which lead to a complex flow pattern superimposed on the primary axial flow. A platform to isolate exosomes using these concepts was devised by Zhou *et al.*[43] They periodically reversed the Dean secondary flow generated by a wavy, serpentine channel with repeated spirals, which caused larger particles (*e.g.*, large extracellular vesicles) to be focused along the central line. In comparison, smaller particles (*e.g.*, exosomes) were concentrated along the edges for separation (Fig. 1D).

In addition to their analytical and clinical applications, inertial microfluidic platforms are being increasingly adapted for large-scale bioprocessing, where robustness and scalability are dominant design constraints. For example, a deformation-free plastic spiral device has been developed for CHO cell clarification, achieving high separation efficiency while minimizing cell damage, even at industrial-scale throughputs (Fig. 1E).[44] The device architecture enables 3D stacking of spiral channels, allowing throughput to be increased *via* parallelization rather than higher flow velocities. This design decouples throughput scaling from shear stress, addressing a key constraint in biomanufacturing applications. Jeon *et al.* introduce an innovative approach to enhance the efficiency of chimeric antigen receptor (CAR) T cell manufacturing, utilizing a multidimensional double spiral inertial microfluidic device that leverages the size differences between activated and inactivated T cells to achieve high-purity separation (Fig. 1F).[45] The study reports

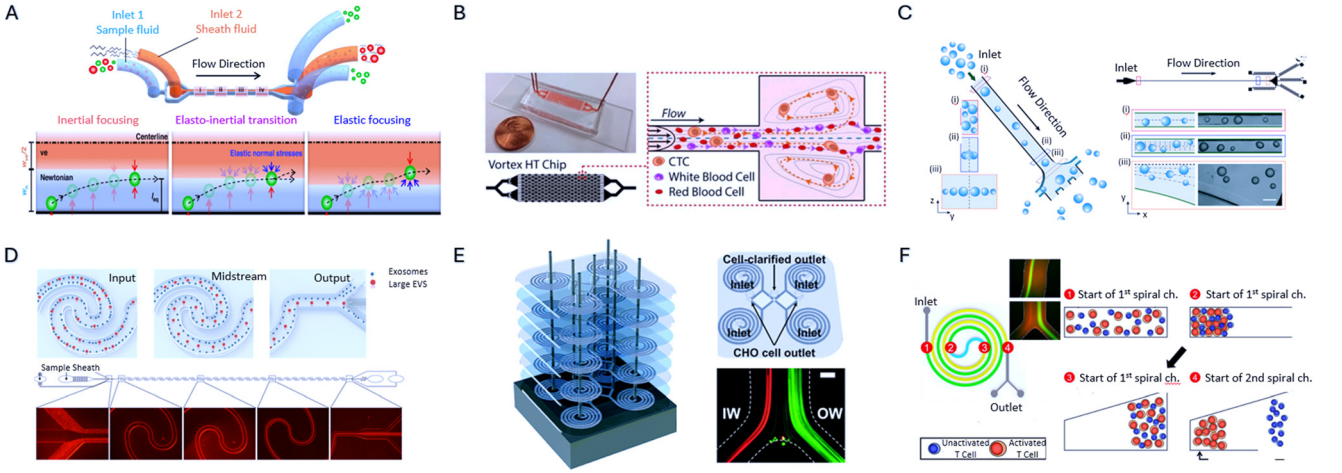

Fig. 1 Inertial and secondary-flow–driven microfluidics for particle and cell manipulation. (A) Elasto-inertial separation of microspheres with submicron resolution, adapted from ref. 40 with permission from Springer Nature, H. Jeon *et al.*, *Microsystems & Nanoengineering*, 2024, **10**, 15, copyright 2024; (B) label-free isolation of prostate circulating tumor cells using vortex microfluidic technology, adapted from ref. 41 with permission from Springer Nature, C. Renier *et al.*, *NPJ Precision Oncology*, 2017, **1**, 15, copyright 2017; (C) size-based sorting of hydrogel droplets using inertial microfluidics, adapted from ref. 42 with permission from Royal Society of Chemistry, M. Li *et al.*, *Lab on a Chip*, 2018, **18**, 2575–2582, copyright 2018; (D) submicron particle focusing and exosome sorting by wavy microchannel structures within viscoelastic fluids, adapted from ref. 43 with permission from American Chemical Society, Y. Zhou *et al.*, *Analytical Chemistry*, 2019, **91**, 4577–4584, copyright 2019; (E) engineering a deformation-free plastic spiral inertial microfluidic system for CHO cell clarification in biomanufacturing, adapted from ref. 44 with permission from Royal Society of Chemistry, H. Jeon *et al.*, *Lab on a Chip*, 2022, **22**, 272–285, copyright 2022; (F) separation of activated T cells using multidimensional double spiral inertial microfluidics for high-efficiency CAR T cell manufacturing, adapted from ref. 45 with permission from American Chemical Society, H. Jeon, C. R. Perez, T. Kyung, M. E. Birnbaum and J. Han, *Analytical Chemistry*, 2024, copyright 2024.

an 85% removal of inactivated T cells and an 80% recovery of activated T cells, resulting in a two-fold increase in CAR transduction efficiency for specific samples.

2.1.2 Geometry- and confinement-based microfluidics. Geometry- and confinement-based passive microfluidic methods achieve label-free manipulation by encoding

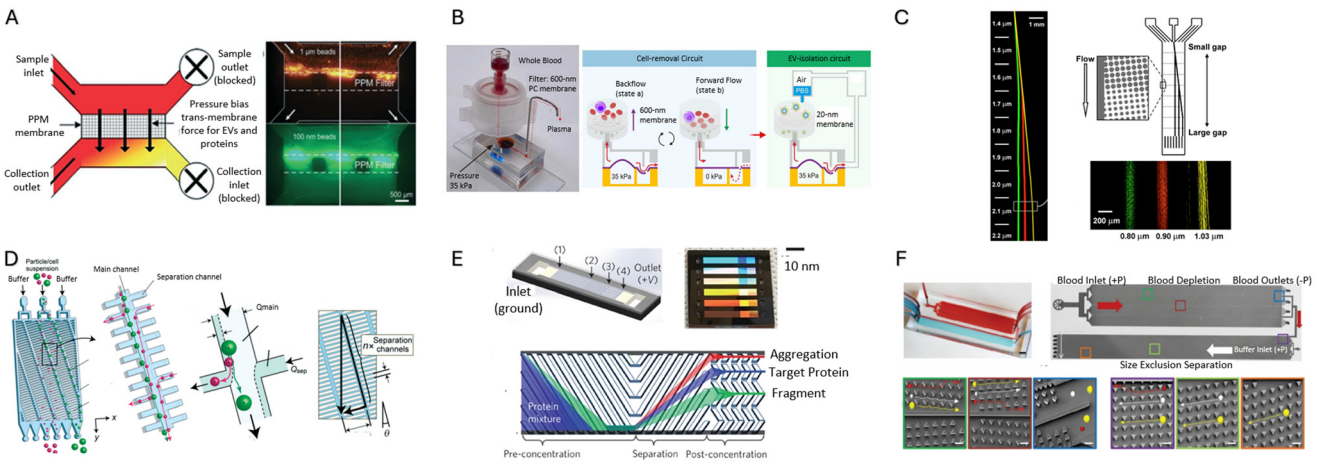

Fig. 2 Geometry- and confinement-based microfluidics for particle manipulation. (A) Microfluidic filtration system for isolating extracellular vesicles directly from blood samples, adapted from ref. 48 with permission from Royal Society of Chemistry, R. T. Davies *et al.*, *Lab on a Chip*, 2012, **12**, 5202–5210, copyright 2012. (B) Cascaded microfluidic circuits generating pulsatile flow conditions for continuous extracellular vesicle filtration from whole blood while mitigating membrane fouling, adapted from ref. 49 with permission from American Association for the Advancement of Science, Z. Li *et al.*, *Science Advances*, 2023, **9**, eade2819, copyright 2023. (C) Deterministic lateral displacement arrays enabling size-based separation of 800–1000 nm spherical particles, adapted from ref. 50 with permission from American Association for the Advancement of Science, L. R. Huang *et al.*, *Science*, 2004, **304**, 987–990, copyright 2004. (D) Slanted, asymmetric microfluidic lattice structures functioning as size-selective sieves for continuous particle and cell sorting *via* repeated interactions with angled obstacles, adapted from ref. 52 with permission from Royal Society of Chemistry, M. Yamada *et al.*, *Lab on a Chip*, 2017, **17**, 304–314, copyright 2017. (E) Nanofluidic device for continuous ultrafiltration and quality assurance of biopharmaceutical products, adapted from ref. 53 with permission from Springer Nature, S. H. Ko *et al.*, *Nature Nanotechnology*, 2017, **12**, 804–812, copyright 2017. (F) Integrated microfluidic platform combining size-based separation and deformability analysis for efficient isolation of circulating tumor cells, adapted from ref. 54 with permission from Wiley, Z. Liu *et al.*, *Advanced Biosystems*, 2018, **2**, 1800200, copyright 2018.

manipulation functionality directly into channel architectures, obstacles, or membrane structures, rather than relying on flow-induced inertial forces.[46,47] In these systems, particle and cell trajectories are deterministically biased through repeated interactions with physical boundaries, constrictions, or porous elements, enabling continuous fractionation based on size, deformability, or transport behavior under flow. Because manipulation arises from structural design rather than externally applied fields or tunable actuation, these approaches offer robust, scalable operation with minimal system complexity. Such methods are particularly well suited for filtration, sieving, and preprocessing of complex biological samples, and are readily integrated upstream of downstream biosensing or molecular analysis modules.

Early microfluidic filtration approaches focused on size-based exclusion using porous membranes and constriction geometries. Davies *et al.* developed a microfluidic filtration device to isolate extracellular vesicles directly from whole blood using nanoscale membrane filters integrated within a microfluidic channel, enabling extracellular vesicle enrichment without ultracentrifugation while preserving vesicle integrity (Fig. 2A).[48] This work demonstrated that on-chip filtration could achieve clinically relevant extracellular vesicle recovery while reducing processing time and sample handling complexity.

To address clogging and throughput limitations inherent to static filtration, more advanced architectures have introduced dynamic or distributed filtration strategies. Li *et al.* created a cascaded microfluidic circuit design generates pulsatile flow conditions that allow continuous extracellular vesicle filtration from whole blood to reduce membrane fouling while preserving high recovery efficiency (Fig. 2B).[49] By distributing filtration across multiple stages and introducing oscillatory flow, this platform enabled robust extracellular vesicle isolation suitable for early cancer diagnostics from unprocessed clinical samples.

Beyond membrane-based filtration, nanofluidic architectures have been used to perform size-selective separation with higher precision and tunability. Huang *et al.* introduced nanoscale deterministic lateral displacement (DLD) arrays capable of separating microspheres with a size resolution of 10 nm (Fig. 2C).[50] Wunsch *et al.* extended this technology for the isolation of exosomes and colloidal particles down to 20 nm based solely on size-dependent transport trajectories.[51] This work extended DLD operation into the true nanoscale regime, demonstrating that carefully engineered pillar geometries can deterministically fractionate vesicles that are inaccessible to conventional microfluidic sieving approaches.

Related lattice-based strategies have further expanded the design space for passive, continuous sorting. Yamada *et al.* developed slanted, asymmetric microfluidic lattice structures that act as size-selective sieves, where particle trajectories are biased by repeated interactions with angled obstacles (Fig. 2D).[52] This approach enables continuous particle and cell sorting without external fields, offering a simple and robust route to size-based fractionation that is compatible with high-throughput operation.

Geometry- and confinement-based microfluidics has also been extended to multiparameter analysis rather than separation alone. Ko *et al.* developed a nanofluidic device for continuous, multiparameter quality assurance of biologics, simultaneously probing size, aggregation state, and transport behavior under flow (Fig. 2E).[53] By integrating nanoscale confinement with electrical and hydrodynamic measurements, this platform enables real-time assessment of biologic heterogeneity without labeling, highlighting the utility of nanofluidics for biomanufacturing and quality control applications.

Beyond size-selective transport, geometric confinement has been leveraged to interrogate cellular mechanical phenotypes. Liu *et al.* developed an integrated microfluidic chip that combines size-based enrichment with deformability analysis to isolate and mechanically profile circulating tumor cells from blood (Fig. 2F).[54] In this platform, controlled constrictions impose well-defined mechanical stresses, allowing malignant cells to be distinguished based on coupled size and deformability signatures. This approach illustrates how geometry-driven microfluidics can bridge passive enrichment with functional phenotyping within a single, continuous workflow.

Collectively, these approaches demonstrate how geometry- and confinement-based passive microfluidic architectures—including filtration, lattice-based sieving, deterministic lateral displacement, and nanoscale confinement—enable label-free, continuous separation and analysis across a broad range of length scales. When integrated upstream of biosensing or molecular assays, these approaches reduce sample complexity while preserving native particle and cell states, providing a robust and scalable alternative to affinity-based or externally actuated microfluidic strategies.

2.2 Active field-driven microfluidic operations

Active field-driven microfluidic operations use externally applied acoustic, electric, or optical fields to manipulate particles, cells, or analytes with high spatial and temporal control. Unlike passive approaches based on fixed geometries, these methods enable dynamic, reconfigurable operation and precise positioning or trapping, but at the cost of increased system complexity, power requirements, and potential field-induced sample perturbations. Despite these trade-offs, active strategies uniquely enable localized analyte concentration and integration with downstream sensing modalities, making them well suited for applications where control and adaptability are prioritized over simplicity and throughput.

2.2.1 Acoustofluidics. Acoustofluidics, the fusion of acoustics with microfluidics, has gained traction for handling cells, particles, and fluids in various biomedical applications.[55–63] In contrast to optical, magnetic, or

electrical manipulation techniques, acoustofluidics is inherently label-free and non-contact, minimizing chemical modification and reducing the risk of phototoxicity, Joule heating, or electrochemical side effects. As a result, acoustic methods are widely regarded as highly biocompatible and are well suited for handling fragile biological specimens, including primary cells, circulating tumor cells, extracellular vesicles, and biomacromolecules.

Acoustic manipulation in microfluidic environments arises primarily from two physical mechanisms: acoustic radiation forces, generated by the scattering of acoustic waves from particles with acoustic impedance mismatches relative to the surrounding medium, and acoustic streaming, which results from viscous dissipation of high-amplitude acoustic oscillations within fluids.[64] The relative contribution of these effects depends on particle size, acoustic wavelength, and device geometry, enabling tunable manipulation across a remarkably wide length scale—from nanoscale objects such as proteins and exosomes to millimeter- and even centimeter-scale particles and droplets such as *C. elegans* and zebra fish.

A key advantage of acoustofluidic systems is their real-time tunability. By modulating acoustic frequency, phase, amplitude, and duty cycle, users can dynamically adjust force magnitude, directionality, and spatial patterning without altering device geometry. This confers a favorable power-biocompatibility balance, in which effective manipulation is achieved at relatively low power densities while maintaining high particle and cell viability, structural integrity, and native biological function. In practice, this balance enables prolonged operation and high-throughput processing without compromising sample integrity, making acoustofluidics particularly attractive for clinical and translational workflows.

Acoustofluidic manipulation is also broadly compatible with diverse sample media. Because acoustic waves couple efficiently to most condensed phases, these systems operate robustly across aqueous buffers, viscous biological fluids, and complex clinical specimens, including saliva, urine, plasma, and whole blood. Moreover, acoustic actuation is compatible with a wide range of substrate materials, such as glass, silicon, and polymers, facilitating integration with existing microfabrication and lab-on-a-chip platforms.

From a practical standpoint, acoustofluidic systems are comparatively cost-effective and scalable. The required hardware—often consisting of piezoelectric transducers and simple radio-frequency driving electronics—is similar in cost and complexity to that of standard optical imaging setups, yet offers substantially higher throughput and force generation. These attributes, combined with gentle operation and broad applicability, have positioned acoustofluidics as a leading active microfluidic modality for applications including cell sorting, biomarker enrichment, molecular diagnostics, drug delivery, and high-throughput screening (Fig. 3A).[65]

In the past 20 years, acoustofluidic devices have emerged as versatile tools in microfluidics, enabling precise manipulation of particles for functions such as separation, trapping, concentration, and sorting.[66–75] For example, Li

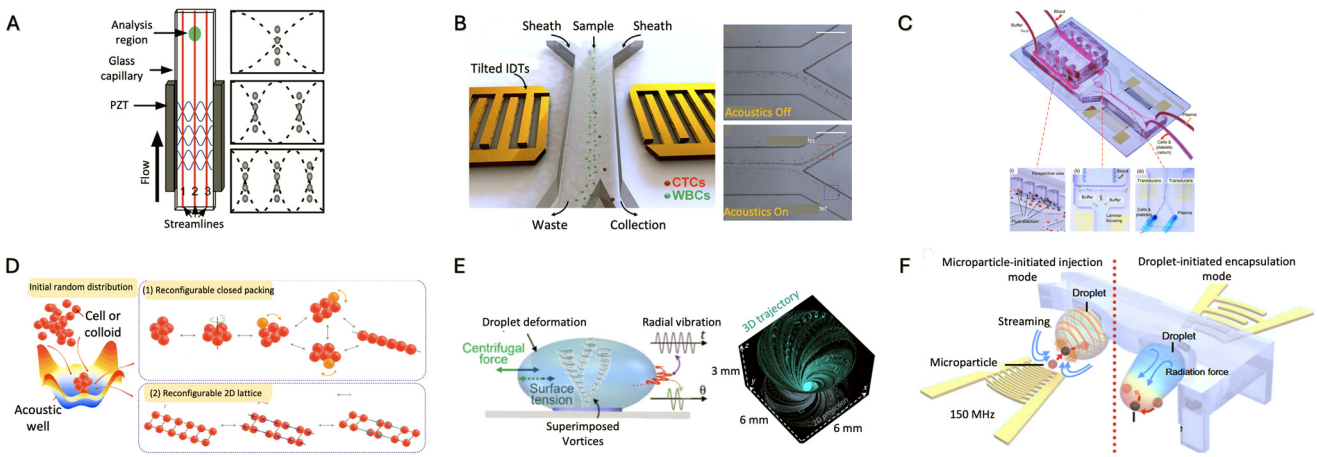

Fig. 3 Acoustofluidics for particle and fluid manipulation. (A) Multinode acoustic focusing for parallel flow cytometry affords simultaneous alignment of multiple particle streams in a capillary channel. Streamlines illustrate acoustic pressure nodes that guide particle movement, adapted from ref. 65 with permission from American Chemical Society, M. E. Piyasena *et al.*, *Analytical Chemistry*, 2012, **84**, 1831–1839, copyright 2012. (B) Acoustofluidic platform for label-free separation of circulating tumor cells from blood, adapted from ref. 76 with permission from National Academy of Sciences, P. Li *et al.*, *Proceedings of the National Academy of Sciences*, 2015, **112**, 4970–4975, copyright 2015. (C) Acoustofluidic therapeutic apheresis system for selective removal of pathogenic substances in whole blood, adapted from ref. 77 with permission from Springer Nature, M. Wu *et al.*, *Nature Communications*, 2024, **15**, 6854, copyright 2024. (D) Harmonic acoustic tweezers generate dynamic and selective manipulation of particles into programmable lattice arrangements, adapted from ref. 80 with permission from Springer Nature, S. Yang *et al.*, *Nature Materials*, 2022, **21**, 540–546, copyright 2022. (E) Acoustofluidic spin control leverages droplet vibrations to achieve 3D rotation and trajectory control of suspended particles, adapted from ref. 83 with permission from American Association for the Advancement of Science, C. Chen *et al.*, *Science Advances*, 2025, **11**, eadx0269, copyright 2025. (F) An acoustofluidic embedding platform for rapid multiphase microparticle injection and droplet encapsulation for bioassays, adapted from ref. 89 with permission from Springer Nature, R. Zhong *et al.*, *Nature Communications*, 2025, **16**, 4144, copyright 2025.

et al. designed a tilted-angle standing surface acoustic wave (SAW) microfluidic device for the high-throughput separation of circulating tumor cells (CTCs) from peripheral blood (Fig. 3B).[76] In this system, the acoustic radiation force pushes particles laterally as they flow through the channel. Since the magnitude of this force scales with particle volume, larger CTCs undergo greater displacement than smaller blood cells. This physical principle enabled the efficient separation of cancer cells from red and white blood cells without the need for labels, achieving a recovery rate exceeding 83% for spiked cancer cell lines at clinically relevant concentrations (~223c100 cells per mL) and successfully isolating viable CTCs from blood samples of breast cancer patients. Building on these capabilities, an acoustofluidic therapeutic apheresis system was developed that continuously processes whole blood at small volumes while maintaining exceptionally low extracorporeal circulation. This design overcomes a key limitation of conventional apheresis technologies, particularly for newborn patients and small animal models, where total blood volume is severely constrained.[77] Operating in a fully label-free manner, the platform enables selective removal of pathogenic factors directly from patient samples and has demonstrated clear therapeutic benefit in preclinical disease models (Fig. 3C).

Beyond conventional SAW and bulk acoustic wave devices, alternative acoustic wave configurations have been developed to further enhance the efficiency and versatility of particle manipulation. Devendran *et al.* developed a diffraction-based acoustic focusing and separation system in which SAWs propagate perpendicular to the flow direction, enabling continuous, label-free particle focusing and separation through laterally patterned acoustic fields.[78] This setup enables periodic rows of trapped particles to form across the width of the channel, similar to traditional standing wave configurations. The primary advantage of this technique is that the acoustic wave energy is distributed across the entire fluid domain, thereby maximizing particle exposure to acoustic forces. By distributing acoustic energy across the full channel cross-section, this approach addresses a common limitation of localized field based methods, in which only a fraction of the sample experiences effective actuation.

Complementing separation, acoustofluidics can also achieve selective particle manipulation. Collins *et al.* applied acoustic streaming vortices within microchannels to capture larger particles while allowing smaller ones to pass through.[79] Since acoustic forces scale with volume, larger cancer cells experience stronger acoustic interactions and are more likely to remain trapped within the vortices. At the same time, the fluid flow carries away smaller blood components. This selective retention mechanism provides an alternative to deterministic size-cutoff methods,[50] offering tunable selectivity without introducing physical barriers that may clog or damage fragile samples.

For single particle manipulation and selective particle assembly, Yang *et al.* introduced a harmonic acoustics platform that utilizes modulated acoustic trapping positions to reversibly assemble colloidal crystals or cells by dynamically switching between trapping and focusing modes (Fig. 3D).[80] Such technology overcomes typical throughput and biocompatibility limitations in studying cell–cell or cell–material interactions by offering dynamic, reversible control over assembly states without physical confinement, surface immobilization, or sustained exposure to high-intensity fields. Xu *et al.* introduced ring-resonator acoustofluidic tweezers that form a high-Q standing wave confined to a micro-ring. When driven at the structure's eigenfrequency, acoustic energy is concentrated around the ring, promoting power-efficient trapping, transport, and mixing of microparticles.[81] Such localized resonant architectures illustrate how acoustofluidic platforms can balance field strength and power efficiency, a tradeoff that becomes increasingly important for portable or integrated systems.

Gu *et al.* generated SAW-driven acoustic streaming within a sessile droplet to create rotational flow patterns that concentrate nanoparticles at the droplet center.[82] This approach operates in an open droplet format rather than enclosed microchannels, it eliminates the need for external pumps or complex fluidic interfacing, simplifying sample loading and improving accessibility for rapid or point-of-use assays. Building on in-droplet manipulation, Chen *et al.* demonstrated acoustic spin control, using rotational acoustic fields to orient and position particles in three-dimensional space within sessile droplets (Fig. 3E).[83]

More recently, acoustofluidic platforms have been applied to mechanobiology, extending beyond particle handling to modulate cellular function directly. To enable mechanical modulation of cells, He *et al.* used micropatterned pillars and an acoustic transducer to deliver controlled nanoscale oscillations to immune cell monolayers for extended durations.[84] This capability distinguishes acoustofluidics from other field-driven methods by enabling sustained mechanical stimulation without direct contact or potentially adverse photothermal or electrical effects. Kim *et al.* developed a microreactor using SAWs to stimulate NK immune cells *via* acoustic streaming dynamically; tuning power and duty cycle avoided cell damage, while enhancement of Ca^{2+} influx, lysosomal protein expression, and tumor cytotoxicity demonstrated functional immune modulation.[85]

Droplet acoustofluidics combines the precision of acoustic wave manipulation with the versatility of flow-based droplet microfluidics, warranting sophisticated control over droplet generation, sorting, and manipulation.[87] Park *et al.* demonstrated the acoustofluidic generation of droplets with tunable chemical concentrations by modulating the amplitude of applied acoustic waves.[86] For droplet sorting, an acoustofluidic sorter was developed using single-phase focused transducers to achieve high-throughput cell-laden droplet sorting at rates exceeding 1000 droplets per second with purities above 99% and cell viability greater than 93%.[88] Zhong *et al.* developed an acoustofluidic embedding module

that utilizes focused acoustic fields to inject multiple types of microparticles into pre-formed droplets in a single step, enabling the controlled co-localization of different particle types for downstream assays (Fig. 3F).[89] Acoustofluidic picoinjection has been developed to deliver high-precision picoliter volume reagents into droplets.[90] This device uses focused acoustic waves to control droplet composition and reagent injections, offering a versatile tool for applications such as single-cell genetic analysis, precise drug delivery testing, and nanoparticle functionalization.

2.2.2 Dielectrophoretic microfluidics. Dielectrophoresis (DEP) is an electrokinetic technique that manipulates and separates particles, cells, and other biological entities based on their dielectric properties.[91,92] This method utilizes the interaction between an irregular electric field and the dielectric properties of particles to warrant exact control over the positioning and sorting of nanoscale and microscale objects. Polarizable particles align with the field through positive dielectrophoresis. In contrast, less polarizable ones oppose the field *via* negative dielectrophoresis, allowing for the precise manipulation of both non-biological and biological particles based on their relative permittivity compared to the fluid medium (Fig. 4A).[93–95] Within microfluidic systems, DEP occupies a distinct niche by enabling selective manipulation based on electrical phenotype rather than size, shape, or affinity interactions, providing access to biophysical contrast mechanisms that are not accessible through passive hydrodynamic or immunoaffinity-based approaches.

This principle has been implemented in various applications for cell manipulation, such as massively parallel cell pairing and fusion using field constriction by a micro-orifice array sheet (Fig. 4B).[96] This system facilitates the simultaneous fusion of ~6000 cells, with a high fusion yield of over 80%. For cell-type-specific manipulation, Li *et al.* generated a selective capture of CTCs using wireless electrode arrays (Fig. 4C). These tumor cells exhibit distinct dielectric properties compared to normal cells and can be captured and visualized through fluorescence imaging.[97] This capability is particularly valuable in heterogeneous clinical samples, where electrically defined phenotypes can enable discrimination between cell populations that overlap in size, a regime where many microfluidic strategies become less effective.

DEP has also been extensively employed for particle separation. Choi *et al.* utilized trapezoidal electrode arrays for negative DEP-based separation of particles based on varying dielectrophoretic velocities (Fig. 4D).[98] Zhao *et al.* extended separation to the nanoscale by developing a DEP device that surrounds a microchannel with a nano-orifice of varying sizes, generating a robust, non-uniform electric field to separate nanoparticles of different sizes.[99] In another example, Viefhues *et al.* demonstrated the separation of polystyrene nanoparticles with diameters of 20 and 100 nm, achieving efficiencies of 85–100%.[100]

DEP has proven highly effective for concentrating and trapping particles into localized regions of high electric field

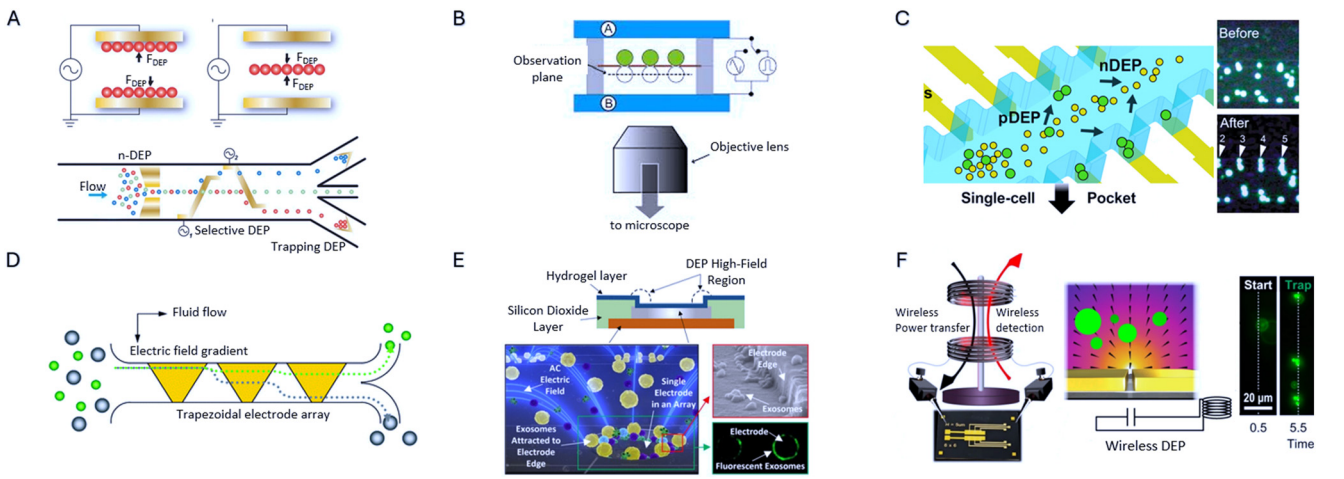

Fig. 4 Integrated dielectrophoretic microfluidics. (A) In inhomogeneous electric fields, polarizable particles align with field (pDEP), less polarizable ones oppose it (nDEP), adapted from ref. 95 with permission from Springer, D. R. Gossett *et al.*, *Analytical and Bioanalytical Chemistry*, 2010, **397**, 3249–3267, copyright 2010. (B) Dielectrophoresis-assisted massively parallel cell pairing and fusion using field constriction created by a micro-orifice array sheet, adapted from ref. 96 with permission from Wiley, Y. Kimura *et al.*, *Electrophoresis*, 2011, **32**, 2496–2501, copyright 2011. (C) High-throughput selective capture of single circulating tumor cells at a wireless electrode array by dielectrophoresis, adapted from ref. 97 with permission from American Chemical Society, M. Li *et al.*, *Journal of the American Chemical Society*, 2017, **139**, 8950–8959, copyright 2017. (D) Trapezoidal electrode arrays enabling dielectrophoretic separation of particles based on differences in polarizability, adapted from ref. 98 with permission from Royal Society of Chemistry, S. Choi *et al.*, *Lab on a Chip*, 2005, **5**, 1161–1167, copyright 2005. (E) Exosomes are attracted to edges of microelectrodes under AC electric field, enabling rapid isolation and fluorescence detection of exosomal biomarkers from plasma, adapted from ref. 102 with permission from American Chemical Society, S. D. Ibsen *et al.*, *ACS Nano*, 2017, **11**, 6641–6651, copyright 2017. (F) Wireless dielectrophoresis trapping and remote impedance sensing through resonant wireless power transfer, adapted from ref. 106 with permission from Springer Nature, C. T. Ertsgaard *et al.*, *Nature Communications*, 2023, **14**, 103, copyright 2023.

strength. This capability is advantageous for applications requiring high particle density, such as biosensing, diagnostics, and particle characterization. For instance, Han *et al.* used alternating current dielectrophoresis and electro-osmosis to augment viruses and proteins, flooding microelectrode high-field regions with nanometer-sized MS2 viruses and troponin I antibodies.[101] Similarly, DEP-driven methods facilitate the rapid concentration of extracellular vesicles from plasma (Fig. 4E).[102] Under an AC electric field, extracellular vesicles are attracted to the edges of microelectrodes, where the DEP high-field region is strongest, allowing for fluorescence detection of critical biomarkers. By spatially concentrating analytes directly at sensing interfaces, DEP facilitated enrichment reduces reliance on long incubation times or bulk amplification steps, strengthening integration with downstream electrical and optical biosensors.

In addition to concentration, DEP has been widely employed for spatial patterning of particles on microfluidic substrates. For example, Faraghat *et al.* used DEP to pattern various cell types into specific arrays depending on their unique interaction with the electric field, facilitating downstream analysis of cell behavior and interactions.[103] Chen *et al.* patterned exosomes along high-field electrodes, enabling subsequent lysis for downstream protein and RNA analysis.[104] Kimbrough *et al.* demonstrated the DEP alignment of carbon nanotubes for wafer-scale fabrication.[105] Such spatial control enables the deterministic organization of biological and nanomaterial components, supporting applications that require precise positioning rather than bulk separation or enrichment.

Recent advances have introduced wireless DEP systems that remove the need for direct electrical connections. Using resonant wireless power transfer, Ertsgaard *et al.* demonstrated wireless DEP trapping capable of concurrent particle capture and electrical characterization (Fig. 4F).[106] Wireless DEP has also been applied to open microfluidics architectures powered through resonant wireless power transfer, expanding DEP to more flexible device architecture for portable biosensing applications.[107] These wireless implementations address longstanding challenges associated with electrode fouling, complex wiring, and system integration, improving the viability of DEP platforms for portable and point-of-care diagnostic applications.

2.2.3 Optofluidics. Optofluidics refers to the integration of optical fields with microfluidic systems to manipulate light, fluids, and particles within microscale environments.[108,109] Unlike traditional optical systems, which rely on static solid-state components, optofluidics takes advantage of the reconfigurable nature of liquids to achieve tunable optical responses inside microchannels. At the same time, light provides a powerful, non-contact means to actuate flows, trap particles, or modulate chemical environments.

One of the primary advantages of optofluidics lies in its ability to induce flow and optical modulation without physical contact, embedded electrodes, or complex channel geometries. Liu *et al.* demonstrated optofluidic control using photothermal nanoparticles, where localized laser heating

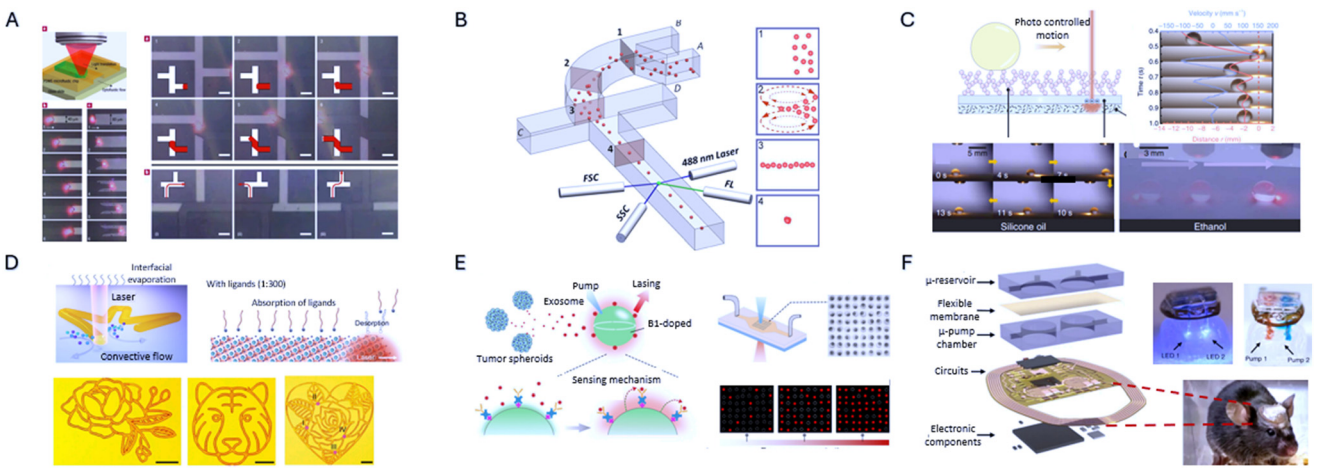

Fig. 5 Optofluidics for light-driven manipulation and sensing. (A) Optofluidic control using photothermal nanoparticles for light-driven fluid manipulation, adapted from ref. 110 with permission from Springer Nature, G. L. Liu *et al.*, *Nature Materials*, 2006, **5**, 27–32, copyright 2006. (B) On-chip flow cytometry chip integrating single-layer 3D hydrodynamic focusing *via* microfluidic drifting with fiber-optic detection, adapted from ref. 112 with permission from AIP Publishing, X. Mao *et al.*, *Biomicrofluidics*, 2012, **6**, copyright 2012. (C) Photopyroelectric microfluidics leverages light-induced pyroelectric effects for contactless droplet actuation and mixing, adapted from ref. 114 with permission from American Association for the Advancement of Science, W. Li *et al.*, *Science Advances*, 2020, **6**, eabc1693, copyright 2020. (D) Optofluidic crystallography directs the growth of single-crystalline halide perovskites with high spatial resolution, adapted from ref. 115 with permission from Springer Nature, X.-G. Chen *et al.*, *Nature Communications*, 2024, **15**, 3677, copyright 2024. (E) Digital lasing biochip detects tumor-derived exosomes by integrating optical resonators with fluidic channels, adapted from ref. 116 with permission from American Chemical Society, T. Zhou *et al.*, *Analytical Chemistry*, 2025, **97**, 5605–5611, copyright 2025. (F) Wireless multilayer optofluidic microsystems allow real-time programmable optogenetics and photopharmacology *in vivo*, adapted from ref. 119 with permission from Springer Nature, Y. Wu *et al.*, *Nature Communications*, 2022, **13**, 5571, copyright 2022.

induced fluid flow and particle transport, providing one of the first clear examples of optical actuation in a microfluidic environment (Fig. 5A).[110] Mao *et al.* described a hydrodynamically tunable optofluidic cylindrical microlens that demonstrated how microfluidics could be used to dynamically reshape optical fields in real time, enabling adjustable focusing and on-chip beam steering.[111] Mao *et al.* showed that by inducing controlled Dean flows in a curved microchannel, their microfluidic drifting approach achieves on-chip three-dimensional hydrodynamic focusing in a single planar device, allowing integrated multiparametric optical detection without external sheath flows (Fig. 5B).[112] These studies highlight how optofluidics enables optical functionality that would otherwise require bulky or complex architectures, emphasizing its utility for compact systems.

Beyond hybrid optical and flow-based fluidic systems, fully integrated optofluidic actuation strategies have emerged as a means to eliminate external pumps, pressure sources, and electrical interfaces. A recent demonstration used a photoresponsive splay-bend strip to generate a traveling peristaltic wave under patterned illumination, achieving all optical pumping without the need for pressure sources or electrodes.[113] Similarly, Li *et al.* demonstrated photopyroelectric microfluidics, where modulated light can be converted into localized pyroelectric fields on a substrate, producing surface charges that actuate droplets with millisecond response times (Fig. 5C).[114] This approach enables versatile digital microfluidics operations such as transport, merging, and concentration. Chen *et al.* utilized localized laser illumination to generate controlled thermal and concentration gradients in precursor flows, thereby directing the nucleation and growth of single-crystalline halide perovskites within microchannels (Fig. 5D).[115] By eliminating hardware such as external pumps, electrodes, or moving parts, these optically driven approaches offer operational simplicity while retaining reconfigurability.

In addition to biosample actuation, optofluidics enables sensing architectures in which optical readout is intrinsically coupled to microfluidic confinement and analyte interaction. Zhou *et al.* created a digital lasing biochip that integrated microfluidic capture arrays with optical microcavities, where exosome binding events altered the cavity environment to switch lasing on or off, producing a digital optical output for extracellular vesicle quantification (Fig. 5E).[116] Jahani *et al.* developed an optofluidic biosensor using dielectric metasurfaces patterned inside microchannels, where vesicle binding produced shifts in optical resonance that could be reconstructed from standard camera images, eliminating the need for spectrometers.[117]

The ability to deliver light and fluids in a wireless, spatially controlled manner has also enabled optofluidic systems to move beyond *in vitro* platforms and into *in vivo* applications. One early wireless neural probe combined microfluidic drug delivery channels with μ-LEDs, for simultaneous infusion of pharmacological agents and optical neural stimulation.[118] Wu *et al.* recently introduced a wireless multilateral optofluidic microsystem that enables optogenetic stimulation and photopharmacological control in freely moving animals by combining programmable microfluidic drug delivery with integrated micro-LEDs (Fig. 5F).[119]

2.2.4 Digital microfluidics. Digital microfluidics represents a fundamentally different paradigm from continuous-flow microfluidics, enabling discrete, programmable manipulation of individual droplets on planar electrode arrays rather than through enclosed channels. Digital microfluidic platforms can transport, split, merge, and mix droplets with high spatial and temporal control, allowing reconfigurable workflows that are not constrained by fixed channel geometries. This architecture enables highly modular assay design, where sample preparation, reaction, and detection steps can be dynamically rearranged within a single device, making digital microfluidics particularly attractive for automated and multiplexed bioanalytical applications.

Most digital microfluidics systems operate using electrowetting-on-dielectric (EWOD), where an applied electric potential locally modulates surface wettability, allowing droplets to be transported, merged, split, and mixed across patterned electrode arrays, as shown in Fig. 6A.[120–122] Pollack *et al.* demonstrated reliable droplet actuation, merging, and splitting on planar electrode arrays, establishing EWOD as a practical platform for discrete fluid handling. Abdelgawad *et al.* extended EWOD operation beyond planar geometries by enabling all-terrain droplet actuation across inclined, vertical, and inverted surfaces, demonstrating compatibility with heterogeneous device architectures.[123] Chatterjee *et al.* showed that EWOD can manipulate droplets containing organic solvents and surfactants, enabling chemical reactions and multiphase processing within digital microfluidic platforms.[124]

While EWOD-based digital microfluidics offers exceptional flexibility, its reliance on direct electrical actuation introduces practical constraints, including dielectric breakdown, electrolysis, surface fouling, and limited compatibility with certain biological samples and solvents. Zhang *et al.* developed digital acoustofluidics, extending the concept of digital microfluidics by using reconfigurable acoustic fields, rather than surface bound electrodes, to manipulate droplets in a fully contactless manner (Fig. 6B).[125] In this work, programmable surface acoustic waves generate pressure nodes and streaming flows that translate, merge, split, and pattern droplets without relying on wettability contrasts or dielectric layers. This approach is particularly useful because it eliminates surface fouling, contact angle hysteresis, and dielectric breakdown issues inherent to EWOD, while enabling robust droplet control across a wide range of fluids, including biofouling-prone and highly conductive samples.

Digital microfluidics has been widely adopted for nucleic acid based diagnostics, where precise reagent handling, contamination control, and thermal cycling are essential. In one early demonstration, Chang *et al.* demonstrated PCR on a digital microfluidics platform by programmatically dispensing, merging, mixing, and thermally cycling droplets

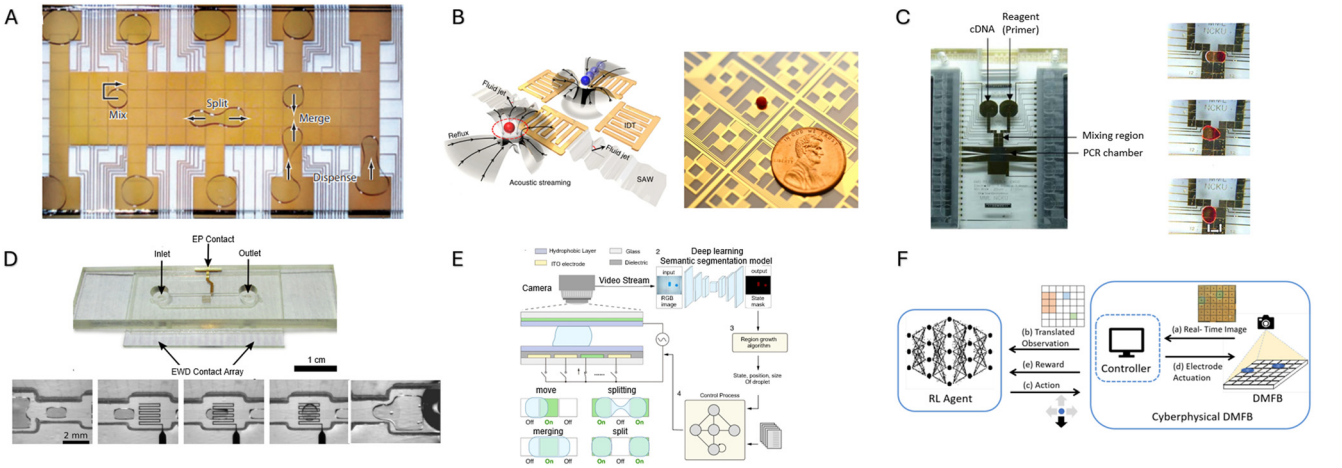

Fig. 6 Digital microfluidics platforms and applications. (A) Representative digital microfluidic device architecture illustrating electrode-based droplet manipulation through electrowetting for programmable liquid handling, adapted from ref. 120 with permission from Annual Reviews, K. Choi *et al.*, *Annual Review of Analytical Chemistry*, 2012, **5**, 413–440, copyright 2012; (B) digital acoustofluidics platform enabling contactless and programmable droplet actuation through acoustic wave-mediated forces, adapted from ref. 125 with permission from Springer Nature, S. P. Zhang *et al.*, *Nature Communications*, 2018, **9**, 2928, copyright 2018. (C) Integrated polymerase chain reaction (PCR) chip implemented on a digital microfluidics platform, incorporating droplet dispensing, mixing, and thermal cycling for on-chip amplification, adapted from ref. 126 with permission from Springer, Y.-H. Chang *et al.*, *Biomedical Microdevices*, 2006, **8**, 215–225, copyright 2006. (D) Scalable device for automated microbial electroporation using digital microfluidics, enabling precise control of droplet-based electrical manipulation, adapted from ref. 130 with permission from American Chemical Society, A. C. Madison *et al.*, *ACS Synthetic Biology*, 2017, **6**, 1701–1709, copyright 2017. (E) AI-assisted digital microfluidic system enabling robust multistate droplet control under fabrication and environmental variability, adapted from ref. 131 with permission from Springer Nature, K. Guo *et al.*, *Microsystems & Nanoengineering*, 2024, **10**, 138, copyright 2024. (F) Reinforcement learning driven digital microfluidic biochip framework enabling dynamic adaptation and closed-loop control of droplet operations, adapted from ref. 132 with permission from Association for Computing Machinery, T.-C. Liang *et al.*, *ACM Transactions on Design Automation of Electronic Systems*, 2024, **29**, 1–24, copyright 2024.

containing PCR reagents on-chip, with integrated heaters used to perform denaturation, annealing, and extension steps (Fig. 6C).[126] This work established the feasibility of executing complete PCR reactions using electrically actuated droplets, without continuous flow channels or external pumping. Subsequent work by Sista *et al.* advanced this concept by introducing droplet shuttling between spatially separated temperature zones, leveraging rapid heat transfer to reduce amplification times and enable faster real-time PCR.[127]

In addition to amplification, the programmability of digital microfluidics makes it well suited for sequencing workflows that require repeated reagent exchange and washing steps. Welch *et al.* extended digital microfluidics to pyrosequencing by automating nucleotide addition, enzymatic reactions, and bead-based washing within droplets, demonstrating sequencing-by-synthesis on a digital microfluidic platform.[128] Building beyond targeted readout, Zhang *et al.* extended digital microfluidics to next-generation sequencing library preparation with the Cilo-seq platform, integrating single-cell isolation through sequencer-ready library construction on chip.[129] This transition highlights how digital microfluidics evolved from controlling individual sequencing reactions to supporting scalable, high-complexity workflows required for single-cell transcriptomics.

Digital microfluidics has also been extended beyond biochemical assays to enable programmable cellular manipulation Madison *et al.* created a scalable digital microfluidics device to perform electroporation of microbial cells by precisely positioning droplets containing cells and DNA between electrode pairs that generate transient, high-intensity electric fields, eliminating manual cuvette based workflows with improved throughput and consistency (Fig. 6D).[130] This approach highlights how digital microfluidics can integrate fluid handling and electrical actuation within the same electrode architecture, providing a flexible route toward automated synthetic biology workflows where precise timing, field strength, and reagent exposure are critical.

Recent efforts have begun to leverage machine learning to enhance the robustness and autonomy of digital microfluidic control. Guo *et al.* developed an artificial intelligence-assisted digital microfluidics system in which a neural network was trained to recognize droplet states and transitions in real time, enabling reliable multistate droplet operations (*e.g.*, transport, splitting, merging) under variabilities such as slight fabrication defects or environmental fluctuations that would challenge traditional rule-based control (Fig. 6E).[131] Complementing this, Liang *et al.* applied deep reinforcement learning to digital microfluidic biochips, allowing the system to autonomously learn actuation policies that optimize droplet routing and error recovery without explicit programming, thereby adapting to new tasks and fault conditions while improving control efficiency (Fig. 6F).[132]

Despite these advantages, digital microfluidics systems face important design constraints that influence their applicability. Reliable operation depends critically on surface coatings, dielectric stability, and electrode patterning, with biofouling and evaporation posing challenges for long-duration assays. Electrical interfacing and high-voltage actuation requirements can complicate system integration, particularly for portable or point-of-care applications. Nevertheless, continued advances in materials, packaging, and intelligent control are steadily improving robustness and manufacturability.

Collectively, digital microfluidics occupies a unique niche within the microfluidics ecosystem: it excels when assay flexibility, programmability, and automation are prioritized over raw throughput. As digital microfluidics continues to integrate alternative actuation modes, embedded sensing, and AI-driven control, it is poised to play an increasingly central role in adaptive diagnostics, automated biology, and closed-loop bioanalytical systems.

2.2.5 Microfluidic immunoassays. Immunoaffinity capture is a ubiquitous technique that leverages the specific binding interactions between antibodies and antigens to isolate and analyze target molecules from complex biological samples.[133,134] In recent years, the integration of immunoaffinity capture into microfluidic platforms has significantly advanced the fields of diagnostics, biomarker discovery, and therapeutic monitoring by providing a means to perform these processes with high efficiency, sensitivity, and speed.[135–137] Microfluidics can process small sample volumes and reduce expensive reagent consumption, saving valuable resources for analyzing rare or precious samples. Moreover, the high surface area-to-volume ratio in microchannels increases antibody and target molecule interactions, improving capture efficiency and detection sensitivity.

Immunoaffinity capture has been utilized extensively to isolate specific cell populations and study cell–cell interactions, enabling advancements in diagnostics, therapeutic development, and fundamental biological research. Dura *et al.* developed a microfluidic system for profiling lymphocyte interactions at the single-cell level, where antibodies are immobilized on the surfaces of microfluidic channels, creating sites for binding to target cell surface markers (Fig. 7A).[138] In contrast to passive enrichment strategies, this platform enables deterministic pairing and interrogation of cells based on defined molecular markers. This platform uses cup-shaped pillars as hydrodynamic traps to position individual lymphocytes within these channels, where antibodies selectively capture the cells through surface antigen–antibody interactions. This binding allows researchers to pair lymphocytes with other cell types for analysis of immune cell interactions and functional responses such as cytokine release or receptor binding. Ronteix *et al.* created a microfluidic assay coupled with probabilistic modeling to quantify T cell cooperation during tumor killing. By capturing and pairing T cells with cancer cells under controlled conditions, the study revealed cooperative behaviors in cytotoxicity that would be difficult to resolve with bulk assays (Fig. 7B).[139]

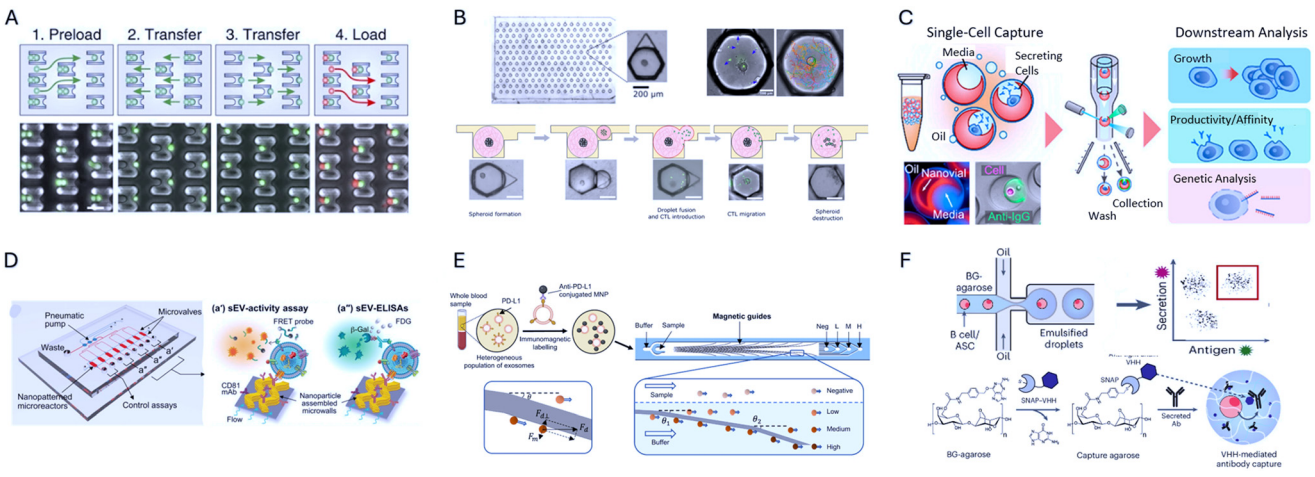

Fig. 7 Microfluidic immunoassays on a chip. (A) Capture and analysis of lymphocyte interactions at the single-cell level, adapted from ref. 138 with permission from Springer Nature, B. Dura *et al.*, *Nature Communications*, 2015, **6**, 5940, copyright 2015. (B) High-resolution microfluidic assay combined with probabilistic modeling reveals cooperative T cell-mediated tumor killing, adapted from ref. 139 with permission from Springer Nature, G. Ronteix *et al.*, *Nature Communications*, 2022, **13**, 3111, copyright 2022. (C) Hydrogel nanovials capture secreted proteins and enrich cells based on antigen-specific binding, adapted from ref. 140 with permission from American Chemical Society, J. De Rutte *et al.*, *ACS Nano*, 2022, **16**, 7242–7257, copyright 2022. (D) Nanopatterned microchips create molecular and functional extracellular vesicle analysis to track tumor progression and metastasis, adapted from ref. 142 with permission from American Association for the Advancement of Science, P. Zhang *et al.*, *Science Translational Medicine*, 2020, **12**, eaaz2878, copyright 2020. (E) Magneto-activated nanoscale cytometry platform for high-throughput profiling of small extracellular vesicles, adapted from ref. 144 with permission from Springer Nature, K. Chen *et al.*, *Nature Communications*, 2023, **14**, 5576, copyright 2023. (F) Microfluidics-enabled fluorescence-activated cell sorting for rapid discovery of monoclonal antibodies from pathogen-specific antibody-secreting cells, adapted from ref. 145 with permission from Springer Nature, K. Fischer *et al.*, *Nature Biotechnology*, 2025, **43**, 960–970, copyright 2025.

Suspendable hydrogel nanovials (Fig. 7C) offer another unique approach for immunoaffinity capture.[140] These nanovials are small, biocompatible microcontainers that are suspended in liquid environments. Antibodies are covalently attached to the hydrogel surfaces to allow for selective binding of target cells based on surface markers. When introduced into a biological sample, the nanovials efficiently capture cells of interest as they bind to the immobilized antibodies. The nanovials can capture thousands of cells in suspension and are ideal for high throughput assays in which screening and profiling on a single-cell level is necessary.

For the ultrasensitive capture and analysis of exosomes, graphene oxide/polydopamine nanostructured coatings on microfluidic chips improve immunoaffinity binding by enhancing both the surface area and the chemical properties of the antibody-immobilized surfaces.[141] Zhang *et al.* introduced a 3D nanopatterned extracellular vesicle capture chip that allowed for detection of MMP14 protease activity using FRET peptides, ELISA quantification of MMP14 protein levels, and measuring total exosome concentration based on total CD63/CD9 markers present in solution (Fig. 7D).[142] Nagase *et al.* utilized thermoresponsive interfaces for temperature-selective capture and release of targeted exosomes by modulating the temperature within the device.[143] Such strategies address a central challenge in exosome analysis, where low antigen density and vesicle heterogeneity limit capture efficiency using conventional planar interfaces.

Immunoaffinity capture is also implemented in flow cytometry based assays. In contrast to conventional flow cytometry, which relies primarily on optical scattering and fluorescence labeling during rapid bulk interrogation, microfluidic immunoaffinity approaches enable upstream molecular selection, enrichment, and stratification of targets prior to analysis. For example, Chen *et al.* implemented antibody-conjugated magnetic nanoparticles and embedded magnetic guides in a microfluidic channel to sort extracellular vesicles into subpopulations according to PD-L1 expression (Fig. 7E).[144] The collected fractions are then profiled by molecular assays, granting high-throughput monitoring of tumor burden and immunotherapy response. Fischer *et al.* combined droplet microfluidics and fluorescence-activated cell sorting with immunocapture of secreted cellular products to identify new monoclonal antibodies against pathogen specific targets (Fig. 7F).[145] By shifting molecular discrimination upstream of detection, these platforms expand flow cytometry from a purely analytical tool into an integrated, preparative workflow capable of handling rare or functionally defined populations.

2.2.6 Microfluidic platforms for dynamic three-dimensional cell culture. Sustaining physiologically relevant 3D tissues is especially challenging, as cells require a constant supply of nutrients, the removal of waste and debris, and often lack the environmental cues, such as shear stresses and oxygen gradients, that strongly influence how cells organize.[146–148] Conventional culture approaches rarely address all these requirements simultaneously, which limits both the functionality and scalability of engineered tissues. Microfluidics overcomes these barriers by embedding perfusable channels, controlling flow, and creating tunable mechanical environments within compact platforms. This direction is increasingly reinforced by policy: on April 29, 2025, NIH announced it is prioritizing human-focused research and reducing animal use.[149,150] As NIH notes, findings from animal studies have often been inconclusive for human diseases such as Alzheimer's and cancer, with translational challenges arising from differences in anatomy, physiology, lifespan, and disease mechanisms. To address these limitations, the National Institutes of Health (NIH) is emphasizing new approach methodologies, including *in vitro* platforms such as organoids and microphysiological systems, which better model human biology, capture patient variability, and improve translational relevance. Against this backdrop, microfluidic 3D culture systems stand out as highly aligned with NIH's priorities, providing human-relevant, patient-specific insight that static cultures or animal models alone cannot achieve.

One of the central challenges in building physiologically relevant organoids and organ-on-chip systems is sustaining cell cultures with functional vasculature and dynamic microenvironments. Early work in this field by Hung *et al.* introduced a 3D dynamic microfluidic cell culture device featuring a stable and uniform microenvironment, which enabled continuous, dynamic cell culturing and offered an affordable and automated alternative to traditional static cell cultures (Fig. 8A).[151] Focusing more specifically on organ-level physiology, Lee *et al.* developed an artificial liver sinusoid with a microfluidic endothelial-like barrier that sustained primary hepatocytes under continuous perfusion, recapitulating nutrient transport and enabling metabolic assays over extended culture periods (Fig. 8B).[152] The nanoliter-scale microbioreactor array, as described by Lee *et al.*, represents an innovative high-throughput microfluidic cell culture platform that provides precise control over the cell environment, making it a valuable tool for exploring and understanding cell systems biology (Fig. 8C).[153] This work presents a microfluidic approach that closely recapitulates the dynamic transport of nutrients and other substances within living tissues, enabling the controlled delivery of soluble factors to cells arranged in an array. Many researchers are actively investigating alternative methods to control the microenvironment, including strategies for positioning individual cells, co-culturing different cell types, patterning the extracellular matrix, and adjusting cell density, all of which help deepen understanding of cellular behavior.

These early contributions highlight the ability of microfluidic systems to sustain and model complex tissues. Recent advances have extended such platforms towards increasingly complex and application-driven studies, producing diverse strategies to vascularize and automate 3D tissues for mechanobiological control and high-throughput testing of sophisticated multicellular interactions. Whisler

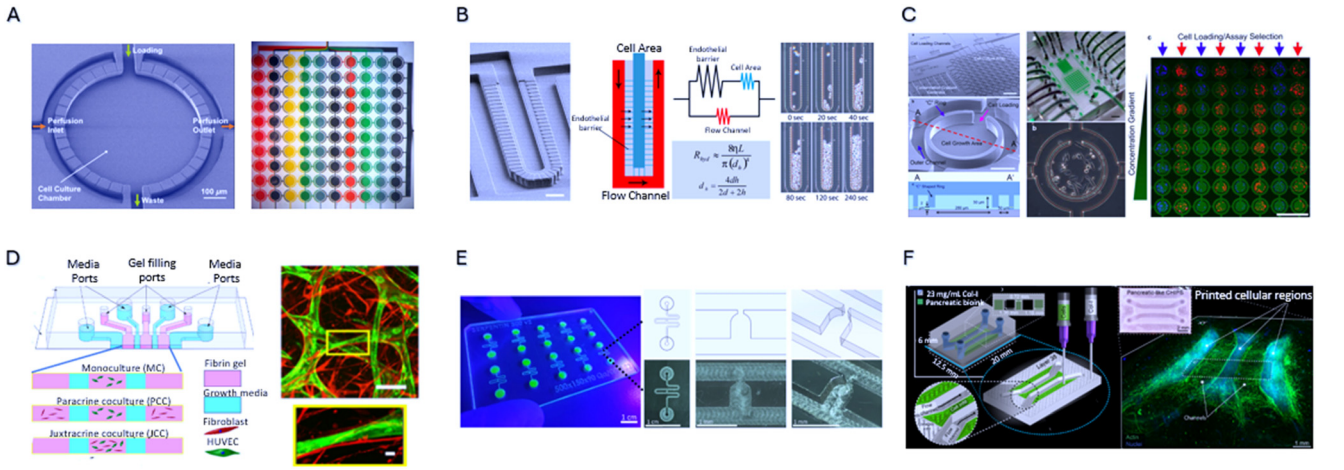

Fig. 8 Dynamic 3D cell culture *via* microfluidics. (A) A high–aspect-ratio microfluidic array providing a stable and uniform microenvironment for mammalian cell culture, adapted from ref. 151 with permission from Royal Society of Chemistry, P. J. Hung *et al.*, *Lab on a Chip*, 2005, **5**, 44–48, copyright 2005. (B) Artificial liver sinusoid with a microfluidic endothelial-like barrier for primary hepatocyte culture, adapted from ref. 152 with permission from Wiley, P. J. Lee *et al.*, *Biotechnology and Bioengineering*, 2007, **97**, 1340–1346, copyright 2007. (C) Nanoliter-scale microbioreactor array enabling high-throughput, quantitative analysis of single-cell growth and microenvironmental responses, adapted from ref. 153 with permission from Wiley, P. J. Lee *et al.*, *Biotechnology and Bioengineering*, 2006, **94**, 5–14, copyright 2006. (D) Microfluidic chip enabling emergent mechanical control of vascular morphogenesis in 3D culture, adapted from ref. 154 with permission from American Association for the Advancement of Science, J. Whisler *et al.*, *Science Advances*, 2023, 9, eadg9781, copyright 2023. (E) Integration of vascularized organoids with controlled biochemical and mechanical cues, adapted from ref. 155 with permission from Springer Nature, C. Quintard *et al.*, *Nature Communications*, 2024, **15**, 1452, copyright 2024. (F) Collagen bioprinted scaffolds with internally perfusable channels for fully biologic tissue systems, adapted from ref. 159 with permission from American Association for the Advancement of Science, D. J. Shiwarski *et al.*, *Science Advances*, 2025, **11**, eadu5905, copyright 2025.

et al. demonstrated how mechanical cues within microchannels can drive vascular morphogenesis, where matrix stiffness and shear stress guided the formation of vascular networks (Fig. 8D).[154] Building on this principle, Quintard *et al.* integrated organoids with microfluidic channels seeded with endothelial cells, allowing long-term vascular coupling and nutrient delivery (Fig. 8E).[155] Lai *et al.* further advanced throughput by developing a multiplexed well-plate that enables the incorporation of organoids into perfusable microcircuits, facilitating parallelized studies of vascularized organoid models.[156]

Microfluidic culture systems have also been adapted for drug testing. Schuster *et al.* applied microfluidics to functional testing by developing an automated instrument for combinatorial drug screening of tumor organoids.[157] This setup enabled precise temporal control of drug dosing and reproduced dynamic concentration profiles that were not achievable in static culture. By integrating tumor organoids with fluidically programmable dosing, the system improved predictive power for preclinical drug screening.

Alongside these functional assays, efforts have been directed toward scaling engineered tissues to clinically relevant dimensions. Grebenyuk *et al.* pushed the upper size scale of microfluidic tissue engineering by creating synthetic 3D soft microfluidics that sustain centimeter-scale constructs with integrated vasculature.[158] In parallel, Shiwarski *et al.* introduced a collagen bioprinting method that fabricates internally flushable scaffolds with high resolution, supporting the engineering of fully biologic tissues (Fig. 8F).[159] Together, these approaches extend microfluidics beyond maintaining organoid-scale cultures toward generating clinically relevant tissues.

3. Microfluidic-based biosensing and molecular analysis

Biosensing and molecular analysis are pivotal techniques in modern biomedical research and diagnostics. These methods allow for detecting and quantifying biological molecules, such as proteins, nucleic acids, and metabolites, which are critical for understanding various physiological and pathological processes.[160] Advances in biosensing technologies have led to the development of highly sensitive, specific, and rapid assays that can be used in various settings, including clinical diagnostics, environmental monitoring, and food safety.[161,162] Biosensors are analytical devices that combine a biological recognition element with a physicochemical transducer to detect the presence or concentration of analytes. The biological recognition element, often an enzyme, antibody, nucleic acid, or receptor, interacts specifically with the target molecule. This interaction generates a signal that the transducer converts into a measurable response, such as an electrical, optical, or thermal signal. In this section, several potent examples of biosensors are introduced (Table 2).

Table 2 Comparative summary of integrated biosensing modalities used in microfluidic platforms, highlighting sensing principles, measured quantities, key advantages, primary limitations, and contexts in which each modality is best suited

Sensing modality	Subtype	What it measures	Key advantages	Primary constraints	When to choose this modality
Electrochemical	Potentiometry	Equilibrium potential changes due to ion activity or molecular binding at electrode interfaces	Label-free operation, low power consumption, compatible with continuous flow	Limited sensitivity for ultra-low abundance targets, drift and fouling	When monitoring ionic species, metabolites, or steady-state binding events
	Amperometric	Current generated by redox reactions	High detection sensitivity, fast response, real-time monitoring	Electrode fouling, mass-transport limitations, requires redox chemistry	When rapid, sensitive detection of electroactive analytes or enzymatic reactions is required
	Impedimetric	Interfacial impedance changes due to binding, cell adhesion, or morphology	Label-free and broad analyte detection, multiplexing capability	Complex signal interpretation, sensitive to nonspecific adsorption	When detecting binding or cellular interactions without electroactive labels
Electrophysiological		Electrical activity, membrane potential, barrier integrity, tissue conductivity	Direct signal readout, high temporal resolution, biologically relevant signals	Limited to electrically active systems, device integration complexity	When probing neural, cardiac, epithelial, or barrier tissue function
Plasmonic	SPR / LSPR	Local refractive index changes near metallic nanostructures	Label-free, high sensitivity, and real-time detection	Sensitive to temperature and bulk refractive index fluctuations	When monitoring biomolecular binding kinetics without labels
	Plasmon-enhanced fluorescence	Fluorescence or vibrational signal amplification	Ultra-high sensitivity, improved signal-to-noise	Requires nanofabrication and optical alignment	When fluorescence sensitivity limits detection or multiplexing is required
Raman/SERS	Label-free	Intrinsic molecular vibrational fingerprints	Direct chemical specificity, rich molecular information	Weak signals, spectral overlap, complex data analysis	When chemical identity is required and samples are sufficiently clean
	Labeled/specific	Raman reporter signals linked to target binding	High sensitivity, strong multiplexing, robust quantification	Requires labeling chemistry, increased assay complexity	When operating in complex biological matrices
Quantum sensors	NV centers, spin defects, quantum plasmonics	Magnetic, thermal, or electronic perturbations at the nanoscale	Extreme detection sensitivity, access to otherwise unmeasurable physical phenomena	Complex instrumentation, lack of detection specificity	When probing nanoscale biophysical or quantum-level biological processes
Distance-based readout	Capillary, bar-chart, density-based	Spatial displacement, flow distance, or volume change	Instrument-free, intuitive readout, low cost	Limited dynamic range, lower resolution	When simplicity, portability, and point-of-care use are prioritized

3.1 Integrated microfluidics with electrochemical sensors

Electrochemical biosensing is an analytical technique that combines the principles of electrochemistry with the specificity of biological recognition elements to detect and quantify various analytes.[12,163,164] This method has garnered significant attention due to its high sensitivity, rapid response, compact size, and ability to perform analysis in diverse environments. Electrochemical biosensors have a wide range of applications, including medical diagnostics, environmental monitoring, food safety, and industrial process control. At the core of an electrochemical biosensor is a biorecognition element, typically enzymes, antibodies, nucleic acids or cells, that specifically interacts with the target analyte leading to a measurable electrochemical signal, used to determine the concentration of the analyte. When integrating with microfluidic systems, electrochemical sensing is particularly attractive because it enables direct electrical transduction at solid–liquid interfaces, is compatible with opaque or optically complex samples, and can be miniaturized without requiring bulky external instrumentation. Electrochemical biosensors typically operate on one of three main electrochemical techniques: potentiometry, amperometry, and impedimetric methods.[165,166]

Potentiometric and voltametric approaches are often well suited for integration with microfluidic sample handling strategies that localize analytes at electrode surfaces. Since

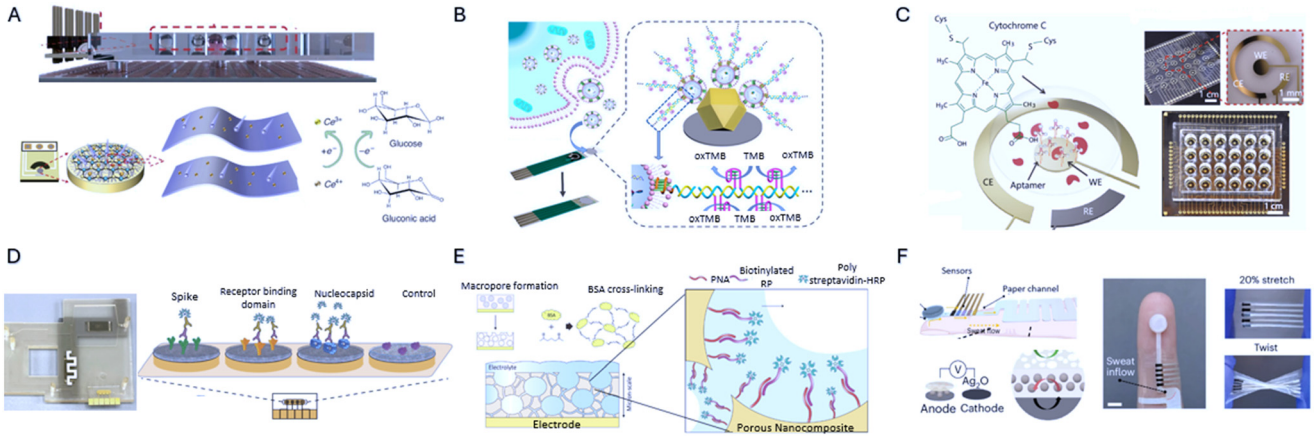

Fig. 9 Integrated microlfuidics with electrochemical sensors. (A) Programmable magnetic digital microfluidic platform integrated with electrochemical detection for versatile biochemical assays, adapted from ref. 168 with permission from Springer Nature, Y. Zhao *et al.*, *Microsystems & Nanoengineering*, 2025, **11**, 82, copyright 2025. (B) Metal–organic framework functionalized paper-based electrochemical biosensor for ultrasensitive exosome detection, adapted from ref. 170 with permission from American Chemical Society, X. Liu *et al.*, *Analytical Chemistry*, 2021, **93**, 11792–11799, copyright 2021. (C) Inkjet-printed electrochemical sensors embedded in a gut bilayer microfluidic chip enable high-performance, real-time monitoring of hypoxia *in vitro*, adapted from ref. 172 with permission from Royal Society of Chemistry, M. A. U. Khalid *et al.*, *Lab on a Chip*, 2022, **22**, 1764–1778, copyright 2022. (D) A lab-on-a-chip platform integrates concurrent electrochemical detection of SARS-CoV-2 RNA and antibodies from saliva and plasma, adapted from ref. 174 with permission from Springer Nature, D. Najjar *et al.*, *Nature Biomedical Engineering*, 2022, **6**, 968–978, copyright 2022. (E) Porous nanocomposite electrode coating providing antifouling performance and enhanced electrochemical signal stability, adapted from ref. 176 with permission from Springer Nature, J.-C. Lee *et al.*, *Nature Communications*, 2024, **15**, 711, copyright 2024. (F) Fingertip-wearable microgrid module enabling autonomous energy management and metabolic biomarker monitoring, adapted from ref. 177 with permission from Springer Nature, S. Ding *et al.*, *Nature Electronics*, 2024, **7**, 788–799, copyright 2024.

these methods rely on equilibrium or near-equilibrium interfacial phenomena, they benefit from microfluidic control over mass transport, residence time, and analyte preconcentration, rather than requiring high current densities or extensive signal amplification. Molazemhosseini *et al.* presented a disposable electrochemical immunosensor for HbA1c detection, employing differential pulse voltammetry as the sensing mechanism.[167] The immunosensor utilizes antibodies immobilized on the working electrode to specifically bind HbA1c. Differential pulse voltammetry works by applying a series of voltage pulses over a linear potential sweep, measuring the changes in current associated with the redox reactions of electroactive species. In this case, the binding of HbA1c alters the electrochemical environment at the electrode surface, leading to a detectable signal. Zhao *et al.* coupled potentiometry with digital microfluidics for programmable droplet positioning on electrode surfaces (Fig. 9A).[168] Salvigni *et al.* redesigned organic electrochemical transistors for potentiometric sensing by maintaining an open circuit potential on the electrode, allowing the device to reach equilibrium without applying external bias. This approach doubled sensitivity, reduced signal drift, and enabled the use of high-impedance materials, resulting in more stable measurements.[169]

Amperometry methods measure the current produced by the oxidation or reduction of an electroactive species at the electrode surface. These approaches are particularly powerful when target recognition can be directly coupled to redox chemistry, enabling rapid, high-sensitivity detection under continuous flow, but they are also more sensitive to electrode fouling and mass-transport limitations than equilibrium-based methods. Liu *et al.* harnessed metal–organic frameworks (MOFs) with a paper-based electrochemical biosensor for the ultrasensitive detection of exosomes (Fig. 9B).[170] MOFs are porous materials with a high surface area and tunable chemical properties, which enhance the immobilization of antibodies or aptamers specific to exosomes. The MOF-functionalized surface increases the density of binding sites for exosomes which triggers a redox reaction that is transduced into a current. This architecture is especially suitable for extracellular vesicles because it compensates for the low intrinsic electrochemical signal of nanoscale vesicles by amplifying surface interactions rather than relying on optical labels or bulk concentration steps.

Peng *et al.* employed amperometry for the sensitive detection of RNA from SARS-CoV-2 virus.[171] The biosensor features probes that hybridize with target RNA molecules and generates an electron transfer signal, making it an ideal choice for monitoring hybridization events. Amperometry has also been integrated into organ-on-chip platforms. For instance, an inkjet-printed electrochemical sensor was embedded within a gut bilayer microfluidic chip to monitor oxygen gradients and detect hypoxia in real time, enabling dynamic tracking of tissue physiology under disease relevant conditions (Fig. 9C).[172] Here, electrochemical sensing enables continuous, spatially resolved measurements that are difficult to achieve with optical reporters in thick or optically scattering tissue constructs.

Impedimetric biosensing offers complementary capabilities in integrated systems by enabling label-free

detection of binding events that do not generate direct redox signals. Impedimetric sensors measure resistance to alternating current, where changes in impedance can indicate the presence of the target analyte. Impedimetric biosensors are advantageous for their ability to detect a wide range of targets, including those that do not produce a direct electrochemical signal.[173] Najjar *et al.* reported a lab-on-a-chip that concurrently detects SARS-CoV-2 RNA and host antibodies. The platform combines isothermal amplification with Cas12a-based electrochemical readout for RNA detection and a sandwich immunoassay with antigen-functionalized electrodes for antibody detection, demonstrating multiplexed electrochemical biosensing in a single device (Fig. 9D).[174] This work illustrates how microfluidic integration enables orthogonal electrochemical modalities to be spatially and electrically isolated on a single chip, supporting multiplexed diagnostics without increasing assay complexity.

Pei *et al.* utilized self-assembled gold nanoparticles for impedimetric and amperometric detection of a prostate cancer biomarker.[175] In this bimodal detection scheme, probe functionalized gold nanoparticles are self-assembled onto the electrode surface for impedimetric detection of prostate cancer biomarkers. Additionally, amperometric detection monitors the redox reactions associated with biomarker binding, providing a dual-mode detection strategy for evaluating binding kinetics.

Despite their advantages, electrochemical biosensors face practical challenges that strongly influence their translational potential, particularly when operated under continuous flow and in complex biological matrices. Among these, surface fouling is often the dominant factor limiting long-term stability, reproducibility, and clinical reliability. To overcome this, Lee *et al.* engineered a micrometer-thick, porous nanocomposite coating that provides exceptional antifouling properties while maintaining high conductivity (Fig. 9E).[176] This material maintained stable electrochemical readouts even in complex biological fluids, directly addressing one of the major bottlenecks in clinical translation. Such materials innovations are critical for moving electrochemical microfluidic systems from short-term demonstrations toward deployable diagnostic platforms.

The compatibility of electrochemical sensing with soft electronics and low-power operation has also facilitated translation beyond benchtop devices. Ding *et al.* demonstrated a fingertip-wearable microgrid system that integrates sweat-powered energy harvesting with on-board electrochemical sensors (Fig. 9F).[177] This self-powered platform measured metabolic biomarkers while autonomously managing energy flow, exemplifying how electrochemical sensing can be embedded into practical, real-world systems.

3.2 Integrated microfluidics with electrophysiological sensors

Electrophysiological biosensors leverage electronic interfaces to record, stimulate, and monitor the electrical activity of biological systems. In contrast to electrochemical sensors that transduce molecular recognition events,

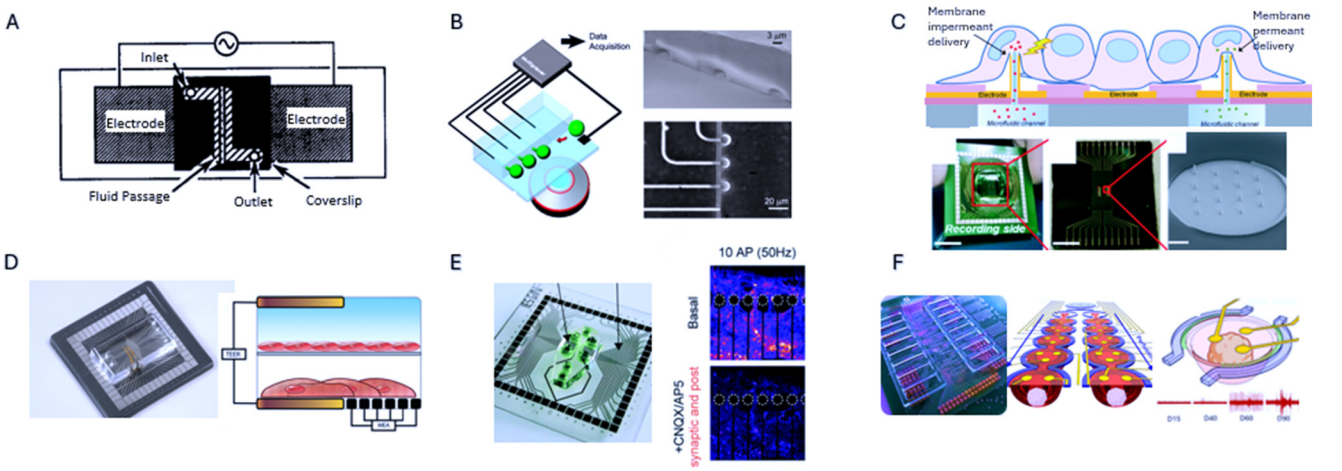

Fig. 10 Integrated microfluidics with electrophysiological sensors. (A) Electrostatic stretch-and-positioning of DNA between electrodes for single-molecule manipulation, adapted from ref. 179 with permission from Institute of Electrical and Electronics Engineers, M. Washizu *et al.*, *IEEE Transactions on Industry Applications*, 2002, **31**, 447–456, copyright 2002. (B) Microfluidic electrophysiology platform for mammalian neuronal recording and stimulation at cellular resolution, adapted from ref. 180 with permission from National Academy of Sciences, C. Ionescu-Zanetti *et al.*, *Proceedings of the National Academy of Sciences*, 2005, **102**, 9112–9117, copyright 2005. (C) Microelectrode array for simultaneous intracellular delivery and intracellular recordings at the single-cell level, adapted from ref. 182 with permission from Royal Society of Chemistry, A. Cerea *et al.*, *Lab on a Chip*, 2018, **18**, 3492–3500, copyright 2018. (D) Organ-on-chip platform with integrated multi-electrode array and TEER measurement capabilities, adapted from ref. 183 with permission from Royal Society of Chemistry, B. M. Maoz *et al.*, *Lab on a Chip*, 2017, **17**, 2294–2302, copyright 2017. (E) Organ-on-chip device incorporating embedded charge sensors and recording microelectrodes for brain circuits, adapted from ref. 184 with permission from Royal Society of Chemistry, E. Moutaux *et al.*, *Lab on a Chip*, 2018, **18**, 3425–3435, copyright 2018. (F) On-chip midbrain organoid development with long-term, non-invasive brainwave-like electrophysiological monitoring, adapted from ref. 185 with permission from Cold Spring Harbor Laboratory, S. Hong *et al.*, *bioRxiv*, 2024, copyright 2024.

electrophysiological sensors directly interrogate functional electrical signaling, making them uniquely suited for excitable cells, barrier tissues, and network-level dynamics. When coupled with microfluidics, these devices enable precise control of the cellular microenvironment while simultaneously capturing dynamic electrical signals from excitable tissues.[146,178] Early demonstrations showed how electronic fields could be coupled to microfluidic systems for biomolecular manipulation. In 2002, Washizu *et al.* presented a microfluidic system for electrostatic stretching and positioning of single DNA molecules, allowing high-resolution optical mapping and sequence analysis (Fig. 10A).[179] This work illustrated the potential of integrating microscale fluid handling with electronic actuation for precise biomolecule manipulation. Building on such concepts, Ionescu-Zanetti *et al.* developed a platform for mammalian electrophysiology, allowing patch-clamp recordings directly within microchannels to monitor the electrical activity of cultured neurons and other excitable cells (Fig. 10B).[180] This integration reduced the operational complexity and variability of traditional patch-clamp techniques, which are labor-intensive, low-throughput, and highly sensitive to manual alignment and seal formation. By confining cells within defined microfluidic geometries, the platform enabled more reproducible access to cells while preserving electrophysiological fidelity, highlighting how microfluidics can mitigate key reliability and scalability limitations of conventional patch clamp.

Recent advances have expanded beyond single parameter sensing to multiplexed readouts. Curto *et al.* created an organic transistor with embedded microchannels capable of in-line, multi-parametric *in vitro* cell monitoring, simultaneously measuring cell adhesion, barrier integrity, and electrophysiological activity in culture.[181] This approach demonstrates how electrophysiological sensing can be co-registered with mechanical and barrier-function readouts, enabling causal interpretation of electrical signals within evolving cellular microenvironments rather than treating them as isolated outputs. Expanding beyond extracellular readouts, microelectrode arrays have been developed to achieve simultaneous intracellular delivery and intracellular recordings at the single-cell level (Fig. 10C).[182] This approach allows simultaneous molecular delivery and electrophysiological measurement within the same cells, providing functional readouts that were previously inaccessible.

In a similar effort to expand multiplexed capabilities, Maoz *et al.* reported an organs-on-chips platform integrated multi-electrode arrays with transepithelial electrical resistance measurements, allowing simultaneous monitoring of electrophysiological activity and barrier integrity within the same device (Fig. 10D).[183] Here, microfluidic control of tissue architecture and flow enables stable, long-term electrophysiological measurements under physiologically relevant shear and nutrient conditions, which are difficult to maintain and measure in static culture systems. Moutaux *et al.* reported an organ-on-chip device with integrated charge sensors and recording microelectrodes for electrophysiological monitoring of brain circuits (Fig. 10E).[184] By embedding sensing electronics directly into the microfluidic chip, the system enabled simultaneous recording of intracellular dynamics and electrical activity in presynaptic axonal projections and in their postsynaptic neuronal targets. Hong *et al.* developed a brain organoid microphysiological analysis platform that enables on-chip formation of human midbrain organoids with real-time, non-invasive monitoring of brainwave-like activity akin to EEG (Fig. 10F).[185] This system captured the developmental transition from early bursts to complex broadband oscillations and modeled Parkinson's disease by revealing neurotoxin-induced beta oscillation abnormalities. Complementing these efforts, high-content drug screening of primary cardiomyocytes has been achieved by combining microfluidics with real-time ultra-large-scale high-resolution imaging, enabling functional readouts of electrophysiological responses to pharmacological compounds at scale.[186]

Integration has also extended into wearable and untethered systems. Bandodkar *et al.* reported a biocompatible, sweat-activated battery technology that could be embedded within soft microchannels.[187] The battery is capable of continuous on-skin documentation of physiological indicators such as heart rate, sweat chloride, and sweat pH. In neuroscience applications, Yang *et al.* developed wireless, soft electronic devices that integrate microfluidic channels for pharmacological delivery with microscale LEDs for optogenetic stimulation, enabling modulation and monitoring of individual and social behaviors in freely moving animals.[188] This work underscores how electrophysiological sensing modalities are particularly well suited for integration with flexible substrates, where mechanical compliance, conformal contact, and low-power operation are critical design constraints.

3.3 Integrated microfluidics with plasmonic sensors

Plasmonic biosensors are gaining significant attention in the field of molecular diagnostics due to their high sensitivity, rapid response time, and ability to operate without the need for labeling.[189,190] These sensors exploit the unique properties of surface plasmon resonance (SPR), a phenomenon that occurs when light strikes a metal surface, such as gold or silver, causing electrons on the metal surface to oscillate and produce a resonant signal. This resonance is highly sensitive to changes in the refractive index near the surface, making plasmonic biosensors ideal for detecting biomolecular interactions. By monitoring shifts in the SPR signal, plasmonic biosensors can detect specific binding events, such as antigen–antibody interactions, nucleic acid hybridization, or enzyme activity, even at very low concentrations of analytes.[191]

One notable development is the use of ordered arrays of metallic nanostructures for surface plasmon-coupled

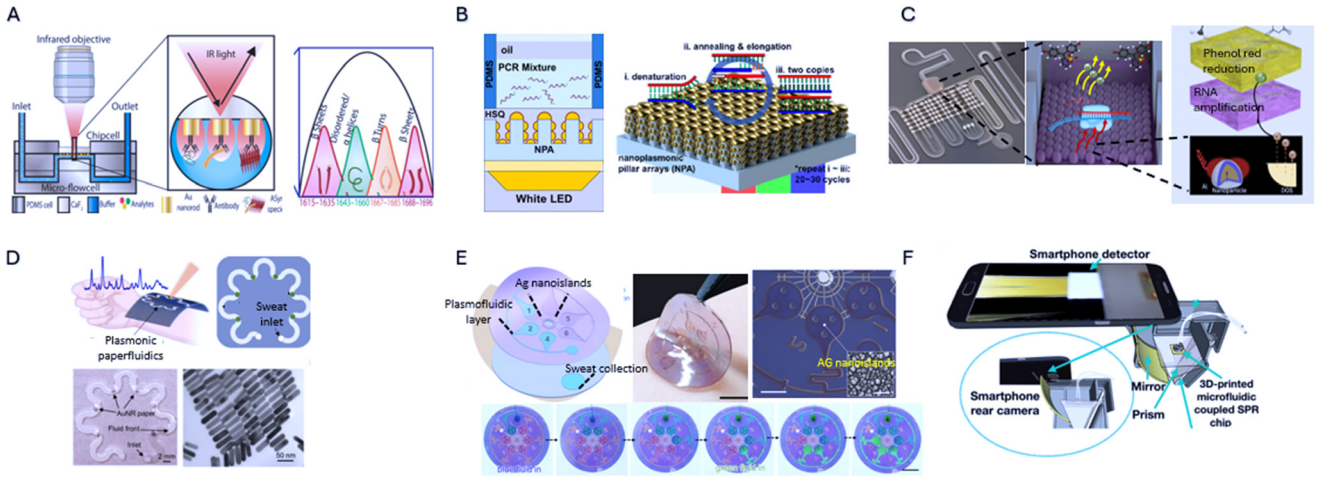

Fig. 11 Integrated plasmonic sensors in microfluidic devices. (A) AI-coupled plasmonic sensor for protein markers in neurodegenerative diseases, adapted from ref. 194 with permission from American Association for the Advancement of Science, D. Kavungal *et al.*, *Science Advances*, 2023, **9**, eadg9644, copyright 2023. (B) Nanoplasmonic PCR using pillar arrays for rapid thermal cycling, achieving faster heating and cooling compared to conventional gold films, improving DNA amplification efficiency, adapted from ref. 197 with permission from American Chemical Society, Y. Lee *et al.*, *ACS Applied Materials & Interfaces*, 2020, **12**, 12533–12540, copyright 2020. (C) Microfluidic plasmonic amplification platform achieves accelerated, colorimetric nucleic acid quantification in pathogen samples, adapted from ref. 198 with permission from Springer Nature, T. AbdElFatah *et al.*, *Nature Nanotechnology*, 2023, **18**, 922–932, copyright 2023. (D) Wearable microfluidics integrated with plasmonics for continuous sweat biomarker analysis in real time, adapted from ref. 199 with permission from American Association for the Advancement of Science, U. Mogera *et al.*, *Science Advances*, 2022, **8**, eabn1736, copyright 2022. (E) Flexible chronoepifluidic nanoplasmonic patch for label-free metabolite profiling in sweat, adapted from ref. 200 with permission from Springer Nature, J. Jeon *et al.*, *Nature Communications*, 2025, **16**, 8017, copyright 2025. (F) Smartphone coupled print-and-stick SPR microfluidic chip (Smart-iSPR) for portable, low-cost biosensing, adapted from ref. 201 with permission from Elsevier, C. Xiao *et al.*, *Analytica Chimica Acta*, 2022, **1201**, 339606, copyright 2022.

fluorescence enhancement, demonstrated by Mei *et al.*[192] The authors designed a biochip incorporating these nanorod arrays, which significantly enhanced fluorescence signals due to the coupling of SPR with fluorescence emissions. This strategy addresses a longstanding limitation of fluorescent assays in microfluidic environments, where small optical path lengths and limited fluorophore numbers often constrain signal-to-noise ratios. Similarly, Luan *et al.* explored ultrabright fluorescent nanoscale labels, coupled with plasmonic nanostructures, for femtomolar detection of analytes.[193] The incorporation of these ultrabright fluorescent nanoparticles into plasmonic biosensing platforms enabled the detection of biomolecules at extremely low concentrations beyond the sensitivity limits of conventional assays. Kavungal *et al.* developed an artificial intelligence–coupled plasmonic infrared sensor for detecting structural protein biomarkers in neurodegenerative disease, demonstrating how plasmonic sensors can be paired with data-driven analysis to extract diagnostically meaningful information from complex, high-dimensional spectral data, thereby mitigating one of the key barriers to clinical translation of label-free plasmonic readouts (Fig. 11A).[194]

In addition to enhancing sensitivity, plasmonic biosensors have also been used for detecting a broader range of analytes using plasmonic resonance energy transfer (PRET). Choi *et al.* demonstrated the use of PRET-based nanospectroscopy for the sensitive and selective detection of metal ions, such as lead and mercury, which are often challenging to detect at trace levels.[195] The study involved coupling plasmonic nanoparticles with fluorescent probes, using the PRET mechanism to enable detection of metal ions based on energy transfer efficiency between the nanoparticles and the probes. Expanding to small-molecule sensing, a nanoplasmonic aptasensor was developed for the real-time detection of dopamine directly from unprocessed whole blood.[196] By coupling aptamer specificity with the refractive index sensitivity of plasmonic nanostructures, the platform enabled selective neurotransmitter detection under physiologically relevant conditions, underscoring the versatility of plasmonic biosensors for complex clinical samples.

On top of optical transduction, plasmonic excitation also generates intense, highly localized thermal effects that can be exploited for active functions within microfluidic systems. One significant advancement in this regard involves the integration of nanoplasmonic devices with PCR workflows. Lee *et al.* explored the use of gold nanoparticle arrays in PCR chips to enhance the amplification and detection of specific DNA sequences (Fig. 11B).[197] Utilizing plasmonic structures in PCR systems improved heat transfer during amplification, facilitating rapid and efficient DNA analysis, which is crucial for molecular diagnostics in clinical settings. Nanoplasmonic amplification has also been harnessed for colorimetric assays, where SPR enhancement enabled rapid colorimetric quantification of pathogen-derived nucleic acid directly from patient samples (Fig. 11C).[198]

Recent efforts have transformed plasmonic sensing technologies into portable and user-friendly devices. Mogera

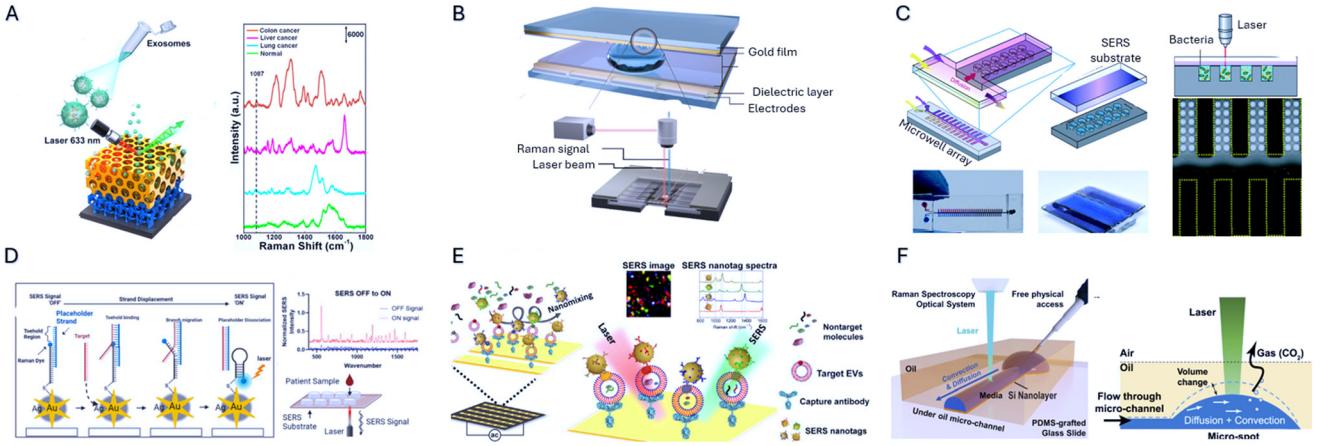

Fig. 12 Integrated microfluidics with Raman spectroscopy. (A) Label-free SERS detection of exosomes with spectral differences distinguishing cancer and normal samples, adapted from ref. 206 with permission from American Chemical Society, S. Dong *et al.*, *ACS Applied Materials & Interfaces*, 2020, **12**, 5136–5146, copyright 2020. (B) Digital droplet microfluidics for seamless sample manipulation and subsequent Raman analysis, adapted from ref. 207 with permission from Elsevier, W. Dong *et al.*, *Biosensors and Bioelectronics*, 2025, **271**, 117036, copyright 2025. (C) Antibiotic concentration gradient microfluidic device with integrated SERS for multiplex antimicrobial susceptibility testing, adapted from ref. 209 with permission from Royal Society of Chemistry, S.-J. Lin *et al.*, *Lab on a Chip*, 2022, **22**, 1805–1814, copyright 2022. (D) Bimetallic nanostar sensing chip for miRNA detection using SERS encoded gene probes, adapted from ref. 211 with permission from Elsevier, A. J. Canning *et al.*, *Biosensors and Bioelectronics*, 2023, **220**, 114855, copyright 2023. (E) Multiplexed SERS mapping of melanoma-derived extracellular vesicles to identify key biomarkers and track phenotypic changes during treatment, adapted from ref. 212 with permission from American Association for the Advancement of Science, J. Wang *et al.*, *Science Advances*, 2020, **6**, eaax3223, copyright 2020. (F) Visualization-enhanced under-oil open microfluidic system for *in situ* characterization of multi-phase chemical reactions, adapted from ref. 214 with permission from Springer Nature, Q. Chen *et al.*, *Nature Communications*, 2024, **15**, 1155, copyright 2024.

et al. introduced a wearable paper-based microfluidic platform integrated with plasmonic nanostructures for continuous sweat analysis (Fig. 11D).[199] Jeon *et al.* created a flexible chronoepifluidic nanoplasmonic patch for label-free profiling of sweat metabolites, integrating fluid handling with nanoplasmonic sensing for continuous and noninvasive biochemical monitoring (Fig. 11E).[200] Complementing this, Xiao *et al.* designed a "print-and-stick" microfluidic SPR chip that connects directly to smartphone cameras for optical readout in resource limited settings (Fig. 11F).[201]

3.4 Integrated microfluidics with Raman spectroscopy

Raman spectroscopy relies on inelastic photon scattering to reveal molecular vibrational modes, providing a chemical fingerprint of target analytes.[202–205] Unlike electrochemical or plasmonic sensors that primarily report on binding, charge transfer, or refractive index changes, Raman spectroscopy directly encodes molecular composition, enabling label-free chemical identification rather than indirect signal transduction. Because conventional Raman signals are weak, surface-enhanced Raman scattering (SERS) utilizes nanostructured metallic substrates to amplify scattering, extending detection down to single molecules or trace analytes. Recent innovations combine SERS with microfluidics, machine learning, and nanomaterials to expand sensitivity and broaden biological applications.

SERS can be categorized into two main subcategories: label-free SERS and specific (labeled) SERS. Label-free SERS directly detects the intrinsic Raman signals of the target molecules without the need for additional labeling agents or tags. For example, Dong *et al.* developed a porous honeycomb gold substrate for the capture and detection of exosomes (Fig. 12A).[206] Here, the exosomes confined within the honeycomb structure can be detected label-free after isolation using centrifugation and polymer precipitation. Digital droplet microfluidics has been integrated with Raman spectroscopy for enrichment of serum derived exosomes. The apparatus gently drives picoliter droplets containing analytes onto a translucent Raman enhancement stack, reducing the risk of biocontamination and enhancing sensitivity (Fig. 12B).[207]

Label-free approaches have several drawbacks, however, as they are largely limited to highly pure samples to prevent interference from co-adsorbed molecules that could affect the accuracy of the SERS spectrum. Furthermore, SERS analysis of heterogeneous biological fluids directly presents challenges due to the complexity and similarity of their vibrational patterns. To circumvent this, machine learning has been applied extensively to tease out the most important information in complicated SERS spectra. Ogunlade *et al.* applied machine learning to SERS spectra of mycobacteria tuberculosis (TB) to enable rapid detection of antibiotic-resistant bacteria.[208] They successfully profiled strains of isogenic Bacillus Calmette-Guérin resistant to one of the four main anti-TB drugs (isoniazid, rifampicin, moxifloxacin, and amikacin) with 98% accuracy in dried samples and 79% accuracy in sputum samples. Building further toward clinical translation, an antibiotic

concentration gradient microfluidic device was developed that integrates SERS for multiplex antimicrobial susceptibility testing, enabling rapid assessment of bacterial response profiles under varying drug dosages (Fig. 12C).[209] This integration highlights a broader design principle for Raman spectroscopy: computational analysis is often essential to compensate for spectral complexity inherent to real biological samples, particularly when operating without purification or labeling.

Specific SERS, also known as labeled SERS, involves using Raman-active labels that are attached to the target molecules or to probes that specifically bind to the target molecules.[203,204] Thanks to the labels' strong and distinct Raman signals, precise identification and quantification of the target analytes is possible. This strategy trades chemical generality for robustness and specificity, offering a practical route to multiplexed detection in heterogeneous samples where label free spectral deconvolution becomes unreliable. Ngo *et al.* developed ultrabright SERS nanorattles for this purpose, which are loaded with reporter probes for facile detection.[210] In the presence of target DNA, a sandwich complex forms between the nanorattle, DNA, and magnetic bead, sanctioning specific SERS quantification of nucleic acids. Expanding into clinical applications, Canning *et al.* designed a bimetallic nanostar biosensor with integrated miRNA probes for multiplexed, amplification-free detection of colorectal cancer biomarkers in patient plasma, achieving sensitive profiling directly from clinical samples (Fig. 12D).[211] By eliminating enzymatic amplification steps such as PCR, this approach reduces assay complexity, avoids amplification bias, and enables direct molecular readout from patient samples—an important advantage for integrated microfluidic platforms where thermal cycling, reagent handling, and contamination control pose significant system-level challenges. Wang *et al.* introduced multiplexed labeling of extracellular vesicles to track multiple biomarkers during treatment response in melanoma patients (Fig. 12E).[212] The study reveals that extracellular vesicles from melanoma cells exhibit distinct Raman spectral changes after treatment with targeted therapies, reflecting shifts in lipid, protein, and nucleic acid composition.

Raman spectroscopy is also being adapted to probe fundamental physicochemical processes. A recent study used electrodeformation to directly quantify the surface tension of metastable aerosol droplets, enabling Raman characterization of droplet stability and interfacial properties that are otherwise inaccessible with conventional techniques.[213] Chen *et al.* introduced an under-oil open microfluidic unit that integrates Raman visualization to monitor multiphase reactions *in situ* (Fig. 12F).[214] By preventing evaporation and maintaining optical clarity, this system allowed tracking of chemical dynamics at picoliter volumes, highlighting the utility of Raman methods for dissecting small-scale interfacial processes beyond traditional biosensing applications.

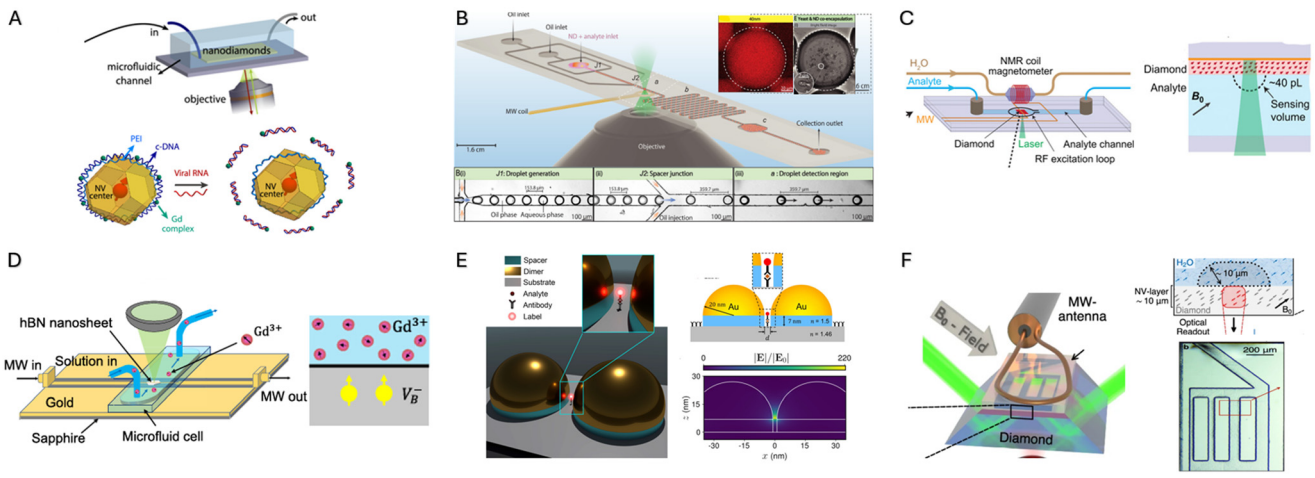

Fig. 13 Integrated microfluidics with quantum sensors. (A) SARS-CoV-2 quantum sensor utilizing nitrogen-vacancy centers in diamond promotes ultrasensitive detection of viral RNA *via* optically detected magnetic resonance, adapted from ref. 218 with permission from American Chemical Society, C. Li *et al.*, *Nano Letters*, 2021, **22**, 43–49, copyright 2021. (B) Chemical quantum sensing in flowing monodisperse microdroplets enables real-time detection of analytes with NV centers, adapted from ref. 219 with permission from American Association for the Advancement of Science, A. Sarkar *et al.*, *Science Advances*, 2024, **10**, eadp4033, copyright 2024. (C) Two-dimensional NMR spectroscopy with a microfluidic diamond quantum sensor provides molecular structural information at picoliter volumes, adapted from ref. 223 with permission from American Association for the Advancement of Science, J. Smits *et al.*, *Science Advances*, 2019, **5**, eaaw7895, copyright 2019. (D) Quantum sensing of paramagnetic spins in liquids using spin qubits in hexagonal boron nitride, adapted from ref. 224 with permission from American Chemical Society, X. Gao *et al.*, *ACS Photonics*, 2023, **10**, 2894–2900, copyright 2023. (E) Quantum plasmonic sensor exploits localized surface plasmons coupled to quantum emitters for sensitive biomolecular detection in an immunoassay, adapted from ref. 225 with permission from American Chemical Society, N. Kongsuwan *et al.*, *Nano Letters*, 2019, **19**, 5853–5861, copyright 2019. (F) Optical widefield nuclear magnetic resonance microscopy in bulk diamond microfluidic sensor, adapted from ref. 227 with permission from Springer Nature, K. D. Briegel *et al.*, *Nature Communications*, 2025, **16**, 1281, copyright 2025.

3.5 Integrated microfluidics with quantum sensors

Quantum biosensing applies principles such as spin coherence, tunneling, and superposition to achieve sensitivities beyond classical techniques and probe nanoscale magnetic fields, temperature shifts, and molecular interactions with single-molecule resolution.[215–217] A diverse array of sensing architectures—including defect centers in diamond, two-dimensional quantum materials, and quantum plasmonic structures—are now being adapted for biological and medical contexts, marking the emergence of a new generation of biosensors that combine quantum physics with life science applications.

Nitrogen-vacancy (NV) centers are defects in diamond lattices that exhibit a multitude of quantifiable properties integral to quantum sensing applications, such as sensitivity to electric fields, magnetics fields, temperature, and other physical properties that affect spin coherence and fluorescence. A recent SARS-CoV-2 biosensor exploited this principle by functionalizing nanodiamonds with viral antibodies and detecting binding events through changes in nitrogen-vacancy T_1 relaxation times (Fig. 13A).[218] The presence of viral proteins generated magnetic noise at the diamond surface, shortening relaxation lifetimes, promising a theoretical limit down to hundreds of RNA copies. Sarkar *et al.* combined flow-based droplet microfluidics with nitrogen-vacancy centers in nanodiamonds to achieve ultrahigh sensitivity and throughput in small-molecule detection (Fig. 13B).[219] In this work, monodisperse microdroplets encapsulate nanodiamond quantum sensors, providing a stable, low-noise environment for detecting paramagnetic ions and small molecules. The system used optically detected magnetic resonance to precisely analyze magnetic fluctuations induced by the presence of target Gd^{3+} molecules in 10^5 droplets per hour. This approach represents a fundamentally different sensing paradigm from affinity-based or other optical assays, where binding events are detected indirectly. Here, biomolecular interactions are sensed through their physical impact on quantum coherence, enabling measurable readouts of unique biological phenomena that would otherwise be invisible to classical approaches.

Local high resolution temperature sensing has also been achieved with nanodiamonds. Conventional temperature measurements typically rely on external thermocouples, infrared cameras, or bulk fluorescent probes, which report spatially averaged values and lack the resolution to capture intracellular or nanoscale thermal heterogeneity. Such approaches are particularly limited when probing localized heat generation associated with metabolism, membrane transport, or nanoscale perturbations. In contrast, nitrogen-vacancy based quantum thermometry enables direct, noninvasive measurement of temperature fluctuations at subcellular length scales, overcoming a fundamental limitation of classical thermal sensing methods. Kucsko *et al.* used nitrogen-vacancy sensors to measure intracellular temperature changes in fibroblast cells, achieving 44 mK sensitivity and nanoscale resolution.[220] Similarly, Tsai *et al.* employed nanodiamonds combined with gold nanorods to monitor temperature changes with mK accuracy during local laser heating, providing insights into cellular membrane stability under thermal stress.[221] Fujiwara *et al.* achieved monitoring of thermogenic responses in *C. elegans*, underscoring the capability of nanodiamonds to probe metabolic activities and cellular responses to environmental stress.[222]

Bulk quantum platforms have also advanced spectroscopy-based biosensing. Smits *et al.* developed a microfluidic diamond quantum sensor for two-dimensional NMR spectroscopy in picoliter-scale volumes achieved by patterning microchannels directly onto the diamond surface to confine analytes near shallow nitrogen-vacancy centers (Fig. 13C).[223] Gao *et al.* introduced a distinct solid-state qubit platform utilizing spin defects in hexagonal boron nitride (hBN) for quantum sensing of paramagnetic spins in liquids (Fig. 13D).[224] The atomically thin nature of hBN places the sensing layer in direct contact with analytes, maximizing sensitivity to weak magnetic fields. Kongsuwan *et al.* introduced a quantum plasmonic immunoassay, where plasmon–quantum emitter coupling enhanced spectral resolution and sensitivity in biomarker detection assays (Fig. 13E).[225] These advances illustrate how diverse quantum architectures are converging to push molecular detection into previously inaccessible regimes.

Quantum sensing has opened new possibilities for direct imaging of dynamic biological and chemical processes at high spatial resolution. Xin *et al.* introduced a quantum biological tunnel junction platform that visualizes electron transfer in live cells by exploiting quantum tunneling currents through biomolecular junctions.[226] This approach enables optical detection of mitochondrial cytochrome c electron transfer during cell life–death transitions, providing a powerful tool for probing quantum aspects of metabolism. Briegel *et al.* developed a platform for optical widefield NMR microscopy, which uses ensembles of nitrogen-vacancy centers in bulk diamond to convert NMR signals into optical signals that are subsequently captured by a high-speed camera (Fig. 13F).[227] This method enables chemical mapping of proton spin signals with submicron resolution across large fields of view, extending NMR beyond its traditional limits. Together, these studies highlight how quantum sensing technologies are moving beyond bulk spectroscopy into the realm of high-resolution imaging, revealing dynamic biological processes with unprecedented detail.

3.6 Microfluidics-enabled distance-based readout strategies for instrument-free biosensing

Distance-based readout strategies provide an alternative biosensing paradigm in which analyte concentration is encoded into a spatial signal, such as fluid travel distance, bar displacement, or volumetric expansion, enabling

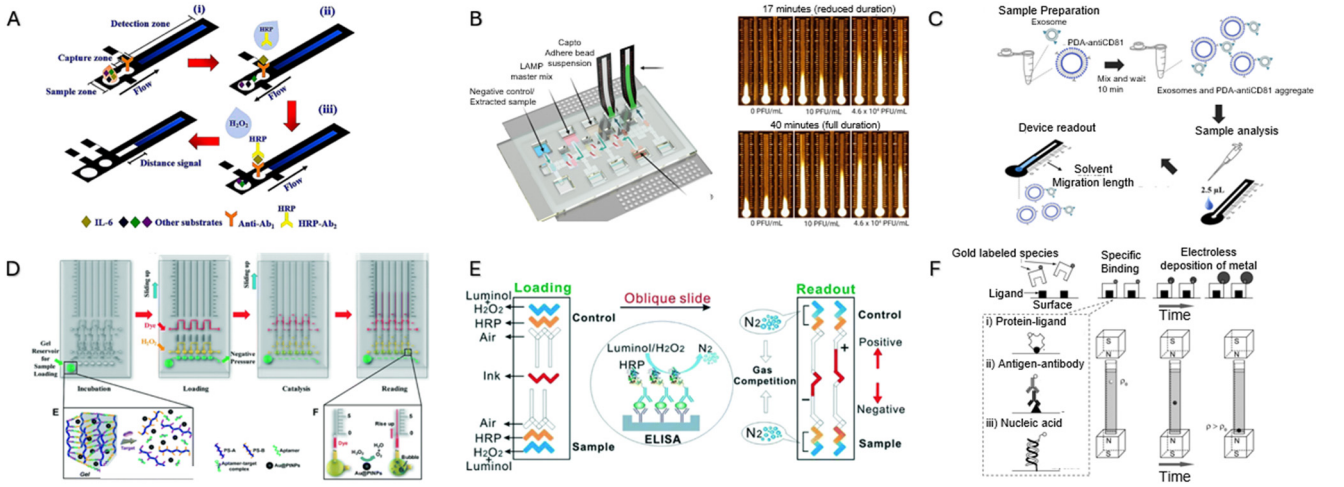

Fig. 14 Distance-based readout strategies for microfluidic biosensing and point-of-care diagnostics. (A) Distance-based all-in-one immunodevice enabling point-of-care monitoring of cytokine interleukin-6 through volumetric signal amplification and spatial bar-chart readout, adapted from ref. 230 with permission from American Chemical Society, K. Khachornsakkul *et al.*, *ACS Sensors*, 2022, **7**, 2410–2419, copyright 2022. (B) Digital microfluidics platform employing distance-based signal transduction for nucleic acid diagnostics, in which assay outputs are encoded as spatial readout lengths rather than optical intensity, adapted from ref. 231 with permission from Royal Society of Chemistry, M. Ho *et al.*, *Lab on a Chip*, 2024, **24**, 63–73, copyright 2024. (C) Stop-flow, paper-based microfluidic device leveraging exosome aggregation to generate distance-based readouts for rapid and portable exosome quantification, adapted from ref. 232 with permission from Wiley, B. Chutvirasakul *et al.*, *Electrophoresis*, 2020, **41**, 311–318, copyright 2020. (D) Target-responsive hydrogel system incorporating Au@Pt nanoparticles and volumetric bar-chart chip readout for quantitative point-of-care testing, adapted from ref. 233 with permission from Wiley, Z. Zhu *et al.*, *Angewandte Chemie International Edition*, 2014, **53**, 12503–12507, copyright 2014. (E) Competitive volumetric bar-chart chip with real-time internal control, enabling robust distance-based quantification in point-of-care diagnostic settings, adapted from ref. 234 with permission from American Chemical Society, Y. Li *et al.*, *Analytical Chemistry*, 2015, **87**, 3771–3777, copyright 2015. (F) Metal-amplified density assays, including density-linked immunosorbent assays, that convert biochemical recognition events into distance-based readouts for instrument-free quantification, adapted from ref. 235 with permission from Royal Society of Chemistry, A. B. Subramaniam *et al.*, *Lab on a Chip*, 2015, **15**, 1009–1022, copyright 2015.

quantitative detection without reliance on optical or electrical instrumentation.[228,229] By translating molecular recognition into a physically measurable length or displacement, these platforms are particularly attractive for point-of-care and low-resource settings where simplicity, robustness, and visual interpretability are prioritized.

Distance-based sensing has been widely applied to protein and nucleic acid detection, where molecular binding or amplification events are converted into changes in flow resistance or displacement length. Distance-based all-in-one immunodevices have been developed for cytokines such as interleukin-6, where antigen–antibody interactions modulate capillary-driven flow to generate a quantitative visual readout (Fig. 14A).[230] For nucleic acids, digital microfluidics with distance-based detection encodes amplification outcomes into spatial readouts rather than fluorescence intensity, offering a visually interpretable alternative to conventional optical PCR or isothermal assays (Fig. 14B).[231] These approaches reduce system complexity while preserving quantitative sensitivity, making them well suited for decentralized molecular testing.

Distance-based readout has also been extended to extracellular vesicle detection, where conventional sensing is challenged by EV heterogeneity and low abundance. Rapid, instrument-free EV quantification is achieved using a stop-flow paper-based device in which exosome-induced aggregation halts capillary flow at distances that scale with analyte concentration (Fig. 14B).[232] By encoding EV concentration directly into a physical stop length, this strategy provides an intuitive and scalable readout for point-of-care diagnostics.

A related class of platforms uses volumetric bar-chart readouts, in which biochemical reactions generate gas, density changes, or volume expansion that displaces liquid columns in microchannels. Zhu *et al.* introduced Au@Pt nanoparticle-encapsulated hydrogels to create target-responsive volumetric bar-chart chips, translating molecular recognition into visually quantifiable displacement lengths (Fig. 14D).[233] Competitive volumetric bar-chart chips further incorporate internal controls, enabling real-time calibration and improved quantitative robustness for point-of-care diagnostics without external readers (Fig. 14E).[234]

Beyond flow and volume based strategies, metal-amplified density assays represent a distinct physical readout mechanism in which target binding triggers metal deposition, producing measurable density changes. Density-linked immunosorbent assays exploit this principle by converting molecular recognition into buoyancy or sedimentation shifts that can be directly observed (Fig. 14F).[235] These density-based approaches expand the distance-readout concept beyond capillarity, highlighting how physical property modulation can serve as a powerful signal transduction mechanism for instrument-free biosensing.

Table 3 Overview of representative applications of integrated microfluidic biosensors, organized by analyte type and application domain, summarizing the roles of microfluidic integration, commonly employed sensing strategies, and key translational challenges

Application category	Representative analytes/-targets	Integrated microfluidic role	Common sensing modalities	Key advantages enabled	Primary translational challenges
Infectious disease diagnostics	Viral RNA/DNA, bacterial proteins, whole pathogens	Sample preparation, concentration, amplification, containment	Electrochemical, plasmonic, Raman/SERS, distance-based	Rapid testing, low sample volume, point-of-care potential	Clinical validation, sample variability, regulatory approval
Cancer diagnostics	Tumor cells, extracellular vesicles, miRNA, proteins	Rare target enrichment, single-entity isolation	Electrochemical, plasmonic, Raman/SERS	Sensitive detection, minimally invasive testing, molecular stratification	Low target abundance, standardization, reproducibility
Extracellular vesicle detection	Exosomes, EV surface markers, EV cargo	Isolation, fractionation, concentration	Electrochemical, Raman/SERS, plasmonic, quantum	Label-free analysis, nanoscale sensitivity	Heterogeneity, lack of standards, inter-lab variability
Single-cell analysis	Individual cells, secreted proteins, electrical activity	Isolation, compartmentalized, controlled stimulation	Electrophysiological, electrochemical, optical, Raman	Resolves population heterogeneity, mechanistic insight	Throughput *vs.* complexity trade-offs
Organ-on-chip	Barrier integrity, electrophysiology, metabolites	Controlled microenvironment, perfusion, long-term culture	Electrophysiological, electrochemical, optical	Human-relevant models, dynamic monitoring	Scalability, standardization, validation against *in vivo* data
Drug screening & toxicology	Cellular response, metabolites, electrical signals	Automated dosing, dynamic exposure, multiplexing	Electrochemical, electrophysiological, optical	Reduced reagent use, functional readouts	Throughput, integration with industry workflows
Biomanufacturing & process monitoring	Cell state, EV yield, metabolites, impurities	Inline monitoring, enrichment, quality control	Raman, quantum, impedance-based	Real-time feedback, process control	Robustness, sensor fouling, long-term stability
Environmental & food safety monitoring	Toxins, pathogens, small molecules	On-site sample handling and detection	Electrochemical, plasmonic, distance-based	Portable, low-cost sensing	Sensitivity in complex matrices
Low resource & point-of-care testing	Proteins, nucleic acids, biomarkers	Minimal preprocessing, instrument-free operation	Distance-based, electrochemical	Accessibility, ease of use	Limited quantitative range, durability

4. Applications of integrated microfluidic biosensors

Integrated microfluidic biosensors are transforming analytical and diagnostic workflows by enabling rapid, low-volume, and highly sensitive detection of biochemical and cellular targets. By integrating fluid handling, target enrichment, and on-chip sensing within a single platform, these systems support applications ranging from point-of-care diagnostics to fundamental studies of molecular and cellular dynamics. The following sections highlight key application areas, beginning from small molecules to small organisms (Table 3).

4.1 Microfluidic devices for small molecule and protein detection

Small molecules and proteins play critical roles in biological processes and disease states. Accurate and rapid detection of these molecules is essential for applications in healthcare, environmental monitoring, and drug development.[236–238] Conventional detection methods such as ELISA and mass spectrometry, though accurate, are slow, resource-intensive, and poorly suited for high-throughput applications.[236,239,240] Faster and more sensitive analysis is achieved as microfluidic biosensors integrate sample handling and signal readout into miniaturized instruments.

Small molecule and protein sensing is constrained by rapid diffusion and limited interaction with the sensing interface. Microfluidic actuation provides a key opportunity to control nanoscale transport and confinement and improve overall sensitivity. To this end, Sonato *et al.* integrated SPR with surface acoustic wave technology to enhance biosensing sensitivity (Fig. 15A).[241] The surface acoustic wave enhanced SPR microfluidic biosensor introduces a hybrid approach where acoustic excitation modulates plasmonic resonance, improving signal stability and detection limits. This device precisely delivers analytes to the SPR sensing region, where the acoustic waves enhance mass transport and reduce diffusion limitations, leading to faster and more sensitive detection of low-abundance protein biomarkers. Similarly, Akther *et al.* combined acoustofluidics with T1 relaxometry in nanodiamond nitrogen-vacancy centers to detect Mn^{2+} concentrations.[242] Here, acoustic waves propagate into a microscale sessile droplet, inducing rapid concentration and localization of the nanodiamond particles. This enables an order of magnitude improvement in the measurement acquisition time and a detection limit of 1 μM Mn^{2+}.

While these approaches enhance sensitivity and specificity, recent advancements have pushed detection limits even further, enabling quantification at the single-molecule

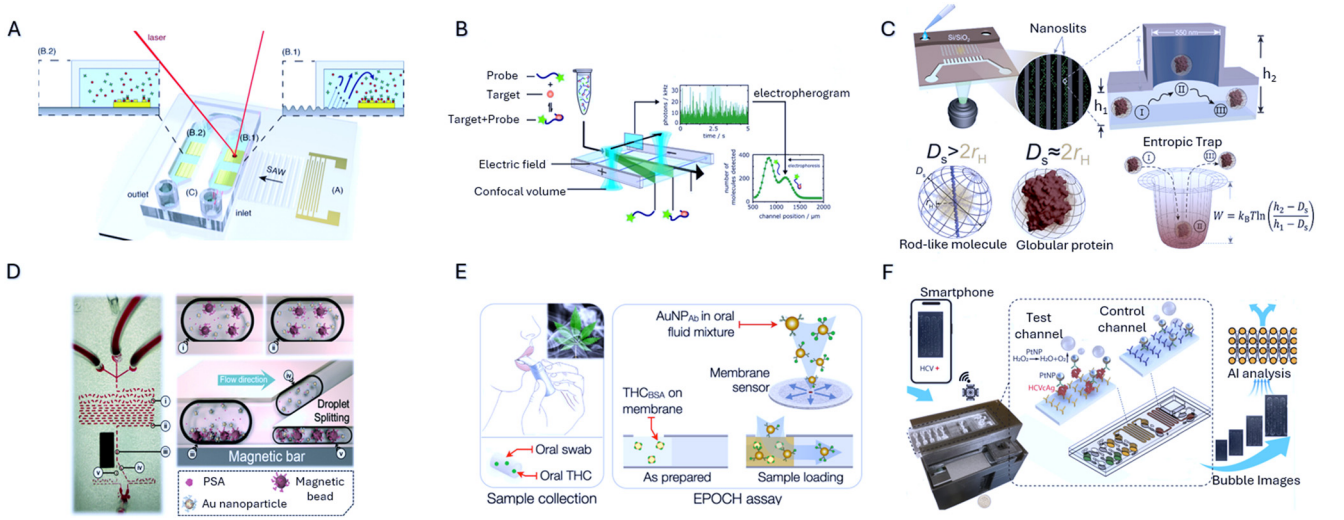

Fig. 15 Small molecule and protein detection. (A) Surface acoustic wave (SAW)-enhanced affinity capture on a localized SPR substrate for label-free analyte detection, adapted from ref. 241 with permission from Royal Society of Chemistry, A. Sonato *et al.*, *Lab on a Chip*, 2016, **16**, 1224–1233, copyright 2016. (B) Aptamer-based electrokinetic biosensing using an electric field for molecular separation, adapted from ref. 243 with permission from Springer Nature, G. Krainer *et al.*, *Nature Communications*, 2023, **14**, 653, copyright 2023. (C) Microfluidic chip for quantitative measurement of molecular size and shape at the single-molecule level, adapted from ref. 245 with permission from American Association for the Advancement of Science, X. Zhu *et al.*, *Science*, 2025, **388**, eadt5827, copyright 2025. (D) Wash-free immunoassay utilizing droplet microfluidics and SERS for PSA detection, adapted from ref. 246 with permission from Royal Society of Chemistry, R. Gao *et al.*, *Lab on a Chip*, 2016, **16**, 1022–1029, copyright 2016. (E) Rapid oral-fluid assay integrating gold nanoparticles for on-site tetrahydrocannabinol (THC) quantification, adapted from ref. 247 with permission from American Association for the Advancement of Science, H. Yu *et al.*, *Science Translational Medicine*, 2021, **13**, eabe2352, copyright 2021. (F) Fully automated deep learning-enabled microfluidic system for rapid HCV antigen detection, adapted from ref. 248 with permission from American Association for the Advancement of Science, H. Chen *et al.*, *Science Advances*, 2025, **11**, eadt3803, copyright 2025.

level. Krainer *et al.* introduced a microfluidic chip for direct digital sensing of protein biomarkers (Fig. 15B).[243] The mechanism uses fluorescently labeled antibodies to capture target proteins, which are separated from unbound targets and funneled into detection chambers using dielectrophoresis. Here, a custom optical setup detects individual fluorescence events, each corresponding to a single biomarker molecule. This digital quantification method eliminates the need for amplification or washing steps, reducing noise and artifacts common in traditional assays. The key advance here is not incremental sensitivity, but a shift from analog signal accumulation to digital molecular counting enforced by microfluidic architecture. By using microfluidics to impose physical partitioning, the system replaces amplification and calibration heavy workflows with a counting-based sensing paradigm.

Building on this, Krainer *et al.* developed a microfluidic system for single-molecule digital sizing of proteins in solution, permitting direct measurement of protein size distributions without labeling or complex sample preparation.[244] The system uses nano-confined microfluidic channels to monitor Brownian motion and molecular diffusion, facilitating high-throughput analysis of heterogeneous protein populations. In this case, microfluidics defines the measurement modality itself rather than serving as a delivery mechanism. The approach illustrates a recurring tradeoff in integrated biosensing: eliminating labels and affinity reagents increases reliance on precise fluidic control and device calibration.

Similarly, Zhu *et al.* introduced escape-time stereometry, an on-chip imaging method that measures molecular size, shape, and interaction strength directly in solution (Fig. 15C).[245] This approach distinguished size differences as small as two carbon atoms among small molecules and quantified molecular interactions across six orders of magnitude. By encoding molecular information into transport dynamics, this work reframes sensing as a physically defined process rather than a chemically selective one. This shift reduces dependence on reagents but increases sensitivity to flow stability and fabrication tolerances, underscoring a key design consideration for label-free microfluidic sensors.

Recent technologies have streamlined drug screening and diagnostics by integrating microfluidic processing with rapid SERS detection. Andreou *et al.* developed a device that efficiently mixed saliva samples with silver nanoparticles under controlled flow, inducing rapid nanoparticle aggregation and analyte adsorption, enhancing Raman scattering for trace-level quantification of methamphetamine. Gao *et al.* introduced a wash-free magnetic immunoassay for detecting the prostate-specific antigen (PSA), a key cancer biomarker, using SERS and droplet microfluidics (Fig. 15D).[246] Their approach eliminated traditional washing steps by introducing droplet microfluidics for precise reagent handling and magnetic particles for selective biomarker capture.

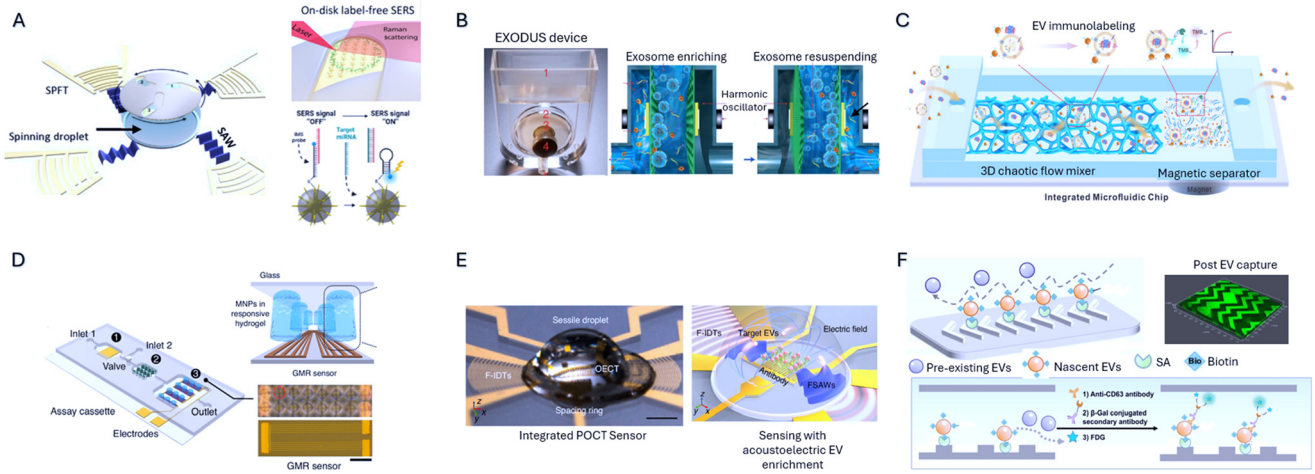

Fig. 16 Exosome separation and detection *via* integrated microfluidics. (A) ASCENDx workflow for exosome concentration and miRNA analysis using an acoustically driven centrifuge with integrated plasmonic nanostars for cancer diagnostics, adapted from ref. 253 with permission from American Association for the Advancement of Science, T. D. Naquin *et al.*, *Science Advances*, 2024, **10**, eadm8597, copyright 2024. (B) EXODUS ultrafast isolation system for high-yield, contamination-free exosome purification using negative pressure oscillations, adapted from ref. 255 with permission from Springer Nature, Y. Chen *et al.*, *Nature Methods*, 2021, **18**, 212–218, copyright 2021. (C) Integrated microfluidic chip combining chaotic flow mixing, magnetic separation, and electrochemical readout for exosome profiling, adapted from ref. 257 with permission from Royal Society of Chemistry, Y.-X. Zhang *et al.*, *Lab on a Chip*, 2025, **25**, 3185–3196, copyright 2025. (D) Magnetic nanoparticle platform with gradient-distributed hydrogel pillars positioned above a giant magnetoresistive sensor array for extracellular vesicle detection, adapted from ref. 258 with permission from Springer Nature, Y. Chen *et al.*, *Nature Communications*, 2024, **15**, 8410, copyright 2024. (E) Point-of-care sensor integrating organic electrochemical transistors with acoustofluidic enrichment for exosome detection, adapted from ref. 259 with permission from Springer Nature, X. Li *et al.*, *Microsystems & Nanoengineering*, 2025, **11**, 65, copyright 2025. (F) Capturing nascent extracellular vesicles *via* metabolic glycan labeling-assisted microfluidics for tracking EV biogenesis, adapted from ref. 261 with permission from Springer Nature, Q. Wu *et al.*, *Nature Communications*, 2023, **14**, 6541, copyright 2023.

Other efforts have extended small molecule detection into portable and user-friendly formats for on-site monitoring. Yu *et al.* implemented a competitive assay using gold nanoparticle–antibody conjugates for the measurement of tetrahydrocannabinol concentration in oral fluid (Fig. 15E).[247] The device features a radial, semipermeable membrane cartridge to promote uniform sample flow and signal acquisition, and results are captured with a standard smartphone camera for facile optical readout, minimizing user intervention for field deployable testing. Chen *et al.* developed a fully automated microfluidic system for hepatitis C virus antigen detection (Fig. 15F).[248] This point-of-care device integrates platinum nanoparticle probes with bubble-based catalytic readouts analyzed by deep learning, providing rapid and accurate diagnostics directly from minimally processed samples. Wang *et al.* reported a wearable microfluidic platform with embedded electrochemical sensing for analysis of sweat associated compounds such as glucose, lactate, and electrolytes.[249] The device features wireless data transmission to mobile devices, supporting applications for personalized health monitoring and sports medicine.

4.2 Microfluidic devices for exosome separation and detection

Extracellular vesicles (EVs), particularly exosomes, are increasingly recognized as critical biomarkers for disease diagnostics and therapeutic monitoring.[57,250,251] While microfluidic techniques have been developed for EV separation or analysis, most lack an integrated approach that simultaneously isolates and characterizes EVs in a single system. Traditional ultracentrifugation-based isolation methods are time-consuming, low-yield, and require large sample volumes, while standard biosensing techniques often rely on pre-enriched EV fractions rather than direct analysis of complex biological fluids. To address this gap, recent microfluidic technologies have been developed for simultaneous EV separation, enrichment, and profiling within a single device.[252]

One such approach, the acoustic separation and concentration of exosomes and nucleotide detection (ASCENDx) platform, utilizes an acoustically driven centrifuge to efficiently separate and concentrate exosomes for nucleotide detection (Fig. 16A).[253] This integrated system enhances exosome recovery from plasma while using plasmonic nanostars for direct detection of exosomal miRNA, facilitating a diagnostic assay for colorectal cancer with 95.8% sensitivity and 100% specificity. Hao *et al.* developed a bimodal microfluidic biosensor integrating acoustofluidics with fluorescence and SERS.[254] This system uses surface acoustic waves to concentrate and enrich EVs within a glass capillary, improving analyte interactions and amplifying available signal for sensing. The dual modality sensing approach leverages fluorescence for highly specific detection and SERS for molecular fingerprinting, offering

complementary detection capabilities to probe complex biological samples. Together, these examples highlight how physical enrichment strategies can be deliberately matched to sensing modalities whose performance depends on analyte proximity and concentration.

Recently, the EXODUS system was introduced for exosome purification, providing rapid, high-yield, and contamination-free recovery (Fig. 16B).[255] By leveraging negative pressure oscillations and dual coupled channels, EXODUS enables clinical grade EV isolation, making it highly attractive for downstream molecular profiling.

Rather than increasing analyte enrichment aggressiveness, complementary strategies have focused on amplifying signal generation at the sensing interface itself. Shi *et al.* introduced a metal–organic framework interfaced ELISA probe to enable ultrasensitive detection of extracellular vesicle biomarkers by significantly increasing antibody loading density and enhancing local redox activity at the electrode surface.[256] By decoupling sensitivity from physical enrichment efficiency, this materials driven approach addresses a key limitation in EV diagnostics, where vesicle scarcity and heterogeneous cargo often constrain downstream detection even after isolation. To further advance extracellular vesicle profiling, Zhang *et al.* introduced an integrated microfluidic chip capable of synchronous drug loading, separation, and detection of plasma exosomes (Fig. 16C).[257] This platform combines chaotic mixers, magnetic nanoparticle-based separation, and electrochemical detection within a single device, enabling streamlined exosome analysis directly from clinical samples. Another recent magnetic nanoparticle platform integrates hydrogel pillars with gradient distributed particles positioned above a giant magnetoresistive sensor array. Binding of target RNAs or proteins releases sensor proximal nanoparticles, producing amplified magnetic signals with sensitivity down to ~10 RNA or ~1000 protein copies (Fig. 16D).[258] Li *et al.* combined acoustofluidic enrichment to propel EV capture in an electrochemical detection unit, causing rapid Alzheimer's detection in under 2minutes (Fig. 16E).[259] In this system, EVs are concentrated within a sessile droplet using acoustic forces, then quantified electrochemically, enabling rapid and label-free detection of Aβ42- and tau-positive EVs.

In addition to physical isolation and enrichment mechanisms, assay level architectural innovations have emerged that reduce reliance on enrichment altogether. Wen *et al.* developed a partitionless digital immunoassay using configurable topographic nanoarrays for direct EV profiling by spatially encoding individual immunobinding events without droplets, wells, or physical compartmentalization.[260] By eliminating partitioning steps that often introduce sample loss, dilution, and fabrication complexity, this strategy illustrates how EV diagnostics can be achieved through surface-engineered signal discretization rather than upstream separation.

Biochemical labeling methods provide a complementary route to physical and affinity-based capture by chemically tagging specific EV populations. Wu *et al.* utilized metabolic glycan labeling to distinguish nascent EVs from pre-existing

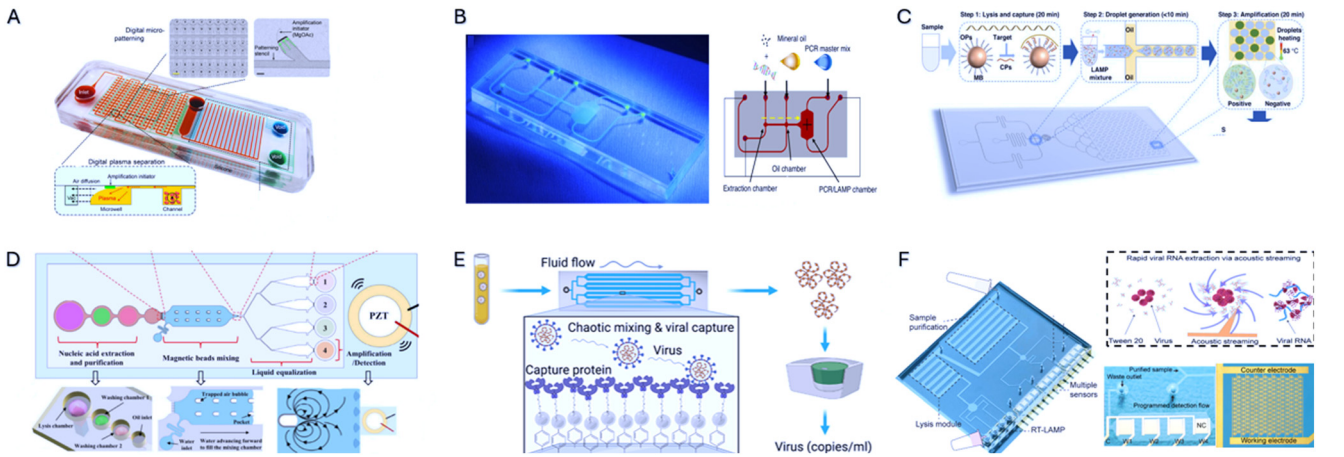

Fig. 17 Integrated microfluidic devices for pathogen detection. (A) Self-powered integrated microfluidic point-of-care low-cost (SIMPLE) chip, which generates multiplexed plasma separation and digital biomarker readout without external instrumentation, adapted from ref. 264 with permission from American Association for the Advancement of Science, E.-C. Yeh *et al.*, *Science Advances*, 2017, **3**, e1501645, copyright 2017. (B) Microfluidic instrument integrating extraction and nucleic acid amplification modules for streamlined nucleic acid testing in a single device, adapted from ref. 265 with permission from Springer Nature, A. Sun *et al.*, *Microsystems & Nanoengineering*, 2024, **10**, 66, copyright 2024. (C) Droplet microfluidics coupling lysis, capture, and loop-mediated isothermal amplification for high-throughput pathogen screening, adapted from ref. 266 with permission from Springer Nature, L. Jiang *et al.*, *Microsystems & Nanoengineering*, 2023, **9**, 118, copyright 2023. (D) Acoustic and magnetic bead microfluidic chip enabling nucleic acid extraction, mixing, and amplification, adapted from ref. 267 with permission from American Chemical Society, J. Li *et al.*, *Analytical Chemistry*, 2024, **96**, 13768–13776, copyright 2024. (E) Viral capture chip using chaotic mixing and immobilized capture proteins for quantitative detection of viral particles, adapted from ref. 268 with permission from American Association for the Advancement of Science, D. C. Rabe *et al.*, *Science Advances*, 2025, **11**, eadh1167, copyright 2025. (F) Acoustofluidic device combining purification, lysis, amplification, and multiplexed electrochemical detection of viral antibodies and nucleic acids, adapted from ref. 269 with permission from American Association for the Advancement of Science, J. Qian *et al.*, *Science Advances*, 2025, **11**, eadt5464, copyright 2025.

populations (Fig. 16F).[261] Incorporating azide-tagged sugar precursors into newly secreted vesicles, the system can profile newly released EVs, providing a unique window into dynamic EV biogenesis and secretion. In a complementary approach, an anion exchange membrane sensor was engineered to profile EGFR and its phosphorylation state directly from CD63-positive EVs in plasma of glioblastoma patients. By leveraging charge-selective ion transport, the platform distinguishes active *versus* inactive receptor populations, providing functional information that conventional EV quantification cannot capture.[262] These systems benefit from strong signal amplification and straightforward electrical interfacing but introduce new constraints related to surface chemistry stability, nonspecific binding, and calibration drift in complex fluids. As such, they are best suited for applications where defined biomarkers are known *a priori* and sample preprocessing can be tightly controlled.

Beyond *in vitro* sensing, microfluidic systems have been adapted for *in vivo* exosome detection to monitor dynamic biomarker expression. In mice, PD-L1-positive EVs were detected *in vivo* using a microfluidic device that directly separates and quantifies tumor-derived EVs within an external blood circulation loop.[263] This device allows for continuous collection of EVs at different stages of tumor progression directly from an *in vivo* source, offering critical information on treatment response while removing confounding effects of traditional EV isolation and preservation used in diagnostics.

4.3 Microfluidic devices for pathogen detection

Rapid and reliable pathogen detection remains a cornerstone of infectious disease control, where diagnostic speed directly impacts treatment decisions and outbreak management. Equally critical are robustness, accessibility, and the ability to operate across diverse clinical and resource settings. One primary objective of microfluidics is the development of complete "sample-to-answer" technologies that automate the entire workflow from patient sample to diagnostic outcome. Importantly, different application contexts impose distinct design constraints: point-of-care platforms prioritize simplicity, low power consumption, and minimal infrastructure, whereas laboratory grade systems emphasize automation, throughput, and assay reproducibility. To this end, Yeh *et al.* created a self-powered nucleic acid detection device from whole blood without the need for external pumps or separation steps (Fig. 17A).[264] Its disposable design emphasizes affordability and simplicity, making it well suited for point-of-care settings. Sun *et al.* developed a nucleic acid diagnostic system for SARS-CoV-2 which fully incorporates microvalves, heaters, and optical readout modules into one machine (Fig. 17B).[265] In contrast to minimalist POC designs, this system is designed for laboratory grade performance and automation for the detection of a large array of pathogens, positioning it for centralized laboratories where infrastructure is available and high assay consistency is required.

Recent pathogen detection platforms have focused on improving sensitivity and multiplexing capabilities. Jiang *et al.* introduced a droplet microfluidic platform with immunoaffinity capture beads to selectively isolate target RNA with minimal background interference (Fig. 17C).[266] This platform facilitates detection at an extremely low concentration of 10 RNA copies per mL within one hour. Li *et al.* developed a microfluidic chip for simultaneous respiratory pathogen detection, which enables multiplexed analysis of multiple pathogens, including influenza, respiratory syncytial virus, and various strains of coronaviruses in a single platform (Fig. 17D).[267] This system combines nucleic acid amplification with microarray hybridization to enable multiplexing, illustrating how microfluidic architectures can scale diagnostic breadth while preserving specificity, an essential capability for differentiating co-infections in clinical settings.

Recent advances are pushing pathogen diagnostics beyond traditional nucleic acid assays toward more complete profiling strategies. A key limitation of amplification-based methods is their susceptibility to inhibitors in complex biofluids and their inability to report on viral integrity. Rabe *et al.* introduced a microfluidic affinity-capture platform for the ultrasensitive detection of intact SARS-CoV-2 particles directly from complex biofluids (Fig. 17E).[268] By bypassing nucleic acid extraction and targeting whole viral particles, this system improves assay fidelity in unprocessed samples where inhibitors often compromise amplification-based methods. The AIMDx platform represents a step toward comprehensive, multi-modal diagnostics by integrating acoustofluidics with molecular assays to simultaneously detect viral nucleic acids and host antibodies within a single chip (Fig. 17F).[269] This dual readout capability provides not only information on current infection status but also the immune response, making it valuable for both acute diagnosis and monitoring of disease progression or immunity.

4.4 Microfluidic devices for single cell analysis

Single-cell analysis has become a cornerstone of modern biology, enabling researchers to uncover cellular heterogeneity that is masked in bulk measurements.[270–272] By integrating sorting, barcoding, sequencing, and biophysical assays into microfluidic platforms, these technologies provide high-throughput access to the molecular and functional states of individual cells with unprecedented precision.[273–277]

Recent advances in microfluidic engineering have transformed how rare and heterogeneous cells are detected, isolated, and characterized. Yeo *et al.* developed a high-throughput microfluidic chip that directs cells into individual chambers. When a target CTC enters and blocks its chamber, subsequent cells are diverted, allowing isolation of single

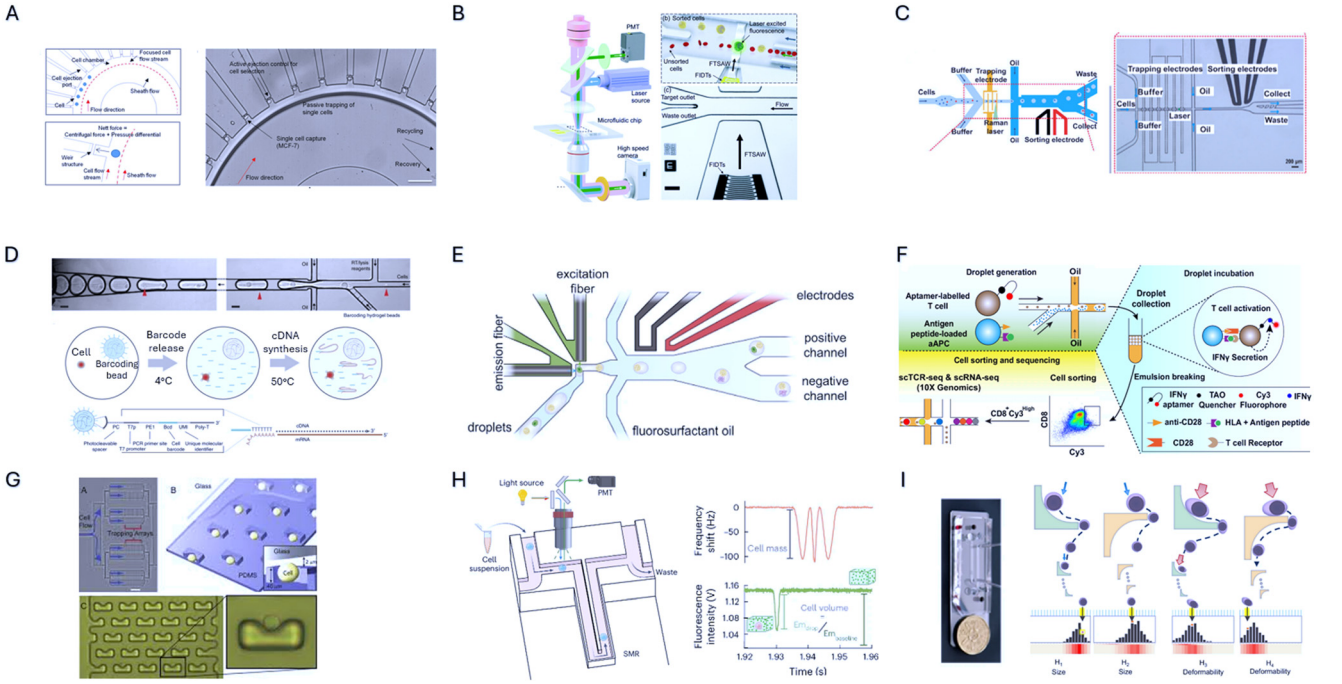

Fig. 18 Single-cell analysis *via* precision microfluidics. (A) Specific selection, isolation, and sequencing of CTCs *via* hydrodynamic focusing, adapted from ref. 278 with permission from Springer Nature, T. Yeo *et al.*, *Scientific Reports*, 2016, **6**, 22076, copyright 2016. (B) Acoustic fluorescence-activated cell sorting using focused traveling surface acoustic waves for label-free cell sorting, adapted from ref. 281 with permission from Royal Society of Chemistry, Z. Ma *et al.*, *Lab on a Chip*, 2017, **17**, 3176–3185, copyright 2017. (C) Raman image–activated cell sorting, integrating optical trapping, imaging, and Raman spectroscopy to classify and sort single cells, adapted from ref. 282 with permission from Springer Nature, N. Nitta *et al.*, *Nature Communications*, 2020, **11**, 3452, copyright 2020. (D) Single-cell barcoding and sequencing using droplet microfluidics, enabling RNA capture and downstream cDNA synthesis from individual cells, adapted from ref. 283 with permission from Springer Nature, R. Zilionis *et al.*, *Nature Protocols*, 2017, **12**, 44–73, copyright 2017. (E) SpinDrop single-cell analysis pipeline. Cells are lysed and encapsulated with barcoded beads in surfactant oil, followed by reverse transcription and downstream molecular profiling, adapted from ref. 284 with permission from Springer Nature, J. De Jonghe *et al.*, *Nature Communications*, 2023, **14**, 4788, copyright 2023. (F) ATLAS-seq for screening antigen-reactive T cells *via* aptamer-based fluorescent molecular sensors and microfluidic sorting, adapted from ref. 285 with permission from Springer Nature, S. Luo *et al.*, *Nature Communications*, 2025, **16**, 216, copyright 2025. (G) Dynamic single-cell culture array featuring cup-shaped pillars for efficient cell capture, adapted from ref. 286 with permission from American Chemical Society, D. D. Carlo *et al.*, *Analytical Chemistry*, 2006, copyright 2006. (H) Suspended micorchannel resonator for single cell density measurments and dynamic profiling of patient drug response, adapted from ref. 287 with permission from Springer Nature, W. Wu *et al.*, *Nature Biomedical Engineering*, 2025, copyright 2025. (I) Mechanical phenotyping device quantifying cell size, deformability, and viscoelastic properties for functional assesment of T-cells, adapted from ref. 288 with permission from Springer Nature, K. K. Zeming *et al.*, *Nature Communications*, 2025, **16**, 4775, copyright 2025.

CTCs at 100% purity from backgrounds as large as 1 in 20 000 white blood cells (Fig. 18A).[278] Nguyen *et al.* employed impedance detection coupled with dielectrophoresis enrichment to analyze lung CTCs.[279] This platform selectively traps and concentrates CTCs from whole blood, followed by electrical impedance measurements that differentiate tumor cells from background leukocytes. Zhang *et al.* developed a microfluidic platform integrating multiplexed SERS nanovectors and multivariate analysis for *in situ* profiling of CTC phenotypes.[280] Within this microfluidic chip, CTCs are captured using spectrally orthogonal SERS aptamer nanovectors, which specifically bind to target biomarkers on the cell surface. These approaches allow for the simultaneous detection and molecular characterization of multiple cell membrane protein biomarkers.

Many applications in oncology and immunology rely on sorting and analyzing heterogeneous cell populations with single-cell precision. Traditional FACS methods require bulky equipment, expensive reagents, and often induce mechanical stress on cells or make the cells unretrievable. These limitations motivate microfluidic alternatives that emphasize gentler actuation, reduced footprint, and improved compatibility with downstream assays. In response, Ma *et al.* developed a FACS system that utilizes focused traveling surface acoustic waves for cell sorting in a high-throughput yet gentle manner (Fig. 18B).[281] This setup achieved a purity above 86% for fluorescently labeled MCF-7 breast cancer cells isolated from blood while maintaining cell viability above 95%. Although fluorescence-based sorting is widely used, label-free approaches provide new opportunities for sorting based on molecular features that are difficult to capture with fluorescent probes. Nitta *et al.* introduced Raman image-activated cell sorting (RICS), a system that directly measures chemically specific intracellular molecular vibrations using ultrafast multicolor stimulated Raman scattering microscopy (Fig. 18C).[282] Unlike traditional sorting methods that rely on

fluorescent labels, RICS sorts cells based on intrinsic chemical composition, allowing isolation of cells by metabolic state, drug response, or cancer phenotype without external labeling.

For applications in genomic profiling, single-cell sequencing technologies have been adapted into microfluidic systems to maximize sequencing yield and information content. A key challenge in single-cell genomics is minimizing molecular loss while preserving reaction efficiency across thousands to millions of cells. By co-encapsulating single cells with uniquely tagged beads in microliter droplets, Zillionis *et al.* established a barcoding strategy that enables RNA sequencing from individual cells (Fig. 18D).[283] Building on this foundation, De Jonghe *et al.* combined droplet microfluidic and picoinjection for multistep chemistry, encouraging separate lysis and reverse transcription within droplets under optimized conditions such as heat denaturation and proteinase K treatment, which substantially improved RNA recovery and gene detection sensitivity (Fig. 18E).[284] Extending these principles to immunology, Luo *et al.* developed ATLASseq, a microfluidic single-cell platform that identifies activated T cells through an aptamer-based fluorescent readout of cytokine secretion, followed by RNA and TCR sequencing to directly map antigen-reactive repertoires (Fig. 18F).[285]

Microfluidic platforms are increasingly applied to probe the functional and mechanical properties of cells, addressing dimensions of cellular state that are invisible to transcriptomic analysis alone. Di Carlo *et al.* established a dynamic single cell culture array, where thousands of cells are captured in hydrodynamic traps and analyzed with functional assays at single cell resolution (Fig. 18G).[286] Wu *et al.* utilized suspended microchannel resonators to characterize single cell mass, volume, and density, enabling dynamic profiling of immune cell states and drug responses based on biophysical characteristics (Fig. 18H).[287] Zeming *et al.* developed a trajectory modulation platform that evaluates CAR-T cells based on their migratory behavior under controlled shear and lateral flows, providing a rapid means of functional phenotyping based on activation state and exhaustion status (Fig. 18I).[288] Complementing these physical assays, Feng *et al.* devised a bead-based system to map the sequence and force dependence of T-cell activation, directly linking molecular recognition to mechanical signaling.[289] Collectively, these technologies extend single-cell analysis into the domain of biophysics and immunotherapy, offering tools to connect cellular function with therapeutic potential.

4.5 Microfluidic platforms for formation of organoid and tissue monitoring

Organoids, organ-on-a-chip models, and other microfluidic tissue systems provide realistic systems that recapitulate drug responses, disease progression, and tissue level physiology more effectively than conventional *in vitro* cultures.[290–294] By integrating flow, biomimetic scaffolds, and embedded biosensors, these platforms provide label-free monitoring of

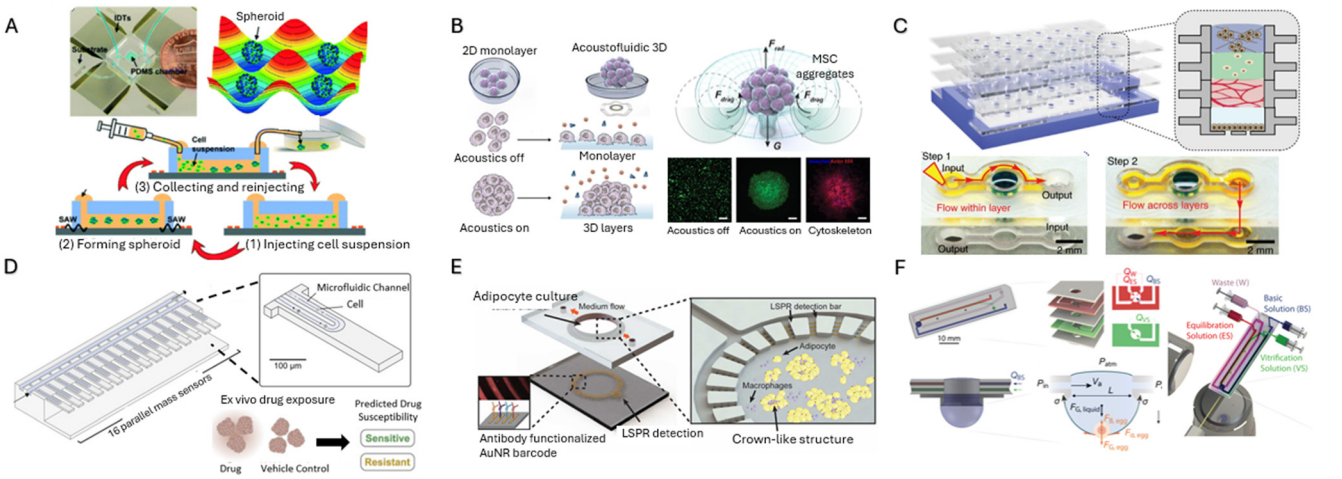

Fig. 19 Integrated microfluidic platforms for organoid and tissue formation and monitoring. (A) 3D acoustic tweezers for rapid formation of size-controllable multicellular spheroids, adapted from ref. 296 with permission from Royal Society of Chemistry, K. Chen *et al.*, *Lab on a Chip*, 2016, 16, 2636–2643, copyright 2016. (B) Acoustofluidic interface for modulating and analyzing the mechanobiological secretome of mesenchymal stem cells, adapted from ref. 297 with permission from Springer Nature, Y. He *et al.*, *Nature Communications*, 2023, **14**, 7639, copyright 2023. (C) Reconfigurable open microfluidic platform enabling dynamic layering, assembly, and disassembly of microenvironments to probe spatiotemporal paracrine signaling, adapted from ref. 298 with permission from Springer Nature, J. Yu *et al.*, *Nature Biomedical Engineering*, 2019, **3**, 830–841, copyright 2019. (D) Suspended microchannel resonator for predicting patient drug response from organoid mass change, adapted from ref. 302 with permission from Elsevier, M. A. Stockslager *et al.*, *Cell Reports*, 2021, **37**, copyright 2021. (E) Multiplexed LSPR biosensor integrated with an adipocyte culture chamber for monitoring macrophage-adipocyte interactions, adapted from ref. 303 with permission from Royal Society of Chemistry, J. Zhu *et al.*, *Lab on a Chip*, 2018, **18**, 3550–3560, copyright 2018. (F) Programmable microfluidic egg vitrification platform inside a hanging droplet, adapted from ref. 304 with permission from Royal Society of Chemistry, H. Feng *et al.*, *Lab on a Chip*, 2024, **24**, 5225–5237, copyright 2024.

organ function and cell–environment interactions. In particular, a growing emphasis has been placed on building physiologically relevant 3D structures and probing their mechanobiological function.[295] Chen *et al.* demonstrated the rapid formation of size-controllable multicellular spheroids *via* 3D acoustic tweezers, enabling the scalable and uniform assembly of spheroids for various downstream applications (Fig. 19A).[296] In addition to assembly, acoustics has also been used to stimulate cells and tissues. He *et al.* developed acoustofluidic interfaces to probe the mechanobiological secretome of mesenchymal stem cells, showing how acoustic forces can regulate cytokine secretion and paracrine signaling in a controlled microenvironment (Fig. 19B).[297]

Yu *et al.* expanded the modularity of 3D culture systems with the Stacks platform, an open, reconfigurable microfluidic architecture composed of vertically layered culture modules that can be assembled and disassembled to study paracrine signaling and spatially organized tissue interactions (Fig. 19C).[298] Each layer functions as an independent microenvironment, and when stacked, the modules permit diffusion driven communication across tissues for dynamic modeling of complex physiological processes such as immune–tumor interactions, vascular invasion, and morphogen gradients.

Yang *et al.* developed a liver-on-a-chip platform integrated with optical biosensors for non-invasive tracking of hepatotoxic effects.[299] This system mimics the natural environment of liver cells by integrating blood flow and nutrient exchange into the culture. Optical biosensors embedded within the chip detect metabolic changes and cellular stress responses under drug exposure, allowing continuous liver function assessment. Yang *et al.* employed fluorescent nanodiamonds for detection of free radical generation in human umbilical vein endothelial cells under shear stress.[300] This system combines microfluidics induced shear stress with quantitative fluorescence tracking of reactive oxygen species production, revealing how vascular cells respond to mechanical forces.

For broader drug response analysis, Zhang *et al.* developed a microfluidic chip for automated whole-course drug response monitoring in organoids.[301] This platform automates media exchange, reagent delivery, and live-cell imaging to analyze the longitudinal effects of drugs on 3D tissue cultures. Stockslager *et al.* utilized suspended microchannel resonators to measure mass accumulation rates in tumor cells under drug exposure (Fig. 19D).[302] This approach was able to predict clinical treatment outcomes in patient-derived neurosphere models, offering a powerful oncology tool for screening drug candidates.

Cytokine profiling for inflammation is also a key factor in metabolic disorders, prompting Zhu *et al.* to develop an adipose-tissue-on-a-chip platform for investigating obesity-associated inflammation (Fig. 19E).[303] This nanoplasmonic biosensing platform enables monitoring of inflammatory

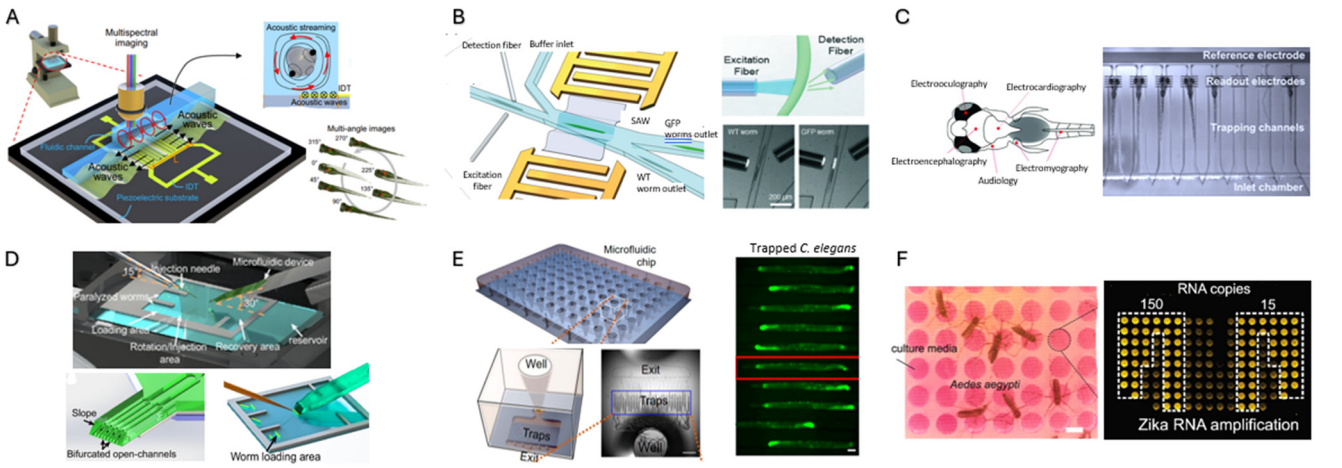

Fig. 20 Integrated microfluidic platforms for small organism studies. (A) Acoustofluidic rotational tweezing achieves high-speed, contactless morphological phenotyping of zebrafish larvae by generating controlled acoustic streaming vortices for rotational imaging, adapted from ref. 309 with permission from Springer Nature, C. Chen *et al.*, *Nature Communications*, 2021, **12**, 1118, copyright 2021. (B) Acoustofluidic sorting and fluorescence detection of *C. elegans*. Surface acoustic waves guide worms for optical characterization, enabling high-throughput phenotypic screening, adapted from ref. 311 with permission from Royal Society of Chemistry, J. Zhang *et al.*, *Lab on a Chip*, 2020, **20**, 1729–1739, copyright 2020. (C) A long-term, multichannel, non-invasive monitoring platform for electrophysiological signals derived from zebrafish larvae, providing simultaneous measurements across multiple modalities (*i.e.*, electrocardiography, electrooculography, electromyography, and audiology), adapted from ref. 314 with permission from Springer Nature, S. Hong *et al.*, *Scientific Reports*, 2016, **6**, 28248, copyright 2016. (D) Robotic microinjection tool for large-scale transgenic studies in *C. elegans*, allowing automated injections into immobilized worms, adapted from ref. 315 with permission from Springer Nature, P. Pan *et al.*, *Nature Communications*, 2024, **15**, 8848, copyright 2024. (E) Screening platform used to identify σ2R/Tmem97 binding ligands that mitigate age-dependent neurodegeneration in *C. elegans*, adapted from ref. 316 with permission from American Chemical Society, S. Mondal *et al.*, *ACS Chemical Neuroscience*, 2018, **9**, 1014–1026, copyright 2018. (F) A microfluidic device for highly parallel "bite-by-bite" profiling of mosquito-borne pathogen transmission, yielding real-time monitoring of viral RNA amplification in individual mosquito feeding events, adapted from ref. 318 with permission from Springer Nature, S. Kumar *et al.*, *Nature Communications*, 2021, **12**, 6018, copyright 2021.

cytokine secretion from adipocytes and immune cells cultured within a 3D microfluidic environment. By integrating plasmonic resonance detection, the system provides label-free, highly sensitive measurements of inflammation-related biomolecules, allowing researchers to study adipose tissue dysfunction and metabolic disease progression with high precision.

Feng *et al.* introduced a microfluidic platform that suspends an egg within a millimeter-scale hanging droplet with programmable pumps for automated cryoprotectant loading for vitrification (Fig. 19F).[304] The system maintains ~95% post-thaw survival rates across more than 100 mouse oocytes, indicating it matches manual protocols in efficacy while enhancing consistency and throughput. Moreover, microscopy monitors egg morphology during the process, opening possibilities for future linkage between morphological changes and functional outcomes.

Brain organoids have also been employed as computational reservoirs, where computing architectures were implemented using living neural networks.[305] This concept utilizes the signaling and network dynamics of organoids for information processing, illustrating a convergence of microfluidics, tissue engineering, and information processing. While still at a proof-of-concept stage, such work highlights how organoid-on-chip systems may extend into both biomedical and biohybrid computational domains.

4.6 Integrated microfluidic platforms for small organism studies

Microfluidic systems have become powerful tools for studying intact small organisms such as *C. elegans*, zebrafish, and *Drosophila.*[306,307] These platforms not only provide imaging and functional readouts but also overcome the limitations of manual handling by providing precise control over positioning, sorting, and stimulation. By integrating physical, optical, acoustic, and electrical forces into chip-scale environments, researchers can now probe organismal physiology and behavior with speed and reproducibility that were not possible with traditional methods.

Precise alignment and rotation of small organisms are essential for high-resolution imaging, morphological phenotyping, and quantitative behavioral analysis. Traditional approaches rely on chemical anesthetics or mechanical traps, which can alter biological responses.[308] To overcome these limitations, Chen *et al.* developed an acoustofluidic rotational tweezing system that uses surface acoustic waves to manipulate zebrafish larvae for high speed and contactless phenotypic analysis (Fig. 20A).[309] Similarly, Zhang *et al.* employed surfaces acoustic waves to induce rotational movement in *C. elegans*, allowing for precise orientation control within microfluidic devices for automated imaging and locomotion studies.[310] Together, these studies illustrate how acoustofluidics can serve both as a non invasive construction tool and as a dynamic mechanical stimulus, offering advantages over static mechanical loading methods that lack temporal tunability.

Automated sorting is critical for large-scale genetic screens and behavioral studies, where manual selection methods are inefficient and error prone. Zhang *et al.* developed a fluorescence-based acoustofluidic sorting system for *C. elegans*, using surface acoustic waves to selectively direct worms based on genetic fluorescence markers, improving sorting speed and accuracy (Fig. 20B).[311] This system eliminates the need for manual pipetting or microscopy guided selection and expedites screening protocols for genetic variants. Mani *et al.* introduced a noninvasive, light-driven microfluidic technique for transporting and sorting zebrafish larvae, eliminating the need for physical manipulation.[312] Aubry *et al.* developed a hydrogel-droplet microfluidic framework for high-resolution imaging and sorting of early *C. elegans* larvae, encapsulating individual organisms in droplet microenvironments to ensure uniform conditions and precise manipulation.[313]

Integrated microfluidic and electrophysiological biosensing technologies offer exciting possibilities for carefully stimulating and monitoring responses in small organisms. Hong *et al.* developed a multi-channel electrophysiology platform that tracks zebrafish neural activity without invasive probes. This innovation paves the way for long-term, non-intrusive monitoring across multiple channels simultaneously. It supports various measurements, including electrocardiography, electrooculography, electromyography, and audiology, making it a versatile and user-friendly tool for researchers (Fig. 20C).[314] Pan *et al.* introduced a robotic microinjection system to automate transgenic studies in *C. elegans*, delivering genetic material into thousands of worms to generate transgenic lines with high throughput (Fig. 17D).[315] For drug discovery applications, Mondal *et al.* designed a high-content microfluidic screening platform to test compounds targeting neurodegeneration in a *C. elegans* Alzheimer's model, allowing for automated tracking of neuronal integrity and behavioral phenotypes (Fig. 20E).[316]

Expanding microfluidic applications to developmental biology, Bai *et al.* introduced a microfluidic system for monitoring the cleavage cycles of Drosophila embryos, granting precise perturbation and observation of early embryonic divisions.[317] This platform allows researchers to control the microenvironment, apply chemical and mechanical stimuli, and track cell division dynamics in real time, providing valuable insights into embryonic development and cellular responses to external perturbations. Researchers have also applied microfluidics to vector biology: a bite-by-bite profiling system was created to study mosquito feeding and pathogen transmission dynamics within a controlled chip environment (Fig. 20F).[318] By supporting parallel monitoring of feeding events and pathogen transfer at single-mosquito resolution, this approach provides a scalable framework for understanding disease transmission mechanisms. These lab-on-a-chip

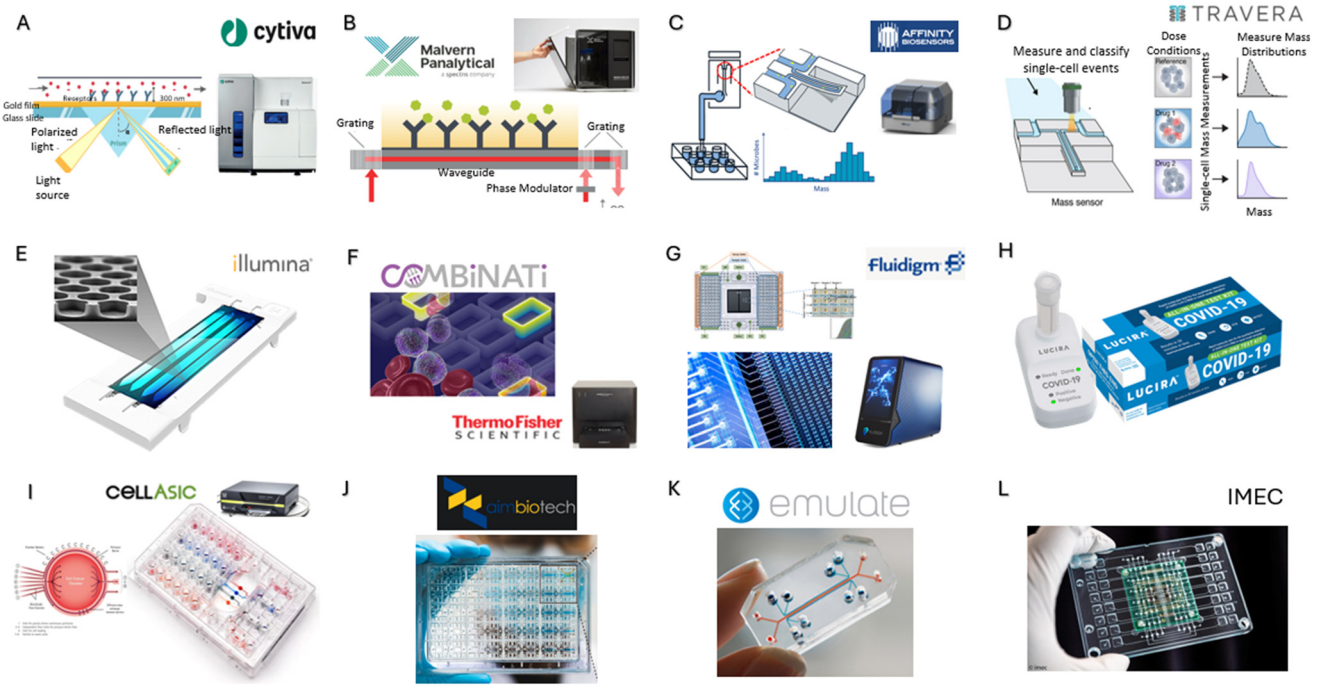

Fig. 21 Commercial systems for microfluidic sensors. (A) Cytiva Biacore SPR system. Schematic of a prism-based SPR imaging setup, where an acousto-optic deflector directs light through a prism and binding events are monitored by a camera.[319] Image reproduced with permission from Cytiva. (B) Malvern Panalytical waveguide system using gratings and phase modulators for highly sensitive refractive index detection.[322] Image reproduced with permission from Malvern Panalytical. (C) Affinity Biosensors suspended microchannel resonator system for mass-based binding assays and molecular interaction profiling.[323] Image reproduced with permission from Affinity Biosensors. Image reproduced with permission from Travera. (D) Travera single-cell mass platform measuring dose–response, drug resistance, and cell mass distributions with machine learning classification.[324] (E) Illumina NovaSeq 6000 for microfluidic enabled next-generation sequencing.[325] Image reproduced with permission from Illumina. (F) Combinati Absolute Q digital PCR system using microfluidic array partitioning for streamlined, high-sensitivity nucleic acid quantification.[326] Image reproduced with permission from Combinati. (G) Fluidigm BioMar X9 microfluidic integrated fluidic circuit used for high-throughput gene expression and genotyping analysis.[327] Image reproduced with permission from Fluidigm. (H) Lucira COVID-19 molecular test strip providing rapid, at-home detection.[328] Image reproduced with permission from Lucira Health. (I) CellASIC's ONIX microfluidic platform enables long-term, dynamically perfused cell culture with precise control of nutrients, gases, and mechanical cues.[329] Image reproduced with permission from CellASIC (J) AIM Biotech 3D microfluidic culture chip enabling physiologically relevant co-culture and perfusion-based tissue modeling.[330] Image reproduced with permission from AIM Biotech. (K) Emulated organ-chip platform with stretchable and rigid microfluidic chips, incorporating tissue–tissue interfaces and flow control.[331] (L) IMEC high-density microelectrode array integrated with microfluidics for large-scale, high-resolution electrophysiological recording.[333] Image reproduced with permission from IMEC.

approaches provide scalable insights into organismal physiology and disease progression, advancing research in neuroscience, toxicology, developmental biology, and regenerative medicine.

4.7 Commercial systems

A number of commercial platforms integrating microfluidics and biosensing have been developed for robust, laboratory-grade research and development. Among these, surface plasmon resonance systems (SPR) dominate, but other novel sensing modalities are beginning to emerge.

Cytiva's Biacore SPR platforms, widely adopted across academia and industry, emphasize versatility with instruments ranging from benchtop to fully automated systems, facilitating routine biomolecular interaction analysis (Fig. 21A).[319] Bruker's Sierra SPR-32 Pro exemplifies the latest in multiplexed SPR technology, allowing simultaneous measurement of up to 32 interactions with high throughput and minimal sample consumption.[320] Similarly, Carterra's LSA system combines flow printing microfluidics with SPR sensing to perform large-scale binding kinetics and epitope mapping, supporting pharmaceutical monoclonal antibody discovery pipelines where screening thousands of interactions in parallel is essential.[321]

As an alternative to SPR, Malvern Panalytical has released the Creoptix WAVEsystem, which relies on waveguide coupled interferometry (Fig. 21B).[322] Unlike SPR, which detects refractive index changes at a metal surface, each photon in WAVEsystem travels through the whole waveguide, resulting in more interactions and increased sensitivity. This makes it particularly valuable for small molecule detection and fragment screening in drug discovery, where sensitivity to low-mass analytes is critical.

Other microfluidic biosensors have found commercial use, such as the suspended microchannel resonator (SMR). Affinity Biosensors has developed the LifeScale AST system, which leverages SMR technology to measure individual

bacterium mass and morphology for antibiotic susceptibility testing (Fig. 21C).[323] Rather than waiting for visible growth, LifeScale detects earlier phenotypic responses—such as changes in mass or shape—allowing many antibiogram results in approximately 41/2 hours following a positive blood culture.

Another SMR derived platform comes from Travera, which measures cancer cell mass accumulation rates with sub-picogram precision (Fig. 21D).[324] This functional biomarker provides readouts of drug efficacy within days, enabling oncologists to rapidly assess how patient-derived tumor cells respond to specific treatments. By directly quantifying growth or shrinkage at the single-cell level, the Travera system translates microfluidic measurement science into a clinically actionable tool for guiding personalized cancer therapy.

Integrated microfluidic biosensors have also translated into commercial molecular testing devices. Illumina's NovaSeq 6000 employs precision microfluidics to automate reagent delivery, fluid exchange, and optical scanning across patterned nanowell flow cells for next-generation sequencing (Fig. 21E).[325] Combinati's Absolute Q digital PCR system is designed for research and clinical laboratories, where it streamlines digital PCR workflows by replacing droplet generation with a microfluidic array of thousands of nanoliter partitions (Fig. 21F).[326] Fluidigm's BioMark X9 platform represents another microfluidic PCR platform, combining pressure-driven microvalve control with nanoliter reaction chambers for high-throughput digital PCR and gene expression analysis (Fig. 21G).[327] The Lucira COVID-19 molecular test kit provides an avenue for point-of-care testing, integrating sample preparation, isothermal amplification, and readout into a disposable strip for rapid, at-home detection of SARS-CoV-2 with clinical-grade accuracy in under 30 minutes (Fig. 21H).[328]

Commercial cell culture platforms have also emerged as a robust foundation for drug development and toxicology testing. CellASIC's ONIX Microfluidic Platform is widely adopted for dynamic cell culture, enabling precise control over perfusion, gas exchange, and mechanical stress in microscale chambers (Fig. 21I).[329] This platform allows long-term culture of mammalian, microbial, and yeast cells under tunable microenvironments, supporting both fundamental biology and high-content imaging assays. AIM Biotech's 3D microfluidic culture chips enable physiologically relevant co-culture and perfusion-based tissue modeling within optically clear, polymer-based channels (Fig. 21J).[330]

Emulate has established itself as a leader in organ-on-chip commercialization, with ready-to-use microfluidic devices preconfigured for models such as liver, gut, lung, and the blood–brain barrier (Fig. 21K).[331] These systems incorporate perfusion, flexible membranes, and co-culture capabilities, allowing researchers to recreate key physiological functions and model disease states with higher fidelity than static culture. Mimetas offers the OrganoReady platform, a collection of pre-seeded, assay-ready 3D tissue models for immediate use in barrier integrity, transport, and toxicity assays without the need for in-house culture.[332] This approach emphasizes compatibility with high-throughput screening while maintaining physiologically relevant microenvironments, making it well-suited for pharmaceutical discovery pipelines.

Imec complements these efforts by developing high-density CMOS microelectrode array chips integrated with microfluidics, providing thousands of recording and stimulation sites across cultured tissues (Fig. 21L).[333,334] These platforms facilitate the creation of detailed maps of neuronal networks, brain organoids, and cardiac tissues. At the same time, they allow for targeted chemical delivery through fluidic channels. By combining large-scale electrophysiological recordings with precise microfluidic control, Imec's systems open up exciting possibilities for drug screening, disease modeling, and basic neuroscience research.

4.8 Potential impact of AI on microfluidic biosensing

As integrated microfluidic biosensors grow in complexity and information density, artificial intelligence (AI) is emerging as a key enabling layer for data interpretation, system control, and device design. A primary impact of AI lies in signal extraction and interpretation. Integrated biosensors routinely generate complex electrochemical, optical, spectroscopic, electrophysiological, and image-based readouts that are confounded by noise, sample variability, and nonlinear responses.[335] Machine learning approaches have demonstrated strong capability in denoising signals, classifying spectral features, and extracting diagnostically relevant information, extending the practical sensitivity and specificity of label-free electrochemical, plasmonic, and Raman sensing in realistic biological samples.[336,337]

AI further enables adaptive and closed-loop operation of microfluidic systems. Active platforms such as acoustofluidic, dielectrophoretic, optofluidic, and digital microfluidic devices involve large, coupled parameter spaces that are difficult to tune manually. Reinforcement learning and adaptive control algorithms offer a pathway toward autonomous operation, where actuation parameters are adjusted in real time based on sensor feedback, enabling self-optimization of sample handling, enrichment, and sensing conditions.[338,339]

In parallel, AI is reshaping device design and optimization. Physics-informed learning and surrogate models accelerate exploration of high-dimensional design spaces spanning channel geometry, field configurations, sensing interfaces, and materials, reducing reliance on trial-and-error optimization.[340] These approaches are particularly valuable for hybrid systems that integrate multiple physical mechanisms, where analytical modeling becomes intractable.

AI also provides a framework for interpreting biological heterogeneity inherent to single cell, single vesicle, and single molecule measurements.[341,342] Rather than treating variability as noise, clustering and predictive modeling

approaches enable functional stratification of populations, supporting precision diagnostics and data-driven biomanufacturing strategies.

Looking ahead, AI is likely to evolve from a post-processing tool into a core architectural component of integrated microfluidic biosensors, enabling closed-loop, adaptive analytical systems. By unifying sensing, control, and decision-making, AI-enabled platforms have the potential to move the field beyond static measurements toward robust, autonomous systems capable of supporting real-world diagnostics and quantitative life science applications.

5. Promise and challenges for translation

5.1 Current readiness landscape

At present, integrated microfluidic biosensors occupy a wide spectrum of technological readiness. Certain components—such as inertial microfluidic separation, electrochemical sensing, and capillary-driven distance-based readouts—have already demonstrated compatibility with scalable fabrication and, in some cases, commercial deployment. In contrast, more complex platforms incorporating active field-driven manipulation, advanced optical sensing, or quantum readout often rely on specialized instrumentation, bespoke fabrication, and expert operation, limiting their near-term translational viability.

Importantly, readiness is rarely determined by a single subsystem. Many platforms exhibit mature microfluidic handling but rely on fragile sensing surfaces, nonstandard materials, or computationally intensive post-processing pipelines. Conversely, highly sensitive sensing modalities may be bottlenecked by upstream sample preparation or downstream data interpretation. Translation therefore depends not only on individual component maturity, but on system-level integration, robustness, and reproducibility across the full workflow.

5.2 Key barriers to clinical and industrial adoption

Several recurring challenges impede the transition from academic prototypes to deployable systems:

1. Manufacturability and scalability present additional hurdles. Devices fabricated using complex multilayer soft lithography, nanoscale patterning, or custom assembly often lack clear pathways to high-volume, low-cost production. Translational success requires early consideration of scalable manufacturing methods—such as injection molding, roll-to-roll processing, wafer-level fabrication, or standardized cartridge architectures—rather than *post hoc* adaptation of research prototypes.

2. System complexity and user burden further constrain adoption. Many integrated microfluidic biosensors require expert calibration, alignment, or interpretation, which is incompatible with clinical workflows or decentralized testing. Even highly sensitive platforms may fail to translate if they impose excessive operational steps, fragile handling, or opaque outputs that do not align with user expectations.

3. Validation and regulatory alignment are also frequently under-addressed in early-stage research. Demonstrations often rely on small sample sizes, spiked analytes, or idealized conditions that do not reflect clinical heterogeneity. Without systematic benchmarking against gold standards, inter-laboratory reproducibility studies, and clearly defined performance metrics, promising technologies struggle to advance beyond exploratory validation.

Successful translation requires a shift from technology driven demonstrations toward user friendly design. Clinical, industrial, and field users prioritize robustness, simplicity, and interpretability over maximal sensitivity or technical sophistication. Designing with end users in mind—from clinicians to technicians to patients—necessitates early engagement with workflow constraints, sample realities, and decision-making needs.

In this context, instrument-free or minimally instrumented readouts, automated operation, and intuitive outputs often provide greater translational value than marginal gains in analytical performance. Similarly, AI-enabled analysis holds promise not only for improving sensitivity, but for simplifying interpretation and reducing operator dependence, provided that models are validated and deployable within realistic computational constraints.

5.3 A translational roadmap

Taken together, the path from proof-of-concept to full deployment can be conceptualized as a four-stage progression:

1. Integration – unifying sample handling, sensing, and analysis into fully enclosed, user-ready systems that function seamlessly as end-to-end platforms.

2. Reproducibility and robustness – rigorous stress-testing of devices under realistic sample conditions and operational scenarios to ensure consistent and reliable performance.

3. Standardization and validation – benchmarking performance against established methods across diverse datasets, ensuring comparability, accuracy, and broad applicability.

4. Manufacturing and deployment – addressing scalability, cost efficiency, and regulatory requirements in parallel with application-specific design to enable real-world adoption.

This staged roadmap provides a clear pathway to translate innovative technologies from the laboratory to practical, deployable solutions.

Integrated microfluidic biosensors are uniquely positioned to impact quantitative life sciences and diagnostics, but realizing this promise requires confronting translational challenges with the same rigor applied to technical innovation. By explicitly addressing readiness, manufacturability, standardization, and user-centered design, the field can move beyond isolated demonstrations toward

reliable, deployable systems that genuinely shape the future of diagnostics and biological measurement.

6. Conclusion

In response to the escalating demand for rapid, precise, and multifunctional biological testing platforms, microfluidic technologies are being increasingly adapted to fulfill the changing needs of both foundational research in quantitative life sciences and clinical diagnostics and therapeutics. The continuous advancement of innovative separation and detection techniques, including dielectrophoresis, acoustofluidics, inertial microfluidics, electrochemical sensors, SERS, and quantum biosensing, will persist in augmenting the capabilities of integrated microfluidic biosensors. Emerging trends in multiplexed detection, AI-driven analytics, and automation are expected to drive these technologies toward widespread clinical adoption and point-of-care applications. Additionally, as these platforms become more cost-effective and user-friendly, their potential for integration into global healthcare systems will increase, enhancing accessibility to high-quality diagnostics worldwide. Despite these advancements, challenges remain in the standardization, reproducibility, and scalability of integrated microfluidic biosensors. Addressing these issues requires interdisciplinary collaboration among engineers, biologists, and clinicians to refine device designs, optimize detection methods, and validate clinical utility. In summary, integrating microfluidics with biosensors holds great promise for advancing the quantitative life sciences, personalized and precision medicine, and fundamental biomedical discoveries in biomedical science. Through the continuous enhancement of sensitivity, specificity, and automation, integrated microfluidic biosensors are poised to play a central role in developing next-generation diagnostic and analytical technologies for quantitative biology and translational medicine.

Author contributions

Conceptualization: T. N., S. Y., L. P. L., and T. J. H. Supervision: S. Y., L. P. L., and T. J. H. writing – original draft: T. N., C. N., Q. W., A. C., K. C., S. Z., Y. L. writing – review and editing: S. Y., C. N., Z. M., K. J., Y. H., L. P. L., and T. J. H.

Conflicts of interest

T. J. H. has co-founded a start-up company, Ascent Bio-Nano Technologies Inc., to commercialize technologies involving acoustofluidics and acoustic tweezers. The remaining authors declare no competing interests.

Data availability

No primary research results, software or code have been included and no new data were generated or analyzed as part of this review.

Acknowledgements

We acknowledge support from the National Institutes of Health R01AG084098 (T. J. H.), R01GM141055 (T. J. H.), R01HD103727 (T. J. H.), R01GM145960 (T. J. H.), R01GM144417 (T. J. H.), R44GM154514 (T. J. H.), R44GM154515 (T. J. H.), and R01GM145960 (L. P. L.)), and the National Science Foundation (CMMI-2104295 (T. J. H.)).

References

1 C. P. Y. Chan, *et al.*, Evidence-based point-of-care diagnostics: current status and emerging technologies, *Annu. Rev. Anal. Chem.*, 2013, **6**, 191–211.
2 P. S. Gaikwad and R. Banerjee, Advances in point-of-care diagnostic devices in cancers, *Analyst*, 2018, **143**, 1326–1348.
3 V. Gubala, L. F. Harris, A. J. Ricco, M. X. Tan and D. E. Williams, Point of care diagnostics: status and future, *Anal. Chem.*, 2012, **84**, 487–515.
4 S. Amartumur, *et al.*, Neuropathogenesis-on-chips for neurodegenerative diseases, *Nat. Commun.*, 2024, **15**, 2219.
5 F. B. Myers and L. P. Lee, Innovations in optical microfluidic technologies for point-of-care diagnostics, *Lab Chip*, 2008, **8**, 2015–2031.
6 J. J. Lai, *et al.*, Exosome processing and characterization approaches for research and technology development, *Adv. Sci.*, 2022, **9**, 2103222.
7 M. E. Badawy, M. A. El-Nouby, P. K. Kimani, L. W. Lim and E. I. Rabea, A review of the modern principles and applications of solid-phase extraction techniques in chromatographic analysis, *Anal. Sci.*, 2022, **38**, 1457–1487.
8 C. Suwanvecho, L. K. Krčmová and F. Švec, Centrifugal-assisted sample preparation techniques: Innovations and applications in bioanalysis, *TrAC, Trends Anal. Chem.*, 2024, 117909.
9 N. T. Holland, M. T. Smith, B. Eskenazi and M. Bastaki, Biological sample collection and processing for molecular epidemiological studies, *Mutat. Res., Rev. Mutat. Res.*, 2003, **543**, 217–234.
10 L. Nováková and H. Vlčková, A review of current trends and advances in modern bio-analytical methods: chromatography and sample preparation, *Anal. Chim. Acta*, 2009, **656**, 8–35.
11 S. Choi, M. Goryll, L. Y. M. Sin, P. K. Wong and J. Chae, Microfluidic-based biosensors toward point-of-care detection of nucleic acids and proteins, *Microfluid. Nanofluid.*, 2011, **10**, 231–247.
12 M. B. Kulkarni, N. H. Ayachit and T. M. Aminabhavi, Biosensors and microfluidic biosensors: from fabrication to application, *Biosensors*, 2022, **12**, 543.
13 A. Y. Jiang, *et al.*, High-throughput continuous dielectrophoretic separation of neural stem cells, *Biomicrofluidics*, 2019, **13**(6), 064111.
14 M. D. Vahey and J. Voldman, High-throughput cell and particle characterization using isodielectric separation, *Anal. Chem.*, 2009, **81**, 2446–2455.

15 D. Ahmed, *et al.*, Neutrophil-inspired propulsion in a combined acoustic and magnetic field, *Nat. Commun.*, 2017, **8**, 1–8.
16 M. Antfolk, P. B. Muller, P. Augustsson, H. Bruus and T. Laurell, Focusing of sub-micrometer particles and bacteria enabled by two-dimensional acoustophoresis, *Lab Chip*, 2014, **14**, 2791–2799.
17 L. Cox, K. Melde, A. Croxford, P. Fischer and B. W. Drinkwater, Acoustic hologram enhanced phased arrays for ultrasonic particle manipulation, *Phys. Rev. Appl.*, 2019, **12**, 064055.
18 N. Xiang and Z. Ni, Inertial microfluidics: current status, challenges, and future opportunities, *Lab Chip*, 2022, **22**, 4792–4804.
19 Z. Zhou, *et al.*, Inertial microfluidics for high-throughput cell analysis and detection: a review, *Analyst*, 2021, **146**, 6064–6083.
20 T. P. Miettinen, *et al.*, Cell size, density, and nutrient dependency of unicellular algal gravitational sinking velocities, *Sci. Adv.*, 2024, **10**, eadn8356.
21 W. Wu, *et al.*, Plasma membrane folding enables constant surface area-to-volume ratio in growing mammalian cells, *Curr. Biol.*, 2025, **35**(7), 1601–1611.
22 M. Andre, *et al.*, Diagnostic potential of exosomal extracellular vesicles in oncology, *BMC Cancer*, 2024, **24**, 322.
23 M. Andre, M. Nair and A. D. Raymond, HIV Latency and nanomedicine strategies for anti-HIV treatment and eradication, *Biomedicines*, 2023, **11**, 617.
24 Z. Liu, *et al.*, Microfluidic biosensors for biomarker detection in body fluids: a key approach for early cancer diagnosis, *Biomark. Res.*, 2024, **12**, 1–29.
25 A. Lenshof and T. Laurell, Continuous separation of cells and particles in microfluidic systems, *Chem. Soc. Rev.*, 2010, **39**, 1203–1217.
26 P. Sajeesh and A. K. Sen, Particle separation and sorting in microfluidic devices: a review, *Microfluid. Nanofluid.*, 2014, **17**, 1–52.
27 M. R. Luskin, M. A. Murakami, S. R. Manalis and D. M. Weinstock, Targeting minimal residual disease: a path to cure?, *Nat. Rev. Cancer*, 2018, **18**, 255–263.
28 T. M. Squires, R. J. Messinger and S. R. Manalis, Making it stick: convection, reaction and diffusion in surface-based biosensors, *Nat. Biotechnol.*, 2008, **26**, 417–426.
29 A. L. Gimpel, *et al.*, Analytical methods for process and product characterization of recombinant adeno-associated virus-based gene therapies, *Mol. Ther. Methods Clin. Dev.*, 2021, **20**, 740–754.
30 P. W. Barone, *et al.*, Viral contamination in biologic manufacture and implications for emerging therapies, *Nat. Biotechnol.*, 2020, **38**, 563–572.
31 V. Narayanamurthy, *et al.*, Advances in passively driven microfluidics and lab-on-chip devices: A comprehensive literature review and patent analysis, *RSC Adv.*, 2020, **10**, 11652–11680.
32 Y. Zhang, *et al.*, From passive to active sorting in microfluidics: A review, *Rev. Adv. Mater. Sci.*, 2021, **60**, 313–324.
33 T. Zhang, *et al.*, Passive microfluidic devices for cell separation, *Biotechnol. Adv.*, 2024, **71**, 108317.
34 H. Amini, W. Lee and D. Di Carlo, Inertial microfluidic physics, *Lab Chip*, 2014, **14**, 2739–2761.
35 Q. Zhao, D. Yuan, J. Zhang and W. Li, A review of secondary flow in inertial microfluidics, *Micromachines*, 2020, **11**, 461.
36 D. Di Carlo, Inertial microfluidics, *Lab Chip*, 2009, **9**, 3038–3046.
37 W. Tang, *et al.*, Channel innovations for inertial microfluidics, *Lab Chip*, 2020, **20**, 3485–3502.
38 J. Zhang, *et al.*, Fundamentals and applications of inertial microfluidics: A review, *Lab Chip*, 2016, **16**, 10–34.
39 A. A. S. Bhagat, S. S. Kuntaegowdanahalli and I. Papautsky, Continuous particle separation in spiral microchannels using dean flows and differential migration, *Lab Chip*, 2008, **8**, 1906–1914.
40 H. Jeon, *et al.*, Elasto-inertial microfluidic separation of microspheres with submicron resolution at high-throughput, *Microsyst. Nanoeng.*, 2024, **10**, 15.
41 C. Renier, *et al.*, Label-free isolation of prostate circulating tumor cells using Vortex microfluidic technology, *npj Precis. Oncol.*, 2017, **1**, 15.
42 M. Li, M. van Zee, K. Goda and D. Di Carlo, Size-based sorting of hydrogel droplets using inertial microfluidics, *Lab Chip*, 2018, **18**, 2575–2582.
43 Y. Zhou, Z. Ma, M. Tayebi and Y. Ai, Submicron particle focusing and exosome sorting by wavy microchannel structures within viscoelastic fluids, *Anal. Chem.*, 2019, **91**, 4577–4584.
44 H. Jeon, T. Kwon, J. Yoon and J. Han, Engineering a deformation-free plastic spiral inertial microfluidic system for CHO cell clarification in biomanufacturing, *Lab Chip*, 2022, **22**, 272–285.
45 H. Jeon, C. R. Perez, T. Kyung, M. E. Birnbaum and J. Han, Separation of Activated T Cells Using Multidimensional Double Spiral (MDDS) Inertial Microfluidics for High-Efficiency CAR T Cell Manufacturing, *Anal. Chem.*, 2024, **96**(26), 10780–10790.
46 H. Kim, A. Zhbanov and S. Yang, Microfluidic systems for blood and blood cell characterization, *Biosensors*, 2022, **13**, 13.
47 R. Nasiri, *et al.*, Microfluidic-based approaches in targeted cell/particle separation based on physical properties: fundamentals and applications, *Small*, 2020, **16**, 2000171.
48 R. T. Davies, *et al.*, Microfluidic filtration system to isolate extracellular vesicles from blood, *Lab Chip*, 2012, **12**, 5202–5210.
49 Z. Li, *et al.*, Cascaded microfluidic circuits for pulsatile filtration of extracellular vesicles from whole blood for early cancer diagnosis, *Sci. Adv.*, 2023, **9**, eade2819.
50 L. R. Huang, E. C. Cox, R. H. Austin and J. C. Sturm, Continuous particle separation through deterministic lateral displacement, *Science*, 2004, **304**, 987–990.
51 B. H. Wunsch, *et al.*, Nanoscale lateral displacement arrays for the separation of exosomes and colloids down to 20 nm, *Nat. Nanotechnol.*, 2016, **11**, 936–940.

52 M. Yamada, W. Seko, T. Yanai, K. Ninomiya and M. Seki, Slanted, asymmetric microfluidic lattices as size-selective sieves for continuous particle/cell sorting, *Lab Chip*, 2017, **17**, 304–314.
53 S. H. Ko, *et al.*, Nanofluidic device for continuous multiparameter quality assurance of biologics, *Nat. Nanotechnol.*, 2017, **12**, 804–812.
54 Z. Liu, *et al.*, Integrated microfluidic chip for efficient isolation and deformability analysis of circulating tumor cells, *Adv. Biosyst.*, 2018, **2**, 1800200.
55 J. Rufo, F. Cai, J. Friend, M. Wiklund and T. J. Huang, Acoustofluidics for biomedical applications, *Nat. Rev. Methods Primers*, 2022, **2**, 30.
56 J. Rufo, P. Zhang, R. Zhong, L. P. Lee and T. J. Huang, A sound approach to advancing healthcare systems: the future of biomedical acoustics, *Nat. Commun.*, 2022, **13**, 3459.
57 W. Wang, *et al.*, H-bonded organic frameworks as ultrasound-programmable delivery platform, *Nature*, 2025, 1–10.
58 S. Wang, *et al.*, Smart patterning for topological pumping of elastic surface waves, *Sci. Adv.*, 2023, **9**, eadh4310.
59 Q. Wu, *et al.*, Active metamaterials for realizing odd mass density, *Proc. Natl. Acad. Sci. U. S. A.*, 2023, **120**, e2209829120.
60 Q. Wu, X. Zhang, P. Shivashankar, Y. Chen and G. Huang, Independent flexural wave frequency conversion by a linear active metalayer, *Phys. Rev. Lett.*, 2022, **128**, 244301.
61 Y. He, *et al.*, Acoustic technologies for the orchestration of cellular functions for therapeutic applications, *Sci. Adv.*, 2025, **11**, eadu4759.
62 M. Wu, *et al.*, Sound innovations for biofabrication and tissue engineering, *Microsyst. Nanoeng.*, 2024, **10**, 170.
63 Y. Ling, *et al.*, Machine learning–driven design of engineered cilia enables hybrid operations in acoustic microrobots, *Nat. Commun.*, 2026, DOI: 10.1038/s41467-026-70048-4.
64 S. Yang, *et al.*, Acoustic tweezers for high-throughput single-cell analysis, *Nat. Protoc.*, 2023, **18**, 2441–2458.
65 M. E. Piyasena, *et al.*, Multinode acoustic focusing for parallel flow cytometry, *Anal. Chem.*, 2012, **84**, 1831–1839.
66 G. Jin, *et al.*, Acoustofluidic scanning nanoscope with high resolution and large field of view, *ACS Nano*, 2020, **14**, 8624–8633.
67 P. Liu, *et al.*, Acoustofluidic black holes for multifunctional in-droplet particle manipulation, *Sci. Adv.*, 2022, **8**, eabm2592.
68 Z. Pei, *et al.*, Capillary-based, multifunctional manipulation of particles and fluids via focused surface acoustic waves, *J. Phys. D: Appl. Phys.*, 2024, **57**, 305401.
69 J. Rich, Z. Tian and T. J. Huang, Sonoporation: Past, present, and future, *Adv. Mater. Technol.*, 2022, **7**, 2100885.
70 T. Godary, *et al.*, Acoustofluidics: Technology Advances and Applications from 2022 to 2024, *Anal. Chem.*, 2025, **97**, 6847–6870.
71 S. Zhao, *et al.*, Topological acoustofluidics, *Nat. Mater.*, 2025, 1–9.
72 J. Rufo, *et al.*, High-yield and rapid isolation of extracellular vesicles by flocculation via orbital acoustic trapping: FLOAT, *Microsyst. Nanoeng.*, 2024, **10**, 23.
73 J. Rich, *et al.*, Aerosol jet printing of surface acoustic wave microfluidic devices, *Microsyst. Nanoeng.*, 2024, **10**, 2.
74 Z. Ma, *et al.*, Acoustofluidic system for targeted antibody removal in transplantation: Enabling small-volume therapeutic apheresis, *Sci. Adv.*, 2025, **11**, eady3262.
75 Q. Wu, H. Chen, H. Nassar and G. Huang, Non-reciprocal Rayleigh wave propagation in space–time modulated surface, *J. Mech. Phys. Solids*, 2021, **146**, 104196.
76 P. Li, *et al.*, Acoustic separation of circulating tumor cells, *Proc. Natl. Acad. Sci. U. S. A.*, 2015, **112**, 4970–4975.
77 M. Wu, *et al.*, Acoustofluidic-based therapeutic apheresis system, *Nat. Commun.*, 2024, **15**, 6854.
78 C. Devendran, *et al.*, Diffraction-based acoustic manipulation in microchannels enables continuous particle and bacteria focusing, *Lab Chip*, 2020, **20**, 2674–2688.
79 D. J. Collins, *et al.*, Selective particle and cell capture in a continuous flow using micro-vortex acoustic streaming, *Lab Chip*, 2017, **17**, 1769–1777.
80 S. Yang, *et al.*, Harmonic acoustics for dynamic and selective particle manipulation, *Nat. Mater.*, 2022, **21**, 540–546.
81 X. Xu, *et al.*, Acoustofluidic tweezers via ring resonance, *Sci. Adv.*, 2024, **10**, eads2654.
82 Y. Gu, *et al.*, Acoustofluidic centrifuge for nanoparticle enrichment and separation, *Sci. Adv.*, 2021, **7**, eabc0467.
83 C. Chen, *et al.*, Acoustofluidic spin control for 3D particle manipulation in droplets, *Sci. Adv.*, 2025, **11**, eadx0269.
84 Y. He, *et al.*, Nanoscale acoustic oscillator for mechanoimmunology: NAOMI, *Sci. Adv.*, 2025, **11**, eadx3851.
85 S. Kim, *et al.*, Acoustofluidic stimulation of functional immune cells in a microreactor, *Adv. Sci.*, 2022, **9**, 2105809.
86 J. Park, G. Destgeer, M. Afzal and H. J. Sung, Acoustofluidic generation of droplets with tunable chemical concentrations, *Lab Chip*, 2020, **20**, 3922–3929.
87 R. Zhong, *et al.*, Cellular immunity analysis by a modular acoustofluidic platform: CIAMAP, *Sci. Adv.*, 2023, **9**, eadj9964.
88 R. Zhong, *et al.*, Acoustofluidic droplet sorter based on single phase focused transducers, *Small*, 2021, **17**, 2103848.
89 R. Zhong, *et al.*, An acoustofluidic embedding platform for rapid multiphase microparticle injection, *Nat. Commun.*, 2025, **16**, 4144.
90 T. Naquin, *et al.*, An acoustofluidic picoinjector, *Sens. Actuators, B*, 2024, **418**, 136294.
91 N. Abd Rahman, F. Ibrahim and B. Yafouz, Dielectrophoresis for biomedical sciences applications: A review, *Sensors*, 2017, **17**, 449.
92 M. Lan and F. Yang, Applications of dielectrophoresis in microfluidic-based exosome separation and detection, *Chem. Eng. J.*, 2024, 152067.
93 C. J. Ramirez-Murillo, J. M. de los Santos-Ramirez and V. H. Perez-Gonzalez, Toward low-voltage dielectrophoresis-based

microfluidic systems: A review, *Electrophoresis*, 2021, **42**, 565–587.
94 H. Zhang, H. Chang and P. Neuzil, DEP-on-a-chip: Dielectrophoresis applied to microfluidic platforms, *Micromachines*, 2019, **10**, 423.
95 D. R. Gossett, *et al.*, Label-free cell separation and sorting in microfluidic systems, *Anal. Bioanal. Chem.*, 2010, **397**, 3249–3267.
96 Y. Kimura, *et al.*, Dielectrophoresis-assisted massively parallel cell pairing and fusion based on field constriction created by a micro-orifice array sheet, *Electrophoresis*, 2011, **32**, 2496–2501.
97 M. Li and R. K. Anand, High-throughput selective capture of single circulating tumor cells by dielectrophoresis at a wireless electrode array, *J. Am. Chem. Soc.*, 2017, **139**, 8950–8959.
98 S. Choi and J.-K. Park, Microfluidic system for dielectrophoretic separation based on a trapezoidal electrode array, *Lab Chip*, 2005, **5**, 1161–1167.
99 K. Zhao, R. Peng and D. Li, Separation of nanoparticles by a nano-orifice based DC-dielectrophoresis method in a pressure-driven flow, *Nanoscale*, 2016, **8**, 18945–18955.
100 M. Viefhues, R. Eichhorn, E. Fredrich, J. Regtmeier and D. Anselmetti, Continuous and reversible mixing or demixing of nanoparticles by dielectrophoresis, *Lab Chip*, 2012, **12**, 485–494.
101 C.-H. Han, S. Y. Woo, J. Bhardwaj, A. Sharma and J. Jang, Rapid and selective concentration of bacteria, viruses, and proteins using alternating current signal superimposition on two coplanar electrodes, *Sci. Rep.*, 2018, **8**, 14942.
102 S. D. Ibsen, *et al.*, Rapid isolation and detection of exosomes and associated biomarkers from plasma, *ACS Nano*, 2017, **11**, 6641–6651.
103 S. A. Faraghat, *et al.*, High-throughput, low-loss, low-cost, and label-free cell separation using electrophysiology-activated cell enrichment, *Proc. Natl. Acad. Sci. U. S. A.*, 2017, **114**, 4591–4596.
104 J. Chen, *et al.*, Rapid and efficient isolation and detection of extracellular vesicles from plasma for lung cancer diagnosis, *Lab Chip*, 2019, **19**, 432–443.
105 J. Kimbrough, L. Williams, Q. Yuan and Z. Xiao, Dielectrophoresis-based positioning of carbon nanotubes for wafer-scale fabrication of carbon nanotube devices, *Micromachines*, 2020, **12**, 12.
106 C. T. Ertsgaard, M. Kim, J. Choi and S.-H. Oh, Wireless dielectrophoresis trapping and remote impedance sensing via resonant wireless power transfer, *Nat. Commun.*, 2023, **14**, 103.
107 C. T. Ertsgaard, D. Yoo, P. R. Christenson, D. J. Klemme and S.-H. Oh, Open-channel microfluidics via resonant wireless power transfer, *Nat. Commun.*, 2022, **13**, 1869.
108 X. Fan and I. M. White, Optofluidic microsystems for chemical and biological analysis, *Nat. Photonics*, 2011, **5**, 591–597.
109 H. Zhang, *et al.*, Optofluidic lasers and their applications in biochemical sensing, *Lab Chip*, 2023, **23**, 2959–2989.
110 G. L. Liu, J. Kim, Y. Lu and L. P. Lee, Optofluidic control using photothermal nanoparticles, *Nat. Mater.*, 2006, **5**, 27–32.
111 X. Mao, J. R. Waldeisen, B. K. Juluri and T. J. Huang, Hydrodynamically tunable optofluidic cylindrical microlens, *Lab Chip*, 2007, **7**, 1303–1308.
112 X. Mao, *et al.*, An integrated, multiparametric flow cytometry chip using "microfluidic drifting" based three-dimensional hydrodynamic focusing, *Biomicrofluidics*, 2012, **6**(2), 024113.
113 K. Dradrach, *et al.*, Light-driven peristaltic pumping by an actuating splay-bend strip, *Nat. Commun.*, 2023, **14**, 1877.
114 W. Li, X. Tang and L. Wang, Photopyroelectric microfluidics, *Sci. Adv.*, 2020, **6**, eabc1693.
115 X.-G. Chen, *et al.*, Optofluidic crystallithography for directed growth of single-crystalline halide perovskites, *Nat. Commun.*, 2024, **15**, 3677.
116 T. Zhou, *et al.*, Digital Lasing Biochip for Tumor-Derived Exosome Analysis, *Anal. Chem.*, 2025, **97**, 5605–5611.
117 Y. Jahani, *et al.*, Imaging-based spectrometer-less optofluidic biosensors based on dielectric metasurfaces for detecting extracellular vesicles, *Nat. Commun.*, 2021, **12**, 3246.
118 J.-W. Jeong, *et al.*, Wireless optofluidic systems for programmable in vivo pharmacology and optogenetics, *Cell*, 2015, **162**, 662–674.
119 Y. Wu, *et al.*, Wireless multi-lateral optofluidic microsystems for real-time programmable optogenetics and photopharmacology, *Nat. Commun.*, 2022, **13**, 5571.
120 K. Choi, A. H. Ng, R. Fobel and A. R. Wheeler, Digital microfluidics, *Annu. Rev. Anal. Chem.*, 2012, **5**, 413–440.
121 J. Lee, H. Moon, J. Fowler, T. Schoellhammer and C.-J. Kim, Electrowetting and electrowetting-on-dielectric for microscale liquid handling, *Sens. Actuators, A*, 2002, **95**, 259–268.
122 R. B. Fair, Digital microfluidics: is a true lab-on-a-chip possible?, *Microfluid. Nanofluid.*, 2007, **3**, 245–281.
123 M. Abdelgawad, S. L. Freire, H. Yang and A. R. Wheeler, All-terrain droplet actuation, *Lab Chip*, 2008, **8**, 672–677.
124 D. Chatterjee, B. Hetayothin, A. R. Wheeler, D. J. King and R. L. Garrell, Droplet-based microfluidics with nonaqueous solvents and solutions, *Lab Chip*, 2006, **6**, 199–206.
125 S. P. Zhang, *et al.*, Digital acoustofluidics enables contactless and programmable liquid handling, *Nat. Commun.*, 2018, **9**, 2928.
126 Y.-H. Chang, G.-B. Lee, F.-C. Huang, Y.-Y. Chen and J.-L. Lin, Integrated polymerase chain reaction chips utilizing digital microfluidics, *Biomed. Microdevices*, 2006, **8**, 215–225.
127 R. Sista, *et al.*, Development of a digital microfluidic platform for point of care testing, *Lab Chip*, 2008, **8**, 2091–2104.
128 E. R. F. Welch, Y. Y. Lin, A. Madison and R. B. Fair, Picoliter DNA sequencing chemistry on an electrowetting-based digital microfluidic platform, *Biotechnol. J.*, 2011, **6**, 165–176.

129 Q. Zhang, *et al.*, Cilo-seq: highly sensitive cell-in-library-out single-cell transcriptome sequencing with digital microfluidics, *Lab Chip*, 2022, **22**, 1971–1979.
130 A. C. Madison, *et al.*, Scalable device for automated microbial electroporation in a digital microfluidic platform, *ACS Synth. Biol.*, 2017, **6**, 1701–1709.
131 K. Guo, *et al.*, An artificial intelligence-assisted digital microfluidic system for multistate droplet control, *Microsyst. Nanoeng.*, 2024, **10**, 138.
132 T.-C. Liang, *et al.*, Dynamic adaptation using deep reinforcement learning for digital microfluidic biochips, *ACM Transact. Des. Autom. Electron. Syst.*, 2024, **29**, 1–24.
133 M. C. Peoples and H. T. Karnes, Microfluidic immunoaffinity separations for bioanalysis, *J. Chromatogr., B*, 2008, **866**, 14–25.
134 A. Bange, H. B. Halsall and W. R. Heineman, Microfluidic immunosensor systems, *Biosens. Bioelectron.*, 2005, **20**, 2488–2503.
135 Y. Xie, *et al.*, Microfluidic isolation and enrichment of nanoparticles, *ACS Nano*, 2020, **14**, 16220–16240.
136 F. Yang, X. Liao, Y. Tian and G. Li, Exosome separation using microfluidic systems: size-based, immunoaffinity-based and dynamic methodologies, *Biotechnol. J.*, 2017, **12**, 1600699.
137 T.-W. Lo, *et al.*, Microfluidic device for high-throughput affinity-based isolation of extracellular vesicles, *Lab Chip*, 2020, **20**, 1762–1770.
138 B. Dura, *et al.*, Profiling lymphocyte interactions at the single-cell level by microfluidic cell pairing, *Nat. Commun.*, 2015, **6**, 5940.
139 G. Ronteix, *et al.*, High resolution microfluidic assay and probabilistic modeling reveal cooperation between T cells in tumor killing, *Nat. Commun.*, 2022, **13**, 3111.
140 J. De Rutte, *et al.*, Suspendable hydrogel nanovials for massively parallel single-cell functional analysis and sorting, *ACS Nano*, 2022, **16**, 7242–7257.
141 P. Zhang, M. He and Y. Zeng, Ultrasensitive microfluidic analysis of circulating exosomes using a nanostructured graphene oxide/polydopamine coating, *Lab Chip*, 2016, **16**, 3033–3042.
142 P. Zhang, *et al.*, Molecular and functional extracellular vesicle analysis using nanopatterned microchips monitors tumor progression and metastasis, *Sci. Transl. Med.*, 2020, **12**, eaaz2878.
143 K. Nagase, K. Yamazaki, Y. Maekawa and H. Kanazawa, Thermoresponsive bio-affinity interfaces for temperature-modulated selective capture and release of targeted exosomes, *Mater. Today Bio*, 2023, **18**, 100521.
144 K. Chen, *et al.*, A magneto-activated nanoscale cytometry platform for molecular profiling of small extracellular vesicles, *Nat. Commun.*, 2023, **14**, 5576.
145 K. Fischer, *et al.*, Rapid discovery of monoclonal antibodies by microfluidics-enabled FACS of single pathogen-specific antibody-secreting cells, *Nat. Biotechnol.*, 2025, **43**, 960–970.
146 D. N. Breslauer, P. J. Lee and L. P. Lee, Microfluidics-based systems biology, *Mol. BioSyst.*, 2006, **2**, 97–112.
147 A. D. Castiaux, D. M. Spence and R. S. Martin, Review of 3D cell culture with analysis in microfluidic systems, *Anal. Methods*, 2019, **11**, 4220–4232.
148 V. Van Duinen, S. J. Trietsch, J. Joore, P. Vulto and T. Hankemeier, Microfluidic 3D cell culture: from tools to tissue models, *Curr. Opin. Biotechnol.*, 2015, **35**, 118–126.
149 N. I. o. Health, *NIH funding announcements to align with NIH initiative to prioritize human-based research*, 2025.
150 N. I. o. H. o. NIH, *NIH to prioritize human-based research technologies: new initiative aims to reduce use of animals in NIH-funded research*, 2025.
151 P. J. Hung, *et al.*, A novel high aspect ratio microfluidic design to provide a stable and uniform microenvironment for cell growth in a high throughput mammalian cell culture array, *Lab Chip*, 2005, **5**, 44–48.
152 P. J. Lee, P. J. Hung and L. P. Lee, An artificial liver sinusoid with a microfluidic endothelial-like barrier for primary hepatocyte culture, *Biotechnol. Bioeng.*, 2007, **97**, 1340–1346.
153 P. J. Lee, P. J. Hung, V. M. Rao and L. P. Lee, Nanoliter scale microbioreactor array for quantitative cell biology, *Biotechnol. Bioeng.*, 2006, **94**, 5–14.
154 J. Whisler, *et al.*, Emergent mechanical control of vascular morphogenesis, *Sci. Adv.*, 2023, **9**, eadg9781.
155 C. Quintard, *et al.*, A microfluidic platform integrating functional vascularized organoids-on-chip, *Nat. Commun.*, 2024, **15**, 1452.
156 B. F. L. Lai, *et al.*, A well plate–based multiplexed platform for incorporation of organoids into an organ-on-a-chip system with a perfusable vasculature, *Nat. Protoc.*, 2021, **16**, 2158–2189.
157 B. Schuster, *et al.*, Automated microfluidic platform for dynamic and combinatorial drug screening of tumor organoids, *Nat. Commun.*, 2020, **11**, 5271.
158 S. Grebenyuk, *et al.*, Large-scale perfused tissues via synthetic 3D soft microfluidics, *Nat. Commun.*, 2023, **14**, 193.
159 D. J. Shiwarski, *et al.*, 3D bioprinting of collagen-based high-resolution internally perfusable scaffolds for engineering fully biologic tissue systems, *Sci. Adv.*, 2025, **11**, eadu5905.
160 A. P. Turner, Biosensors: sense and sensibility, *Chem. Soc. Rev.*, 2013, **42**, 3184–3196.
161 T. Vo-Dinh, Nanobiosensors: probing the sanctuary of individual living cells, *J. Cell. Biochem.*, 2002, **87**, 154–161.
162 T. Vo-Dinh and B. Cullum, Biosensors and biochips: advances in biological and medical diagnostics, *Fresenius' J. Anal. Chem.*, 2000, **366**, 540–551.
163 G. Luka, *et al.*, Microfluidics integrated biosensors: A leading technology towards lab-on-a-chip and sensing applications, *Sensors*, 2015, **15**, 30011–30031.
164 L. M. Schmidt-Speicher and K. Länge, Microfluidic integration for electrochemical biosensor applications, *Curr. Opin. Electrochem.*, 2021, **29**, 100755.

165 J. Baranwal, B. Barse, G. Gatto, G. Broncova and A. Kumar, Electrochemical sensors and their applications: A review, *Chem*, 2022, **10**, 363.
166 R. Singh, R. Gupta, D. Bansal, R. Bhateria and M. Sharma, A review on recent trends and future developments in electrochemical sensing, *ACS Omega*, 2024, **9**, 7336–7356.
167 A. Molazemhosseini, L. Magagnin, P. Vena and C.-C. Liu, Single-use disposable electrochemical label-free immunosensor for detection of glycated hemoglobin (HbA1c) using differential pulse voltammetry (DPV), *Sensors*, 2016, **16**, 1024.
168 Y. Zhao, *et al.*, A programmable magnetic digital microfluidic platform integrated with electrochemical detection system, *Microsyst. Nanoeng.*, 2025, **11**, 82.
169 L. Salvigni, *et al.*, Reconfiguration of organic electrochemical transistors for high-accuracy potentiometric sensing, *Nat. Commun.*, 2024, **15**, 6499.
170 X. Liu, X. Gao, L. Yang, Y. Zhao and F. Li, Metal–organic framework-functionalized paper-based electrochemical biosensor for ultrasensitive exosome assay, *Anal. Chem.*, 2021, **93**, 11792–11799.
171 Y. Peng, *et al.*, An electrochemical biosensor for sensitive analysis of the SARS-CoV-2 RNA, *Biosens. Bioelectron.*, 2021, **186**, 113309.
172 M. A. U. Khalid, *et al.*, High performance inkjet printed embedded electrochemical sensors for monitoring hypoxia in a gut bilayer microfluidic chip, *Lab Chip*, 2022, **22**, 1764–1778.
173 H. S. Magar, R. Y. Hassan and A. Mulchandani, Electrochemical impedance spectroscopy (EIS): Principles, construction, and biosensing applications, *Sensors*, 2021, **21**, 6578.
174 D. Najjar, *et al.*, A lab-on-a-chip for the concurrent electrochemical detection of SARS-CoV-2 RNA and anti-SARS-CoV-2 antibodies in saliva and plasma, *Nat. Biomed. Eng.*, 2022, **6**, 968–978.
175 H. Pei, *et al.*, A DNA nanostructure-based biomolecular probe carrier platform for electrochemical biosensing, *Adv. Mater.*, 2010, **22**, 4754.
176 J.-C. Lee, *et al.*, Micrometer-thick and porous nanocomposite coating for electrochemical sensors with exceptional antifouling and electroconducting properties, *Nat. Commun.*, 2024, **15**, 711.
177 S. Ding, *et al.*, A fingertip-wearable microgrid system for autonomous energy management and metabolic monitoring, *Nat. Electron.*, 2024, **7**, 788–799.
178 Y. Huang, J. C. Williams and S. M. Johnson, Brain slice on a chip: opportunities and challenges of applying microfluidic technology to intact tissues, *Lab Chip*, 2012, **12**, 2103–2117.
179 M. Washizu, O. Kurosawa, I. Arai, S. Suzuki and N. Shimamoto, Applications of electrostatic stretch-and-positioning of DNA, *IEEE Trans. Ind. Appl.*, 2002, **31**, 447–456.
180 C. Ionescu-Zanetti, *et al.*, Mammalian electrophysiology on a microfluidic platform, *Proc. Natl. Acad. Sci. U. S. A.*, 2005, **102**, 9112–9117.
181 V. F. Curto, *et al.*, Organic transistor platform with integrated microfluidics for in-line multi-parametric in vitro cell monitoring, *Microsyst. Nanoeng.*, 2017, **3**, 1–12.
182 A. Cerea, *et al.*, Selective intracellular delivery and intracellular recordings combined in MEA biosensors, *Lab Chip*, 2018, **18**, 3492–3500.
183 B. M. Maoz, *et al.*, Organs-on-Chips with combined multi-electrode array and transepithelial electrical resistance measurement capabilities, *Lab Chip*, 2017, **17**, 2294–2302.
184 E. Moutaux, B. Charlot, A. Genoux, F. Saudou and M. Cazorla, An integrated microfluidic/microelectrode array for the study of activity-dependent intracellular dynamics in neuronal networks, *Lab Chip*, 2018, **18**, 3425–3435.
185 S. Hong, M. Song, W. S. Yang, I.-H. Park and L. P. Lee, Brainwaves Monitoring via Human Midbrain Organoids Microphysiological Analysis Platform: MAP, *bioRxiv*, 2024, preprint, DOI: 10.1101/2024.09.24.613225.
186 L. Huang, X. Zhang, Y. Feng, F. Liang and W. Wang, High content drug screening of primary cardiomyocytes based on microfluidics and real-time ultra-large-scale high-resolution imaging, *Lab Chip*, 2022, **22**, 1206–1213.
187 A. Bandodkar, *et al.*, Sweat-activated biocompatible batteries for epidermal electronic and microfluidic systems, *Nat. Electron.*, 2020, **3**, 554–562.
188 Y. Yang, *et al.*, Wireless multilateral devices for optogenetic studies of individual and social behaviors, *Nat. Neurosci.*, 2021, **24**, 1035–1045.
189 W. Liu, K. Chung, S. Yu and L. P. Lee, Nanoplasmonic biosensors for environmental sustainability and human health, *Chem. Soc. Rev.*, 2024, **53**(21), 10491–10522.
190 A. Neettiyath, K. Chung, W. Liu and L. P. Lee, Nanoplasmonic sensors for extracellular vesicles and bacterial membrane vesicles, *Nano Convergence*, 2024, **11**, 23.
191 Q. Duan, Y. Liu, S. Chang, H. Chen and J.-h. Chen, Surface plasmonic sensors: Sensing mechanism and recent applications, *Sensors*, 2021, **21**, 5262.
192 Z. Mei and L. Tang, Surface-plasmon-coupled fluorescence enhancement based on ordered gold nanorod array biochip for ultrasensitive DNA analysis, *Anal. Chem.*, 2017, **89**, 633–639.
193 J. Luan, *et al.*, Ultrabright fluorescent nanoscale labels for the femtomolar detection of analytes with standard bioassays, *Nat. Biomed. Eng.*, 2020, **4**, 518–530.
194 D. Kavungal, *et al.*, Artificial intelligence–coupled plasmonic infrared sensor for detection of structural protein biomarkers in neurodegenerative diseases, *Sci. Adv.*, 2023, **9**, eadg9644.
195 Y. Choi, Y. Park, T. Kang and L. P. Lee, Selective and sensitive detection of metal ions by plasmonic resonance energy transfer-based nanospectroscopy, *Nat. Nanotechnol.*, 2009, **4**, 742–746.
196 A. Biswas, *et al.*, Nanoplasmonic aptasensor for sensitive, selective, and real-time detection of dopamine from unprocessed whole blood, *Sci. Adv.*, 2024, **10**, eadp7460.

197 Y. Lee, *et al.*, Nanoplasmonic on-chip PCR for rapid precision molecular diagnostics, *ACS Appl. Mater. Interfaces*, 2020, **12**, 12533–12540.
198 T. AbdElFatah, *et al.*, Nanoplasmonic amplification in microfluidics enables accelerated colorimetric quantification of nucleic acid biomarkers from pathogens, *Nat. Nanotechnol.*, 2023, **18**, 922–932.
199 U. Mogera, *et al.*, Wearable plasmonic paper–based microfluidics for continuous sweat analysis, *Sci. Adv.*, 2022, **8**, eabn1736.
200 J. Jeon, *et al.*, All-flexible chronoepifluidic nanoplasmonic patch for label-free metabolite profiling in sweat, *Nat. Commun.*, 2025, **16**, 8017.
201 C. Xiao, J. Eriksson, A. Suska, D. Filippini and W. C. Mak, Print-and-stick unibody microfluidics coupled surface plasmon resonance (SPR) chip for smartphone imaging SPR (Smart-iSRP), *Anal. Chim. Acta*, 2022, **1201**, 339606.
202 T. Vo-Dinh, *et al.*, SERS nanosensors and nanoreporters: golden opportunities in biomedical applications, *Wiley Interdiscip. Rev.:Nanomed. Nanobiotechnol.*, 2015, **7**, 17–33.
203 L. Guerrini, E. Garcia-Rico, A. O'Loghlen, V. Giannini and R. A. Alvarez-Puebla, Surface-enhanced Raman scattering (SERS) spectroscopy for sensing and characterization of exosomes in cancer diagnosis, *Cancers*, 2021, **13**, 2179.
204 A. J. Canning, J. Q. Li, S. Atta, H.-N. Wang and T. Vo-Dinh, Nanoplasmonics biosensors: At the frontiers of biomedical diagnostics, *TrAC, Trends Anal. Chem.*, 2024, 117973.
205 A. J. Canning, *et al.*, Advancing precision photothermal therapy by integrating armored gold nanostars with real-time photoacoustic thermometry and imaging, *Sci. Adv.*, 2025, **11**, eadx6350.
206 S. Dong, *et al.*, Beehive-inspired macroporous SERS probe for cancer detection through capturing and analyzing exosomes in plasma, *ACS Appl. Mater. Interfaces*, 2020, **12**, 5136–5146.
207 W. Dong, *et al.*, Digital microfluidics with integrated Raman sensor for high-sensitivity in-situ bioanalysis, *Biosens. Bioelectron.*, 2025, **271**, 117036.
208 B. Ogunlade, *et al.*, Rapid, antibiotic incubation-free determination of tuberculosis drug resistance using machine learning and Raman spectroscopy, *Proc. Natl. Acad. Sci. U. S. A.*, 2024, **121**(25), e2315670121.
209 S.-J. Lin, *et al.*, An antibiotic concentration gradient microfluidic device integrating surface-enhanced Raman spectroscopy for multiplex antimicrobial susceptibility testing, *Lab Chip*, 2022, **22**, 1805–1814.
210 H. T. Ngo, N. Gandra, A. M. Fales, S. M. Taylor and T. Vo-Dinh, Sensitive DNA detection and SNP discrimination using ultrabright SERS nanorattles and magnetic beads for malaria diagnostics, *Biosens. Bioelectron.*, 2016, **81**, 8–14.
211 A. J. Canning, *et al.*, miRNA probe integrated biosensor platform using bimetallic nanostars for amplification-free multiplexed detection of circulating colorectal cancer biomarkers in clinical samples, *Biosens. Bioelectron.*, 2023, **220**, 114855.
212 J. Wang, *et al.*, Tracking extracellular vesicle phenotypic changes enables treatment monitoring in melanoma, *Sci. Adv.*, 2020, **6**, eaax3223.
213 V. Shahabadi, *et al.*, Quantifying surface tension of metastable aerosols via electrodeformation, *Nat. Commun.*, 2024, **15**, 1–11.
214 Q. Chen, H. Zhai, D. J. Beebe, C. Li and B. Wang, Visualization-enhanced under-oil open microfluidic system for in situ characterization of multi-phase chemical reactions, *Nat. Commun.*, 2024, **15**, 1155.
215 N. Nunn, A. I. Shames, M. Torelli, A. I. Smirnov and O. Shenderova, Luminescent diamond: A platform for next generation nanoscale optically driven quantum sensors in *Luminescent nanomaterials*, Jenny Stanford Publishing, 2022, pp. 1–95.
216 O. A. Shenderova, M. Torelli, N. Nunn and A. Marek, Fluorescent nanodiamond for emerging quantum sensing applications, in *Quantum Effects and Measurement Techniques in Biology and Biophotonics II (SPIE)*, 2025, p. PC133400A.
217 R. D. Allert, *et al.*, Microfluidic quantum sensing platform for lab-on-a-chip applications, *Lab Chip*, 2022, **22**, 4831–4840.
218 C. Li, R. Soleyman, M. Kohandel and P. Cappellaro, SARS-CoV-2 quantum sensor based on nitrogen-vacancy centers in diamond, *Nano Lett.*, 2021, **22**, 43–49.
219 A. Sarkar, *et al.*, High-precision chemical quantum sensing in flowing monodisperse microdroplets, *Sci. Adv.*, 2024, **10**, eadp4033.
220 G. Kucsko, *et al.*, Nanometre-scale thermometry in a living cell, *Nature*, 2013, **500**, 54–58.
221 P.-C. Tsai, *et al.*, Gold/diamond nanohybrids for quantum sensing applications, *EPJ Quantum Technol.*, 2015, **2**, 1–12.
222 M. Fujiwara, *et al.*, Real-time nanodiamond thermometry probing in vivo thermogenic responses, *Sci. Adv.*, 2020, **6**, eaba9636.
223 J. Smits, *et al.*, Two-dimensional nuclear magnetic resonance spectroscopy with a microfluidic diamond quantum sensor, *Sci. Adv.*, 2019, **5**, eaaw7895.
224 X. Gao, *et al.*, Quantum sensing of paramagnetic spins in liquids with spin qubits in hexagonal boron nitride, *ACS Photonics*, 2023, **10**, 2894–2900.
225 N. Kongsuwan, *et al.*, Quantum plasmonic immunoassay sensing, *Nano Lett.*, 2019, **19**, 5853–5861.
226 H. Xin, B. Namgung and L. P. Lee, Nanoplasmonic optical antennas for life sciences and medicine, *Nat. Rev. Mater.*, 2018, **3**, 228–243.
227 K. D. Briegel, *et al.*, Optical widefield nuclear magnetic resonance microscopy, *Nat. Commun.*, 2025, **16**, 1281.
228 S. Chung, C. M. Jennings and J. Y. Yoon, Distance versus Capillary Flow Dynamics-Based Detection Methods on a Microfluidic Paper-Based Analytical Device (μPAD), *Chem. – Eur. J.*, 2019, **25**, 13070–13077.
229 T. Tian, *et al.*, Distance-based microfluidic quantitative detection methods for point-of-care testing, *Lab Chip*, 2016, **16**, 1139–1151.

230 K. Khachornsakkul, W. Dungchai and N. Pamme, Distance-based all-in-one immunodevice for point-of-care monitoring of cytokine interleukin-6, *ACS Sens.*, 2022, **7**(8), 2410–2419.
231 M. Ho, *et al.*, Digital microfluidics with distance-based detection–a new approach for nucleic acid diagnostics, *Lab Chip*, 2024, **24**, 63–73.
232 B. Chutvirasakul, N. Nuchtavorn, L. Suntornsuk and Y. Zeng, Exosome aggregation mediated stop-flow paper-based portable device for rapid exosome quantification, *Electrophoresis*, 2020, **41**, 311–318.
233 Z. Zhu, *et al.*, Au@ Pt nanoparticle encapsulated target-responsive hydrogel with volumetric bar-chart chip readout for quantitative point-of-care testing, *Angew. Chem., Int. Ed.*, 2014, **53**, 12503–12507.
234 Y. Li, *et al.*, Competitive volumetric bar-chart chip with real-time internal control for point-of-care diagnostics, *Anal. Chem.*, 2015, **87**, 3771–3777.
235 A. B. Subramaniam, M. Gonidec, N. D. Shapiro, K. M. Kresse and G. M. Whitesides, Metal-amplified density assays,(MADAs), including a density-linked immunosorbent assay (DeLISA), *Lab Chip*, 2015, **15**, 1009–1022.
236 R. A. Becker, *et al.*, Optical probing of gastrocnemius in patients with peripheral artery disease characterizes myopathic biochemical alterations and correlates with stage of disease, *Physiol. Rep.*, 2017, **5**, e13161.
237 O. Alkhamis, J. Canoura, H. Yu, Y. Liu and Y. Xiao, Innovative engineering and sensing strategies for aptamer-based small-molecule detection, *TrAC, Trends Anal. Chem.*, 2019, **121**, 115699.
238 S. Lyu, Z. Wu, X. Shi and Q. Wu, Optical fiber biosensors for protein detection: a review, *Photonics*, 2022, **9**, 987.
239 D. C. Duffy, Digital detection of proteins, *Lab Chip*, 2023, **23**, 818–847.
240 J. C. Rolando, A. V. Melkonian and D. R. Walt, The present and future landscapes of molecular diagnostics, *Annu. Rev. Anal. Chem.*, 2024, **17**, 459–474.
241 A. Sonato, *et al.*, A surface acoustic wave (SAW)-enhanced grating-coupling phase-interrogation surface plasmon resonance (SPR) microfluidic biosensor, *Lab Chip*, 2016, **16**, 1224–1233.
242 A. Akther, *et al.*, Acoustomicrofluidic concentration and signal enhancement of fluorescent nanodiamond sensors, *Anal. Chem.*, 2021, **93**, 16133–16141.
243 G. Krainer, *et al.*, Direct digital sensing of protein biomarkers in solution, *Nat. Commun.*, 2023, **14**, 653.
244 G. Krainer, *et al.*, Single-molecule digital sizing of proteins in solution, *Nat. Commun.*, 2024, **15**, 7740.
245 X. Zhu, *et al.*, Measurements of molecular size and shape on a chip, *Science*, 2025, **388**, eadt5827.
246 R. Gao, Z. Cheng, A. J. Demello and J. Choo, Wash-free magnetic immunoassay of the PSA cancer marker using SERS and droplet microfluidics, *Lab Chip*, 2016, **16**, 1022–1029.
247 H. Yu, *et al.*, A rapid assay provides on-site quantification of tetrahydrocannabinol in oral fluid, *Sci. Transl. Med.*, 2021, **13**, eabe2352.
248 H. Chen, *et al.*, Reducing hepatitis C diagnostic disparities with a fully automated deep learning–enabled microfluidic system for HCV antigen detection, *Sci. Adv.*, 2025, **11**, eadt3803.
249 M. Wang, *et al.*, A wearable electrochemical biosensor for the monitoring of metabolites and nutrients, *Nat. Biomed. Eng.*, 2022, **6**, 1225–1235.
250 R. Tikhomirov, *et al.*, Exosomes: from potential culprits to new therapeutic promise in the setting of cardiac fibrosis, *Cell*, 2020, **9**, 592.
251 Y. Zhang, Y. Liu, H. Liu and W. H. Tang, Exosomes: biogenesis, biologic function and clinical potential, *Cell Biosci.*, 2019, **9**, 1–18.
252 M. Andre, *et al.*, Magnetoelectric Extracellular Vesicle Latency-Targeting (MELT) Nanotherapeutic for the Block-Lock-and-Kill HIV Eradication Strategy, *Biomedicines*, 2025, **13**, 147.
253 T. D. Naquin, *et al.*, Acoustic separation and concentration of exosomes for nucleotide detection: ASCENDx, *Sci. Adv.*, 2024, **10**, eadm8597.
254 N. Hao, *et al.*, Acoustofluidics-assisted fluorescence-SERS bimodal biosensors, *Small*, 2020, **16**, 2005179.
255 Y. Chen, *et al.*, Exosome detection via the ultrafast-isolation system: EXODUS, *Nat. Methods*, 2021, **18**, 212–218.
256 J. Shi, S. C. Barman, S. Cheng and Y. Zeng, Metal–organic framework-interfaced ELISA probe enables ultrasensitive detection of extracellular vesicle biomarkers, *J. Mater. Chem. B*, 2024, **12**, 6342–6350.
257 Y.-X. Zhang, *et al.*, An integrated microfluidic chip for synchronous drug loading, separation and detection of plasma exosomes, *Lab Chip*, 2025, **25**, 3185–3196.
258 Y. Chen, *et al.*, Magnetic augmentation through multi-gradient coupling enables direct and programmable profiling of circulating biomarkers, *Nat. Commun.*, 2024, **15**, 8410.
259 X. Li, *et al.*, Extracellular vesicle-based point-of-care testing for diagnosis and monitoring of Alzheimer's disease, *Microsyst. Nanoeng.*, 2025, **11**, 65.
260 Y. Wen, *et al.*, Partition-less digital immunoassay using configurable topographic nanoarrays for extracellular vesicle diagnosis of ewing sarcoma, *ACS Nano*, 2025, **19**, 11973–11986.
261 Q. Wu, *et al.*, Capturing nascent extracellular vesicles by metabolic glycan labeling-assisted microfluidics, *Nat. Commun.*, 2023, **14**, 6541.
262 N. H. Maniya, *et al.*, An anion exchange membrane sensor detects EGFR and its activity state in plasma CD63 extracellular vesicles from patients with glioblastoma, *Commun. Biol.*, 2024, **7**, 677.
263 X.-Z. Cong, *et al.*, Microfluidic device-based in vivo detection of PD-L1-positive small extracellular vesicles and its application for tumor monitoring, *Anal. Chem.*, 2024, **96**, 2658–2665.
264 E.-C. Yeh, *et al.*, Self-powered integrated microfluidic point-of-care low-cost enabling (SIMPLE) chip, *Sci. Adv.*, 2017, **3**, e1501645.

265 A. Sun, *et al.*, An integrated microfluidic platform for nucleic acid testing, *Microsyst. Nanoeng.*, 2024, **10**, 66.
266 L. Jiang, *et al.*, Single-molecule RNA capture-assisted droplet digital loop-mediated isothermal amplification for ultrasensitive and rapid detection of infectious pathogens, *Microsyst. Nanoeng.*, 2023, **9**, 118.
267 J. Li, *et al.*, Simultaneous Detection of Multiple Respiratory Pathogens Using an Integrated Microfluidic Chip, *Anal. Chem.*, 2024, **96**, 13768–13776.
268 D. C. Rabe, *et al.*, Ultrasensitive detection of intact SARS-CoV-2 particles in complex biofluids using microfluidic affinity capture, *Sci. Adv.*, 2025, **11**, eadh1167.
269 J. Qian, *et al.*, Rapid and comprehensive detection of viral antibodies and nucleic acids via an acoustofluidic integrated molecular diagnostics chip: AIMDx, *Sci. Adv.*, 2025, **11**, eadt5464.
270 T. Stuart and R. Satija, *et al.*, *Nat. Rev. Genet.*, 2019, **20**, 257–272.
271 L. Heumos, *et al.*, Best practices for single-cell analysis across modalities, *Nat. Rev. Genet.*, 2023, **24**, 550–572.
272 G.-C. Yuan, *et al.*, Challenges and emerging directions in single-cell analysis, *Genome Biol.*, 2017, **18**, 84.
273 D. Di Carlo, N. Aghdam and L. P. Lee, Single-cell enzyme concentrations, kinetics, and inhibition analysis using high-density hydrodynamic cell isolation arrays, *Anal. Chem.*, 2006, **78**, 4925–4930.
274 S. Hong, Q. Pan and L. P. Lee, Single-cell level co-culture platform for intercellular communication, *Integr. Biol.*, 2012, **4**, 374–380.
275 S. Lindström and H. Andersson-Svahn, Overview of single-cell analyses: microdevices and applications, *Lab Chip*, 2010, **10**, 3363–3372.
276 R. Zhong, *et al.*, Enhancing cancer therapy via acoustics: chemotherapy-enhanced tunable acoustofluidic permeabilization (ChemoTAP), *Lab Chip*, 2025, **25**, 6314–6323.
277 K. Yang, *et al.*, Precision acoustofluidics for high-throughput mechanobiology in suspension cells, *Sci. Adv.*, 2026, **12**, eady1136.
278 T. Yeo, *et al.*, Microfluidic enrichment for the single cell analysis of circulating tumor cells, *Sci. Rep.*, 2016, **6**, 22076.
279 N.-V. Nguyen and C.-P. Jen, Impedance detection integrated with dielectrophoresis enrichment platform for lung circulating tumor cells in a microfluidic channel, *Biosens. Bioelectron.*, 2018, **121**, 10–18.
280 Y. Zhang, *et al.*, Combining multiplex SERS nanovectors and multivariate analysis for in situ profiling of circulating tumor cell phenotype using a microfluidic chip, *Small*, 2018, **14**, 1704433.
281 Z. Ma, Y. Zhou, D. J. Collins and Y. Ai, Fluorescence activated cell sorting via a focused traveling surface acoustic beam, *Lab Chip*, 2017, **17**, 3176–3185.
282 N. Nitta, *et al.*, Raman image-activated cell sorting, *Nat. Commun.*, 2020, **11**, 3452.
283 R. Zilionis, *et al.*, Single-cell barcoding and sequencing using droplet microfluidics, *Nat. Protoc.*, 2017, **12**, 44–73.
284 J. De Jonghe, *et al.*, spinDrop: a droplet microfluidic platform to maximise single-cell sequencing information content, *Nat. Commun.*, 2023, **14**, 4788.
285 S. Luo, A. Notaro and L. Lin, ATLAS-seq: a microfluidic single-cell TCR screen for antigen-reactive TCRs, *Nat. Commun.*, 2025, **16**, 216.
286 D. D. Carlo and L. P. Lee, *Dynamic single-cell analysis for quantitative biology*, ACS Publications, 2006.
287 W. Wu, *et al.*, High-throughput single-cell density measurements enable dynamic profiling of immune cell and drug response from patient samples, *Nat. Biomed. Eng.*, 2025, 1–10.
288 K. K. Zeming, *et al.*, Cell trajectory modulation: rapid microfluidic biophysical profiling of CAR T cell functional phenotypes, *Nat. Commun.*, 2025, **16**, 4775.
289 Y. Feng, X. Zhao, A. K. White, K. C. Garcia and P. M. Fordyce, A bead-based method for high-throughput mapping of the sequence-and force-dependence of T cell activation, *Nat. Methods*, 2022, **19**, 1295–1305.
290 L. A. Low, C. Mummery, B. R. Berridge, C. P. Austin and D. A. Tagle, Organs-on-chips: into the next decade, *Nat. Rev. Drug Discovery*, 2021, **20**, 345–361.
291 M. W. van Der Helm, A. D. Van Der Meer, J. C. Eijkel, A. van den Berg and L. I. Segerink, Microfluidic organ-on-chip technology for blood-brain barrier research, *Tissue Barriers*, 2016, **4**, e1142493.
292 M. Stavrou, N. Phung, J. Grimm and C. Andreou, Organ-on-chip systems as a model for nanomedicine, *Nanoscale*, 2023, **15**, 9927–9940.
293 H. Liu, *et al.*, Advances in Hydrogels in Organoids and Organs-on-a-Chip, *Adv. Mater.*, 2019, **31**, 1902042.
294 M. Zhang, *et al.*, Biomimetic human disease model of SARS-CoV-2-induced lung injury and immune responses on organ chip system, *Adv. Sci.*, 2021, **8**, 2002928.
295 K. Yum, S. G. Hong, K. E. Healy and L. P. Lee, Physiologically relevant organs on chips, *Biotechnol. J.*, 2014, **9**, 16–27.
296 K. Chen, *et al.*, Rapid formation of size-controllable multicellular spheroids via 3D acoustic tweezers, *Lab Chip*, 2016, **16**, 2636–2643.
297 Y. He, *et al.*, Acoustofluidic interfaces for the mechanobiological secretome of MSCs, *Nat. Commun.*, 2023, **14**, 7639.
298 J. Yu, *et al.*, Reconfigurable open microfluidics for studying the spatiotemporal dynamics of paracrine signalling, *Nat. Biomed. Eng.*, 2019, **3**, 830–841.
299 J. W. Yang, *et al.*, Liver-on-a-Chip Integrated with Label-Free Optical Biosensors for Rapid and Continuous Monitoring of Drug-Induced Toxicity, *Small*, 2024, **20**, 2403560.
300 R. Sharmin, *et al.*, Fluorescent nanodiamonds for detecting free-radical generation in real time during shear stress in human umbilical vein endothelial cells, *ACS Sens.*, 2021, **6**, 4349–4359.
301 K. Zhang, *et al.*, A Microfluidic Chip-Based Automated System for Whole-Course Monitoring the Drug Responses of Organoids, *Anal. Chem.*, 2024, **96**(24), 10092–10101.

302 M. A. Stockslager, *et al.*, Functional drug susceptibility testing using single-cell mass predicts treatment outcome in patient-derived cancer neurosphere models, *Cell Rep.*, 2021, **37**(1), 109788.
303 J. Zhu, *et al.*, An integrated adipose-tissue-on-chip nanoplasmonic biosensing platform for investigating obesity-associated inflammation, *Lab Chip*, 2018, **18**, 3550–3560.
304 H. Feng, *et al.*, A microfluidic hanging droplet as a programmable platform for mammalian egg vitrification, *Lab Chip*, 2024, **24**, 5225–5237.
305 H. Cai, *et al.*, Brain organoid reservoir computing for artificial intelligence, *Nat. Electron.*, 2023, **6**, 1032–1039.
306 N. Frey, U. M. Sönmez, J. Minden and P. LeDuc, Microfluidics for understanding model organisms, *Nat. Commun.*, 2022, **13**, 3195.
307 M. M. Crane, K. Chung, J. Stirman and H. Lu, Microfluidics-enabled phenotyping, imaging, and screening of multicellular organisms, *Lab Chip*, 2010, **10**, 1509–1517.
308 G. Sun and H. Lu, Recent advances in microfluidic techniques for systems biology, *Anal. Chem.*, 2018, **91**, 315–329.
309 C. Chen, *et al.*, Acoustofluidic rotational tweezing enables high-speed contactless morphological phenotyping of zebrafish larvae, *Nat. Commun.*, 2021, **12**, 1118.
310 J. Zhang, *et al.*, Surface acoustic waves enable rotational manipulation of Caenorhabditis elegans, *Lab Chip*, 2019, **19**, 984–992.
311 J. Zhang, *et al.*, Fluorescence-based sorting of Caenorhabditis elegans via acoustofluidics, *Lab Chip*, 2020, **20**, 1729–1739.
312 K. Mani, Y.-C. Hsieh, B. Panigrahi and C.-Y. Chen, A noninvasive light driven technique integrated microfluidics for zebrafish larvae transportation, *Biomicrofluidics*, 2018, **12**(2), 021101.
313 G. Aubry, M. Zhan and H. Lu, Hydrogel-droplet microfluidic platform for high-resolution imaging and sorting of early larval Caenorhabditis elegans, *Lab Chip*, 2015, **15**, 1424–1431.
314 S. Hong, P. Lee, S. C. Baraban and L. P. Lee, A novel long-term, multi-channel and non-invasive electrophysiology platform for zebrafish, *Sci. Rep.*, 2016, **6**, 28248.
315 P. Pan, *et al.*, Robotic microinjection enables large-scale transgenic studies of Caenorhabditis elegans, *Nat. Commun.*, 2024, **15**, 8848.
316 S. Mondal, *et al.*, High-content microfluidic screening platform used to identify σ2R/Tmem97 binding ligands that reduce age-dependent neurodegeneration in C. elegans SC_APP model, *ACS Chem. Neurosci.*, 2018, **9**, 1014–1026.
317 Z. Bai, *et al.*, Real-time observation of perturbation of a Drosophila embryo's early cleavage cycles with microfluidics, *Anal. Chim. Acta*, 2017, **982**, 131–137.
318 S. Kumar, *et al.*, A microfluidic platform for highly parallel bite by bite profiling of mosquito-borne pathogen transmission, *Nat. Commun.*, 2021, **12**, 6018.
319 http://cytivalifesciences.com, Biacore™ SPR systems.
320 http://bruker.com, Sierra SPR®-32 Pro, 2025.
321 http://carterra-bio.com, Carterra LSA for Antibody Discovery & Development.
322 http://malvernpananalytical.com, WAVEsystem.
323 http://affinitybio.com, Affinity Biosensors Technolgoy, 2025.
324 http://travera.com, The first and Only Technology enabling 2-day Therapy Selection.
325 http://illumina.com, Chemistry and Imaging on NovaSeq 6000.
326 http://thermofisher.com, Thermo Fisher Scientific Adds Digital PCR to Genetic Analysis Capabilities, 2025.
327 http://standardbio.com, Biomark One Run and Done.
328 https://www.lucirabypfizer.com, Meet the 1st and only at-home molecular test to quickly tell you if it is COVID-19 or the flu—in just 30 minutes.
329 http://sigmaaldrich.com, CellASIC® ONIX2 Live Cell Imaging System.
330 http://aimbiotech.com, 3D microvascular networks (MVNs) are key building blocks for dynamic disease models & predictive drug testing.
331 http://wyss.harvard.edu, Human Organs-on-Chips.
332 http://mimetas.com, OrganoReady®.
333 http://imec-int.com, Imec Presents Novel Organ-on-Chip Platform for Drug Screening, 2018.
334 A. Venz, B. Duckert, L. Lagae, S. E. Takalloo and D. Braeken, Impedance mapping with high-density microelectrode array chips reveals dynamic heterogeneity of in vitro epithelial barriers, *Sci. Rep.*, 2025, **15**, 1592.
335 E. J. Topol, High-performance medicine: the convergence of human and artificial intelligence, *Nat. Med.*, 2019, **25**, 44–56.
336 R. Luo, J. Popp and T. Bocklitz, Deep learning for Raman spectroscopy: A review, *Analytica*, 2022, **3**, 287–301.
337 S. N. A. B. M. Nashruddin, F. H. M. Salleh, R. M. Yunus and H. B. Zaman, Artificial intelligence– powered electrochemical sensor: Recent advances, challenges, and prospects, *Heliyon*, 2024, **10**(18), e37964.
338 J. Park, Y. W. Kim and H.-J. Jeon, Machine learning-driven innovations in microfluidics, *Biosensors*, 2024, **14**, 613.
339 R. J. Hickman, P. Bannigan, Z. Bao, A. Aspuru-Guzik and C. Allen, Self-driving laboratories: A paradigm shift in nanomedicine development, *Matter*, 2023, **6**, 1071–1081.
340 D. McIntyre, A. Lashkaripour, P. Fordyce and D. Densmore, Machine learning for microfluidic design and control, *Lab Chip*, 2022, **22**, 2925–2937.
341 C. Trapnell, Defining cell types and states with single-cell genomics, *Genome Res.*, 2015, **25**, 1491–1498.
342 A. Wagner, A. Regev and N. Yosef, Revealing the vectors of cellular identity with single-cell genomics, *Nat. Biotechnol.*, 2016, **34**, 1145–1160.